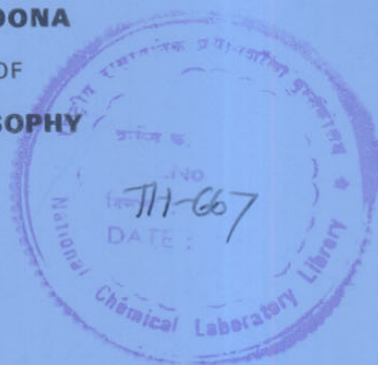


# **STUDIES IN MULTIPHASE REACTORS**

A THESIS  
SUBMITTED TO THE  
**UNIVERSITY OF POONA**  
FOR THE DEGREE OF  
**DOCTOR OF PHILOSOPHY**  
IN CHEMISTRY

COMPUTERISED



BY  
**CHANDRASHEKHAR VASANT RODE**

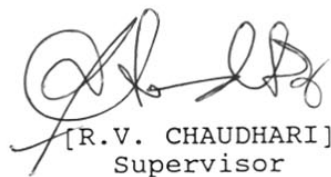
66-023(043)  
ROD

CHEMICAL ENGINEERING DIVISION  
**NATIONAL CHEMICAL LABORATORY**  
PUNE 411 008 (INDIA)

**JUNE 1990**

FORM - A

CERTIFIED that the work incorporated in thesis  
Studies in Multiphase Reactors', submitted by Shri. C.V.  
Rode was carried out by the candidate under my  
supervision. Such material as has been obtained from the  
other sources has been duly acknowledged in the thesis.



[R.V. CHAUDHARI]  
Supervisor

## A C K N O W L E D G E M E N T S

I take this opportunity to express my debt of gratitude to Dr. R.V. Chaudhari, Asst. Director, Chemical Engineering Division, National Chemical Laboratory, Pune, for initiation of the problem and his inspiring guidance throughout the course of this work.

I am grateful to Dr. R.A. Mashelkar, Director, NCL for permitting me to carry out this research work in NCL and to submit this thesis to the University of Pune.

It is my great pleasure to acknowledge my colleagues for their ever willing support, helpful hand and sympathetic ear. I also wish to thank Mr. K. Radhakrishnan for elegant typing of this thesis, within a very short time.

Pune  
June 1990



C.V. Rode

## CONTENTS

SUMMARY AND CONCLUSIONS		1
PART I <b>MODELLING OF A BUBBLE COLUMN REACTOR :</b>		
<b>OXIDATION OF ETHYLENE TO ACETALDEHYDE</b>		
<b>USING PdCl<sub>2</sub>-CuCl<sub>2</sub> CATALYST</b>		
<u>CHAPTER</u>	1	<b>INTRODUCTION AND LITERATURE SURVEY</b>
	1.1	General background 15
	1.2	Literature survey 17
	1.2.1	Bubble column reactor 17
	1.2.2	Wacker process 26
	1.2.2.1	Kinetics and mechanism 32
	1.3	Scope and objective 37
		REFERENCES 38
<u>CHAPTER</u>	2	<b>EXPERIMENTAL</b>
	2.1	Materials 42
	2.2	Reactor 42
	2.3	Experimental procedure 43
	2.4	Analysis 44

<u>CHAPTER</u>	<b>3</b>	<b>RESULTS AND DISCUSSION</b>	
	3.1	Theoretical model	47
	3.2	Parameter estimation	52
	3.3	Comparison of experimental data with theory	59
	3.4	Critical concentration of oxygen	69
		3.4.1 Introduction	69
		3.4.2 Experimental	72
		3.4.3 Results and discussion	73
	3.5	Conclusions	83
		NOMENCLATURE	85
		REFERENCES	87

<u>CHAPTER</u>	<b>4</b>	<b>GAS HOLDUP AND FLOW REGIMES IN A BUBBLE COLUMN REACTOR</b>	
	4.1	General background and Literature survey	89
	4.2	Experimental	97
		4.2.1 Materials	97
		4.2.2 Apparatus	97
		4.2.3 Experimental procedure	98
	4.3	Results and discussion	99
		4.3.1 Gas hold-up in air-water system	99
		4.3.2 Effect of electrolytes on gas hold-up	101

4.3.3	Effect of surfactants on gas hold-up	109
4.3.4	Correlation of data	113
4.3.5	Flow regimes	128
4.4	Conclusions	135
	NOMENCLATURE	137
	REFERENCES	138

**PART II    HYDROGENATION OF META-NITROCHLORO BENZENE  
TO    META-CHLORO ANILINE**

**CHAPTER    1            INTRODUCTION**

1.1	General background	144
1.1.1	Reaction	147
1.1.2	Literature survey	148
1.1.3	Kinetics and mechanism	154
1.2	Analysis of slurry reactors	155
1.2.1	General	155
1.2.2	Literature survey	159
1.2.3	Theory	161
1.2.3.1	Analysis of differential reactors	164
1.2.3.2	Overall rate of mass transfer	165
1.2.3.3	Rate of chemical reaction	166
1.2.3.4	L-H Type kinetics	168

	1.3	Objective of the present work	170
<u>CHAPTER</u>	2	<b>EXPERIMENTAL</b>	
	2.1	Materials	171
	2.2	Apparatus	171
	2.3	Experimental procedure	172
	2.4	Analysis	172
<u>CHAPTER</u>	3	<b>RESULTS AND DISCUSSION</b>	
	3.1	Analysis of initial rate data	180
	3.1.1	Effect of catalyst loading	185
	3.1.2	Effect of agitation speed	185
	3.1.3	Effect of H <sub>2</sub> pressure	186
	3.1.4	Effect of substrate and product concentration	186
	3.1.5	Analysis of mass transfer effects	186
	3.1.5.1	Gas-liquid mass transfer	193
	3.1.5.2	Liquid-solid mass transfer	194
	3.1.5.3	Intra-particle diffusion	197
	3.2	Kinetic model	198
	3.2.1	Model discrimination and parameter estimation	206

3.2.2	Interpretation of rate data at 353 and 363K	212
3.3	Batch reactor model	214
3.4	Non-isothermal modelling	225
3.5	Conclusions	233
	NOMENCLATURE	235
	REFERENCES	237



## SUMMARY AND CONCLUSIONS

Multiphase reactors involving gas and liquid reactants, are extensively used in several industrial scale chemical processes. Some of the well known examples are found in oxidation and hydrogenation of organic compounds, hydroprocessing of coal derived and petroleum oils, Fischer-Tropsch synthesis and polymerization reactions. Recently, these reactors have also found applications in the fields of food, biotechnology and pharmaceutical (FBP) engineering, namely in the production of antibiotics and wastewater treatment. The performance of these reactors is dependent on various factors such as gas-liquid, liquid-solid and intraparticle heat and mass transfer, reaction kinetics and mixing of the fluid phases. In the proper design of such a reactor, the contribution of the above steps needs to be incorporated. The reaction engineering of Multiphase Catalytic Reactors has considerably progressed and this subject has been reviewed in books by Ramachandran and Chaudhari (1983) and Shah (1979).

The commonly used multiphase reactors in industry are : bubble column reactors, agitated reactors, trickle bed reactors, packed bed and three phase fluidized bed reactors. For gas-liquid catalytic processes involving homogeneous catalysts, the bubble column reactors are

commonly used. While extensive work on this subject has been done, there is lack of data on real systems involving gas-liquid catalytic (homogeneous) reactions and industrially important hydrogenation reactions in a slurry phase. The aim of the present work was to study the following problems :

- \* Oxidation of ethylene to acetaldehyde using  $\text{PdCl}_2$ - $\text{CuCl}_2$  catalyst system, in a bubble column reactor.
- \* Hydrogenation of m-nitrochlorobenzene (MNCB) to m-chloroaniline (MCA), using Pt/C, catalyst in a stirred slurry reactor.

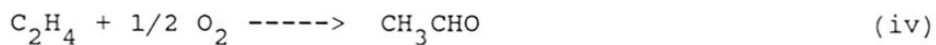
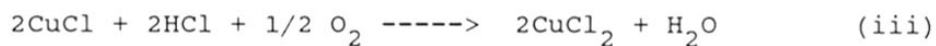
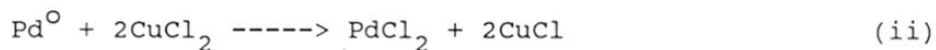
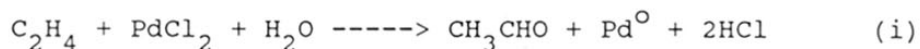
Both these reactions are industrially important and provide good case studies for investigations on the modelling of multiphase reactors. Though, much work has been published so far on the chemistry of Wacker process (Henry, 1964; Jira, 1969), there is little information available, on the reaction engineering aspects of this process under conditions of practical relevance. This system is also interesting as it involves reaction of two gases, namely, ethylene and oxygen, in a liquid and there are only a few experimental studies on such cases (Moiseev, 1970; and Henry, 1980). The second problem on hydrogenation of MNCB is also important industrially and there are no published reports on the kinetics and reaction engineering aspects of this reaction. A brief

summary of the work carried out is presented here :

PART I

MODELLING OF A BUBBLE COLUMN REACTOR : OXIDATION OF  
ETHYLENE TO ACETALDEHYDE USING PdCl<sub>2</sub>-CuCl<sub>2</sub> CATALYST

The liquid phase oxidation of olefins using transition metal complex catalysts to carbonyl compounds is of great industrial significance. These processes involve gas-liquid reactions in the presence of a homogeneous or a heterogeneous catalyst, with continuous flow of reactants and the products. An important example of this class is the liquid phase oxidation of ethylene to acetaldehyde, using a homogeneous, redox type of catalyst system (Smidt et al. 1962). The present work was undertaken with the aim of understanding the reaction engineering aspects of this important reaction. The reaction scheme involved in the Wacker Process is as follows :



The following specific problems were studied :

- \* Performance of a bubble column reactor for oxidation of ethylene to acetaldehyde (Wacker Process) : An experimental and theoretical study.
- \* Critical oxygen concentration for the oxidation of ethylene to acetaldehyde : Comparison of experimental data with the predictions of the model.
- \* Gas hold-up and flow regimes in a bubble column reactor : Role of electrolytes and surfactants.

Chapter 1 presents a general background and literature survey on the oxidation of ethylene to acetaldehyde. A critical review of the various routes for acetaldehyde manufacture and its applications, the catalysts used, kinetic studies, and reaction mechanism has been presented. Generally, liquid-phase oxidation of ethylene to acetaldehyde is carried out using redox type of catalyst consisting of  $\text{PdCl}_2\text{-CuCl}_2$ . More recently, the use of heteropolyacids has been suggested, in place of  $\text{CuCl}_2$ , for regeneration of  $\text{PdCl}_2$  catalyst. The scope of the work on this subject has been outlined.

Chapter 2 presents details of the experimental reactor assembly, the procedure for obtaining reactor performance data and the analysis of reactants and

products. All the experiments were carried out in a single stage bubble column reactor, of 0.05 m diameter and 1.5 m height. This was operated in a semi-batch manner, with respect to the catalyst solution.

Chapter 3 presents the results and discussion on the reactor performance and studies on critical oxygen concentration for ethylene oxidation. Experimental data were obtained in a temperature range of 333-363 K. The effect of superficial gas velocity,  $\text{PdCl}_2$  concentration,  $\text{CuCl}_2$  concentration, ratio of gas phase concentration and temperature on the conversion of ethylene was investigated. The performance equations for the bubble column reactor were developed assuming that i) the gas phase moves in a plug flow manner and the liquid is thoroughly backmixed, ii) the reactions of dissolved  $\text{C}_2\text{H}_4$  and  $\text{O}_2$  occur in the bulk liquid, and the reactions in the film are negligible; iii) isothermal conditions prevail in the reactor; iv) the gas-side mass transfer resistance is negligible; and v) the change in the superficial velocity of the gas phase is considered negligible. The form of rate equation, (based on the earlier kinetics studies (Henry, 1964), considered was :

$$r_A = \frac{k_1 AC_I}{E_2 (E_1 + 2B + E_2)^2} \quad (1)$$

where,

- $k_1$  = rate constant,  $(\text{kmol}/\text{m}^3)^2/\text{s}$   
 $A$  = species A (ethylene) or concentration of ethylene,  $\text{kmol} / \text{m}^3$   
 $C_I$  = initial concentration of  $\text{PdCl}_2$ ,  $\text{kmol}/\text{m}^3$   
 $B$  = concentration of cupric chloride,  $\text{kmol}/\text{m}^3$   
 $E_1$  = concentration of cuprous chloride,  $\text{kmol}/\text{m}^3$   
 $E_2$  = concentration of  $\text{HCl}$ ,  $\text{kmol}/\text{m}^3$

It was observed that the conversion of ethylene ( $X_A$ ) decreased with increase in the linear gas velocity and was found to vary linearly with the catalyst concentration. Kinetic parameters were evaluated using one set of our own experimental data and using these parameters, the performance at other conditions was predicted and compared with the experimental results. The agreement was found to be good showing validity of the model at all temperatures and also the applicability of the kinetics under wider range of conditions.

A study on the critical concentration of oxygen, for ethylene oxidation process was also carried out. Under a given set of operating conditions, the achievable steady state conversion of ethylene will be attained, only if the oxygen concentration at the reactor inlet is higher than a certain level. Below this critical concentration level, the catalytic cycle will not operate leading to a lower efficiency of the reactor. A theoretical analysis has been presented to predict the

critical inlet  $O_2$  concentration, by way of a steady state analysis of the above reactor and also the effect of other process and operating parameters on this important variable has been studied. It was found that the conversion of ethylene decreases with time when the ratio of inlet concentration of oxygen to ethylene ( $\alpha_3$ ) was below 2. In the extreme cases, i.e. when  $\alpha_3 < 0.5$ ,  $X_A$  was very low and Pd black was found to be deposited along the walls of the reactor. For the purpose of obtaining such data, a particular run was carried out for a duration of 4-6 hours and depletion in the catalyst activity was observed over a period of time. Experiments were carried out under different conditions. Experimental results were found to be in good agreement with the theoretical predictions.

Chapter 4 presents a study on the gas hold-up and flow regimes in a bubble column reactor, particularly to investigate the effect of electrolytes and surfactants. A knowledge of these parameters is useful in the scale up and design of reactors. The effect of various system parameters like gas velocity, concentration of electrolytes and surfactants, and temperature, on the gas hold-up and flow regime has been studied. The experimental data were compared with the predictions of various literature correlations. It was found that none of the correlations could predict the increased gas hold-up observed in presence of

electrolytes and surfactants. On careful examination of the models on coalescence of bubbles (Marrucci, 1969; Andrew, 1960; and Sagert and Quinn 1978), it was noticed that one of the important dimensionless group ( $N_{CO}$ ), describing the process of bubble coalescence is defined as :

$$N_{CO} = \frac{Crk^2}{\gamma} \quad (2)$$

where,

$$C = \frac{2c}{RT} \left( \frac{d\gamma}{dc} \right)^2 \quad (3)$$

and

$$k = \left( \frac{12\pi\gamma}{Ar} \right)^{1/3} \quad (4)$$

Based on this theory, the correlation for gas hold-up as proposed by Hikita et al. (1980), was modified as follows

$$\epsilon_g = 1.145 \left( \frac{u_g \mu_L}{\gamma} \right)^{0.578} \left( \frac{\mu_L^4 g}{\rho_L \gamma^3} \right)^{-0.131} \left( \frac{\rho_G}{\rho_L} \right)^{0.062} \times \left( \frac{\mu_G}{\mu_L} \right)^{0.107} \left( \frac{Crk^2}{\gamma} \right)^{0.0917} \quad (5)$$



Since Hikita's correlation represented the data for air-water system at room temperature in the present work satisfactorily, it was used as the basis for modification. The agreement between the predictions by the equation (5) with the experimental data was excellent, indicating the correlation proposed here suitably accounts for the coalescence effect. Similarly, for the gas hold-up data for surfactants, the following correlation was obtained :

$$\epsilon_g = 0.672 \left( \frac{u_g \mu_L}{\gamma} \right)^{0.578} \left( \frac{\mu_L^4 g}{\rho_L \gamma^3} \right)^{-0.131} \left( \frac{\rho_G}{\rho_L} \right)^{0.062} \times \left( \frac{\mu_G}{\mu_L} \right)^{0.107} \times \left( \frac{0.82 Crk^2/\gamma}{1 + 0.154 Crk^2/\gamma} \right) \dots (6)$$

Here also the agreement between the theory and the experimental results was excellent. While both these correlations were tested for the data at room temperature they can be extended to incorporate the effect of temperature and the vapour pressure of the solvent.

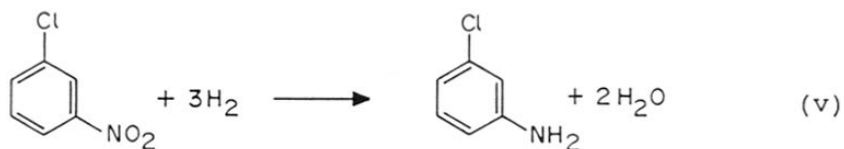
The effect of temperature on flow regime characteristics of a bubble column was studied for air-water, air-aqueous electrolyte and air-aqueous surfactant systems. At lower temperature (303K), the bubble flow

regime was operating over a wide range of gas velocities, while increase in temperature resulted in substantial decrease in the gas velocity  $u_{gT}$ , at which transition from bubble flow to churn turbulent flow occurs. For the solutions of electrolytes and surfactants,  $u_{gT}$  was found to be higher than in the air-water system. Nevertheless,  $u_{gT}$  was found to decrease with temperature even for electrolytes and surfactants.

## PART II

### HYDROGENATION OF m-NITROCHLOROBENZENE TO m- CHLOROANILINE IN A SLURRY REACTOR

Slurry reactors have extensive applications in chemical industries and particularly in the liquid phase catalytic hydrogenation processes. For any specific system of practical importance, a knowledge of the intrinsic kinetics of the reaction is essential, for predicting the reactor performance. In the present work, some of the reaction engineering aspects of an industrially important reaction such as hydrogenation of m-nitrochlorobenzene to m-chloroaniline, in a liquid-phase, using 1% Pt-S/C, was studied.



In Chapter 1, general background of the problem and literature survey on slurry reactors and also the reaction under study, is presented. m-Chloroaniline is used as an intermediate in dyes, drugs and pesticides manufacture. Liquid phase catalytic hydrogenation of halo nitrocompounds is, therefore, a reaction of industrial significance and a three phase slurry reactor is commonly used for this process. It was noted from the literature, that there is hardly any published information on the kinetics of the catalytic hydrogenation of halonitrocompounds and most of the information is in the form of patents. Therefore, it was thought important to study the kinetics of hydrogenation of m-nitrochlorobenzene.

Chapter 2, presents details of the apparatus, experimental procedure and the analysis of reactants and products. The experiments were carried out in a mechanically stirred autoclave, having provisions for gas inlet, sampling, gas vent and automatic temperature control. Hydrogenation experiments were carried out in a temperature range of 313-363 K, and over a  $H_2$  pressure range of  $0.656 \times 10^3$  kPa to  $6.8 \times 10^3$  kPa.

Chapter 3 presents the results and discussion on the kinetics of the hydrogenation of m-nitrochlorobenzene to m-chloroaniline. The effect of catalyst loading,  $H_2$  pressure, concentration of reactants

and products on the rate of hydrogenation as well as the concentration profile in a batch reactor were investigated. The rate was found to be linearly dependent on  $H_2$  pressure, while it was zero order with respect to both substrate as well as the product concentrations. The initial rate data were analyzed for the significance of mass transfer effects. It was found that in the temperature range of 313-333 K, mass transfer effects were unimportant, while at 353 and 363 K, the gas-liquid mass transfer resistance was significant. The initial rate data were fitted to several forms of rate equations, some purely empirical and some Langmuir Hinshelwood type of models. After a rigorous discrimination procedure, the following rate equation was found to represent the rate data satisfactorily :

$$r_A = \frac{wk_1 A^* B_{10}}{1 + K_B B_{10}} \quad (7)$$

where,

- $A^*$  = concentration of hydrogen,  $\text{kmol/m}^3$
- $B_{10}$  = concentration of MNCB,  $\text{kmol/m}^3$
- $k_1$  = rate constant,  $(\text{m}^3/\text{kg}) \cdot (\text{m}^3/\text{kmol} \cdot \text{s})$
- $K_B$  = adsorption equilibrium constant,  $\text{m}^3/\text{kmol}$
- $w$  = catalyst loading,  $\text{kg/m}^3$

The kinetic parameters were evaluated and the activation energy was found to be 30.63 kJ/mol.

In order to verify the applicability of the kinetic model over a wide range of conditions, integral batch reactor data were also obtained at a constant  $H_2$  pressure. Using the rate model proposed earlier, based on the initial rate data, the concentration time behaviour was predicted from the batch reactor model. The experimental and predicted concentration profiles of m-nitrochlorobenzene and m-chloroaniline vs. time, agreed very well, which suggests that the proposed rate model can be reliably used for design and scale-up purposes. Even the results at higher temperatures agreed with model predictions after the gas-liquid mass transfer contribution was incorporated.

Also, a few experiments were carried out under non-isothermal conditions, at different initial temperatures in which  $H_2$  consumption and temperature vs. time profiles were observed. It was found that these data could be well represented by the proposed non-isothermal theoretical model.

## REFERENCES

- 1 Andrew, S.P.S., 'Int. Symp. on distillation', Ed. P.A. Rottenburg, Inst. of Chem. Engrs., London, (1960).
- 2 Henry, P.M., J. Am. Chem. Soc., **86**, 3246, (1964)
- 3 Henry, P.M., "Palladium catalyzed oxidation of Hydrocarbons" D. Reidel Pub. Co. London, (1980).
- 4 Jira, R., "Ethylene and its Industrial Derivatives" Benn, London, (1969).
- 5 Marrucci, G., Chem. Eng. Sci., **24**, (1969), 975.
- 6 Moiseev, I.I., Kinet. Katal., **11** (1970), 342.
- 7 Ramachandran, P.A. and Chaudhari, R.V., "Three Phase Catalytic Reactors", Gordon Breach Sci. Pub. New York, (1983).
- 8 Sagert, N.H., and Quinn, M.J., Chem. Eng. Sci. **33** (1978), 1087.
- 9 Shah, Y.T., "Gas-Liquid-Solid Reactor Design", McGraw-Hill, New York, (1979).
- 10 Smidt, J., Hafner, W., Jira, R., Sedmetier, J., Sieber, R., Ruttenger, R., Kojer, H., Angew. Chem., Int. Ed. Engl., **1** (1962), 80.

**PART I**

**MODELLING OF A BUBBLE COLUMN  
REACTOR : OXIDATION OF ETHYLENE  
TO ACETALDEHYDE USING  
PdCl<sub>2</sub> - CuCl<sub>2</sub> CATALYST**

## **CHAPTER 1**

### **INTRODUCTION AND LITERATURE SURVEY**



## 1.1 GENERAL BACKGROUND

Bubble column reactors are extensively used in industries, both in chemical as well as bio-chemical processes. Some of the important examples are found in homogeneous catalytic gas-liquid reactions, such as, oxidation, carbonylation, hydroformylation and hydrogenation reactions. In these reactors, the gas phase is dispersed through a deep pool of liquid containing either a homogeneous or suspended solid catalyst. The performance of such reactors is strongly dependent on the mixing of gas and liquid phases, mass transfer processes and reaction kinetics. It is important to develop mathematical models which will allow prediction of performance of such reactors incorporating the various complexities associated with multiphase contacting and chemical reactions. Such a study provides a scientific basis for the design of these reactors. While extensive work on the modelling of bubble column reactors has been reported in the literature, there is lack of information on modelling of real systems and particularly, the experimental studies with the aim of verification of the reactor models. The aim of the present work was to undertake an experimental programme on the performance of a bubble column reactor for oxidation of ethylene to acetaldehyde (Wacker Process). Since the Wacker Process is one of the important examples of applications of

bubble column reactors, such a study would be useful from practical considerations. The Wacker Process is a typical example of this, which involves the liquid phase oxidation of ethylene to acetaldehyde using a homogeneous, redox type catalyst system. Acetaldehyde is an important raw material in industrial synthesis of acetic acid, acetic anhydride, cellulose acetate, vinyl acetate resins, acetate esters, pyridine derivatives, crotonaldehyde, terphthalic acid and peracetic acid.

The oxidation of ethylene has been studied by several investigators, in the past (Stern, 1967; Aguilo, 1967; Henry, 1968; Moiseev, 1970), with emphasis on reaction mechanism, product distribution and kinetics. However, the reaction engineering features of this important process have not been investigated earlier. As this process involves simultaneous absorption of two gases (ethylene and oxygen) with a complex catalytic reaction, the role of mass transfer on the efficiency of the process needs to be understood. Also, the catalytic solution is an electrolyte and hence, will have significant influence on both hydrodynamic and mass transfer characteristics of the reactor. There is a need to develop a mathematical model for predicting the bubble column reactor performance incorporating the above effects.

The aim of the present work was to attempt the investigations on reaction engineering aspects of this important process that would be useful in understanding the design aspects of the reactor. It was also the aim of this work to compare the experimental results with theoretical models and bring out the important implications of such a study to the design of the reactors.

The relevant literature on modelling of bubble column reactors as well as the Wacker Process is summarized in the following sections.

## 1.2 LITERATURE SURVEY

### 1.2.1 Bubble Column Reactors

Bubble column reactors are contactors, for gas liquid reactions, in which a continuous gas phase moves in the form of bubbles relative to a continuous liquid phase. In industrial processes, the various modes of operation are practised. These could be single stage or multistage bubble columns operated in a batch or continuous mode with regard to the liquid phase. Continuous bubble column reactors can be operated cocurrently or countercurrently. Some of the major advantages of these reactors over other multiphase contactors are :

66.023(043)  
ROD

TH-667

- Less maintenance, no sealing problem due to the absence of moving parts.
- efficient mass transfer characteristics.
- solids can be handled without significant erosion or plugging problems.
- simple design and hence less expensive.

The performance of bubble column reactor depends on mass transfer, hydrodynamic characteristics and the chemical reaction kinetics. The various aspects concerning design and modelling of these reactors have been reviewed by Mashelkar (1970), Shah et al. (1982), Ramachandran and Chaudhari (1983), and Deckwer (1985).

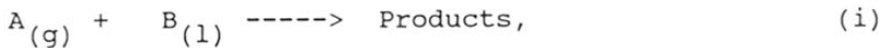
Mathematical models for the performance of bubble column reactors can be developed from different view points. Various authors (Chaudhari and Ramachandran, 1980; Ramachandran and Chaudhari, 1983; Lohse, et al., 1983), have proposed models for bubble column reactors based on the assumption of a backmixed liquid phase. The following situations can be considered in general,

- o Both gas and liquid phases completely backmixed (CSTR).
- o Gas moves in a plug flow manner and liquid is backmixed.
- o Both gas and liquid phases are partially mixed as described by the axial dispersion model.

These situations can be analyzed for both isothermal and non-isothermal conditions. Generally, the bubble column reactors are operated at conditions wherein the liquid phase is nearly backmixed and the gas moves in a plug flow manner. The bubble column reactors are well suited for carrying out reactions in the slow regime of absorption. Due to the high liquid holdup, bubble column reactors provide a large liquid volume, where the reaction can take place. Therefore, in this chapter the models applicable for gas-liquid reactions operating in slow reaction regime will be presented for semibatch mode of operation.

1. Gas and liquid phases completely backmixed

If we consider a gas liquid reaction, of the type,



and assume that the reaction occurs in bulk liquid (slow reaction regime) and isothermal conditions, then the material balance equations for species A and B will be given as ,

$$Q_g (A_{gi}) - (A_{go}) = k_L a V_L (A_{go}/H_A - A_l) \quad (1)$$

$$k_L a (A_{go}/H_A - A_l) = k_1 A_l B_l \quad (2)$$

The conversion of A, can be expressed as,

$$X_A = 1 - \frac{A_{g0}}{A_{gi}} \quad (3)$$

Equations (1) and (2) can be solved for evaluating an unknown  $A_{g0}$  and substituting this in equation (3) the performance equation expression becomes,

$$X_A = \frac{\frac{k_L a V_L}{H_A} \left( \frac{\beta}{\beta + 1} \right)}{\frac{k_L a V_L}{H_A} \left( \frac{\beta}{\beta + 1} \right) + Q_g} \quad (4)$$

where,  $\beta = \frac{k_1 B_1}{k_L a}$  (5)

Another form of performance equation, obtained was

$$r_A = \frac{u_{gi}}{L} A_{gi} X_A \quad (6)$$

where,  $\frac{u_{gi}}{L} = \tau$ , residence time,  $s^{-1}$  (7)

This expression relates in a simple way, the four terms  $X_A$ ,  $r_A$ , residence time ( $\tau$ ) and  $A_{gi}$ ; thus, knowing any three allows the fourth to be found directly. In design then the size of reactor needed for a given extent of conversion is found directly.

2. Gas-phase in plug flow, liquid completely backmixed. In a plug flow reactor the composition of gas varies along the length. For the same stoichiometry, as given in equation (i), the mass balance of gas A as a function of height measured from the point of gas inlet is :

$$-u_g \left[ \frac{dA_g}{dz} \right] = k_L a \left[ \frac{A_g}{H_A} - A_1 \right] \quad (8)$$

For the reactor as a whole the expression (8), upon integration yields,

$$\frac{A_g - H_A A_1}{A_{gi} - H_A A_1} = e^{(-\alpha_A z)} \quad (9)$$

$$\text{Where, } \alpha_A = \frac{k_L a}{u_g H_A} \quad (10)$$

The rate of absorption of gas per unit volume of reactor is :

$$r_A = \frac{H_A Q}{V_L} \left[ 1 - e^{-\alpha_A L} \right] \left[ \frac{A_{gi}}{u_g H_A} - A_1 \right] \quad (11)$$

The rate of reaction is also given as,

$$r_A = k_1 A_1 B_1 \quad (12)$$

Solving these two equations for  $A_1$ , the rate expression

can be given as ,

$$r_A = k_1 B_1 A_{gi} \left[ \frac{L}{u_{gi}} - \frac{k_1 B_1}{1 - e^{-\alpha L}} + H_A \right]^{-1} \quad (13)$$

Similarly, a model considering dispersion of both gas and liquid phases, can be followed (Chaudhari and Ramachandran 1980).

For various practical systems, bubble column reactor models have also been developed, a summary of which is given in Table 1.I.

Goto and Smith (1978) compared the performance of slurry, trickle bed and packed bed reactors for the oxidation of sulfur dioxide. They developed equations to predict the fractional conversion of the gas phase reactant.

Satterfield and Huff (1980), investigated the effect of mass transfer in a bubble column slurry reactor, for F-T synthesis. They derived a reactor model, assuming gas phase in plug flow and liquid and solid phases completely backmixed. This model was different from that of Calderbank et al. (1963), where they assumed that both the liquid and gas phases are in plug-flow. The same reaction (F-T synthesis) was dealt with by Deckwer, et al. (1981a, 1981b), using a reactor model which assumed both gas and liquid phases in plug flow.



Recently, Bukur (1983), studied the effect of model parameters on the prediction of reactor performance for F-T synthesis in a bubble column slurry reactor, considering plug flow of gas and no mixing (PF model) or complete mixing (PM model) in the liquid phase.

Lohse, et al. (1983), proposed a model for the batch catalytic chlorination of toluene in a bubble column reactor, assuming complete backmixing of the liquid phase.

More recently, Jaganathan, et al. (1987) developed a mixing cell model for a continuous bubble column slurry reactor. The system under study was the hydrogenation of butynediol, which showed substrate inhibited kinetics.

In a similar manner, several other models, considering complex kinetics, continuous operation of the liquid phase, mixing cell model and non-isothermal reactions, can be developed. Some aspects of the modelling of bubble column reactor are covered by Deckwer (1985,1986).

In order to predict the performance of bubble column reactors, using these theoretical models, a knowledge of physico-chemical properties, kinetic parameters, hydrodynamics and mass transfer effects is

most essential. While, the kinetics and physico-chemical parameters can be determined experimentally for the system under consideration, the mass transfer and hydrodynamic parameters can be predicted using literature correlations. A summary of such correlation for bubble column reactors is presented by Shah, et al. (1982). While, extensive studies on mass transfer and hydrodynamic behaviour is reported in the literature, the contribution of the system properties ( for electrolytic and organic solutions) has not been incorporated satisfactorily. This is primarily due to lack of understanding of coalescence behaviour of gas bubbles in such systems. Primarily, one requires parameters such as  $k_L a$ , which depends on bubble size, gas hold-up, flow regime, and diffusivity. Therefore, understanding of the effect of system properties on these parameters is important. Since, the reaction system considered in the present work involves electrolytic solution, as a first step it was thought important to study the flow regimes, and gas holdup, in a bubble column reactor. The details of literature on this subject are covered in chapter 4.

TABLE 1.1: STUDIES ON BUBBLE COLUMN REACTOR MODELLING

Str. No.	System studied	Model used	Reference
1.	F - T synthesis	Plug flow for both gas and liquid	Calderbank et al. (1963)
2.	Oxidation of sulfur dioxide		Goto and Smith (1978)
3.	F - T synthesis	Gas in plug flow, liquid completely backmixed	Satterfield and Huff (1980)
4.	F - T synthesis	Gas phase in plug flow, no mixing in the liquid phase	Deckwer et al. (1981)
5.	Chlorination of toluene	Gas in plug flow, liquid backmixed	Lohse et al. (1983)
6.	F - T synthesis	Gas in plug flow, no mixing or complete mixing in the liquid phase	Bukur (1983)
7.	Hydrogenation of butynediol	Mixing cell model, liquid completely backmixed	Jaganathan et al. (1987)

1.2.2 Wacker process

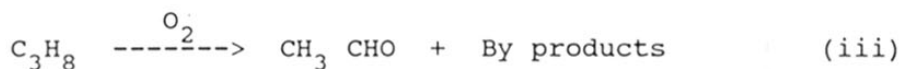
Various commercial routes for the manufacture of acetaldehyde are :

1) Oxidation of Ethyl Alcohol

In this process, vapour phase oxidation of ethyl alcohol, using air is carried out in a temperature range of 450-500°C and at 3atmospheres, over a silver catalyst. (Neelay, 1966).

2) Oxidation of Saturated Hydrocarbon

A catalyst free oxidation of propane or a mixture of propane and butane, at 425-460°C and 7-20 atm. pressure, produces acetaldehyde (Weissermel and Arpe 1978).

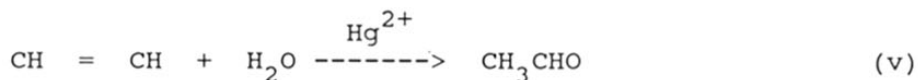
3) Dehydrogenation of Ethyl Alcohol

In this process, a catalytic dehydrogenation of ethyl alcohol, using supported copper or chromium catalyst, in a temperature range of 270-300°C, gives acetaldehyde, (Faith et al., 1957).



#### 4) Hydration of Acetylene

Liquid phase catalytic hydration of acetylene to give acetaldehyde, was a very well known manufacturing process for acetaldehyde in the past (Szoni, 1968).



In this process, a homogeneous catalyst ( $\text{Hg}^{2+}$ ) is used in a temperature range of 70-90°C and under a pressure of 2 atmospheres.

A process involving a direct oxidation of ethylene to acetaldehyde was first developed by Wacker-Chemie and is commonly known as the Wacker process (Smidt, et al., 1959).

Prior to the discovery of this process of oxidation of ethylene, acetaldehyde was manufactured by one or the other routes, described above. A comparison of the various manufacturing routes is presented in Table 1-II. It is clearly seen from this table, that all these processes, except the vapour phase oxidation of hydrocarbons, give very high yields of acetaldehyde. In spite of this, the Wacker process has been preferred in most countries due to a significantly lower net raw

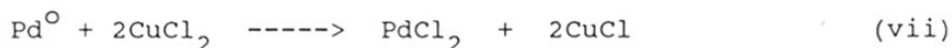
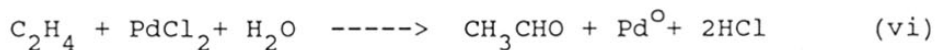
TABLE I.II: MANUFACTURING PROCESSES FOR ACETALDEHYDE\*

Process	Reaction conditions	Catalyst	Per Pass conversion %	Yield %	By products
Oxidation of ethyl alcohol	500°C, 1 atm, vapour phase	Ag or Cu	25 - 35	85 - 95	Acetic acid, ethyl acetate, CO <sub>2</sub> , CH <sub>4</sub>
Oxidation of butane	450°C, 6-7 atm, vapour phase	non-catalytic	25 - 35	90	Aldehydes, ketones, alcohols, acids, CO <sub>2</sub>
Hydration of acetylene	70 - 100°C, 1 atm liquid phase	Hg <sup>2+</sup>	50 - 60	93 - 98	Acetic acid, diacetyl crotonaldehyde
Dehydrogenation of ethyl alcohol	260 - 290°C, 1 atm vapour phase	Cu, Cr	30 - 50	90	H <sub>2</sub> , acetic acid, ethyl acetate, CO <sub>2</sub>
Oxidation of ethylene					
- single stage	100 - 130°C, 3 atm	Pd	75	93 - 95	Acetic acid, CO <sub>2</sub>
- two stage	125 - 130°C, 10 atm	Pd	99.5	93 - 95	Chlorinated aldehydes, crotonaldehyde

\* Aguilo and Penrod (1977)

material cost, low energy consumption and low capital investment factor. (Hagemeyer, 1978).

The direct oxidation of ethylene to acetaldehyde (Smidt, et al. 1959) was a technological breakthrough for Wacker-Chemie, and the process was later known as the Wacker Process. The first commercial plant for acetaldehyde, based on Wacker process was built in Europe, in 1960 (Jira, 1969). The reaction scheme involved is :



The overall reaction is a combination of three stoichiometric reactions, known individually since long (Smidt et al. 1959). In the process,  $\text{PdCl}_2$  is required in catalytic quantities, which is reduced to  $\text{Pd}^0$ , and then reoxidized insitu to  $\text{Pd}^{\text{II}}$  by  $\text{CuCl}_2$  which in turn gets regenerated with oxygen and the catalytic cycle is completed. This series of oxidation-reduction reactions, keeps the catalyst always in the active form thus the life of the catalyst would be practically indefinite.

In the one stage process, ethylene together with oxygen is fed to the reactor, thus allowing all the reactions, to take place simultaneously, keeping the catalyst composition constant. Depending on the reaction conditions, such as temperature, ethylene and oxygen partial pressures and initial catalyst composition, a steady state is achieved, which is characterized by the fact that reaction and regeneration (oxidation) proceed at appropriate rates to give high productivity of acetaldehyde. For a single stage operation, low oxygen concentration is used in order to avoid the explosion hazards of the ethylene-oxygen mixture. Therefore, in this operation, higher Cl/Cu ratio is required so that even at low oxygen concentration, Pd metal does not precipitate. The pH of the solution is carefully maintained in a range of 1.5 - 2.0 so that, copper oxychloride precipitation is avoided. Ethylene conversion in a single stage process is about 75% (Morse, 1967) therefore, a gas recycle is necessary, for which the gas-liquid separator is provided and the catalyst solution is fed back to the reactor by gravity flow. The vapours from the gas-liquid separator are condensed and then scrubbed with water, which has acetaldehyde concentration of about 9 wt% . This is then subjected to distillation, where methyl and ethyl chlorides and crotonaldehyde are removed and pure acetaldehyde is recovered.



In the two stage process, ethylene and oxygen (air) are fed to two separate reactors. Almost complete conversion of ethylene is achievable in one pass, and since no recycle is required, air can be used for the oxidation of cuprous chloride. Acetaldehyde formed in the first reactor is removed by flashing and the catalyst solution is recycled to the second reactor for regeneration.

Advantages of two stage over the one stage process are: 1) Since ethylene and air are reacted separately in two different reactors, the operation is more safe 2) Due to complete conversion of ethylene, no gas recycle is required and ethylene feed can tolerate some inerts 3) Less liquid effluent 4) Use of air as oxidant is possible.

Advantages of the one stage over the two stage process are : 1) Catalyst solution stays in one reactor thereby avoiding expensive liquid circulation equipment and minimizing catalyst losses, 2) Less byproduct formation 3) Lower operating pressure 4) Lower volume of vent gases 5) Liquid effluent may be biologically treated due to higher dilution of chlorinated acetaldehydes and 6) Lower investment costs.

Since, both variations offer advantages and disadvantages, both the one and two-stage reactors are in

operation for the manufacture of acetaldehyde.

The main drawback of the Wacker Process, is that the catalyst solution is highly corrosive, therefore, titanium or brick-lined equipment has to be used, which poses difficulties in fabrication. An alternative involves the use of heteropolyacids as oxidizing agents, in place of copper chloride (Kozheinikov and Matveev, 1983). Matveev (1977), has discussed the kinetics and mechanism of oxidation of ethylene in the presence of halide-free catalysts based on heteropolyacids.

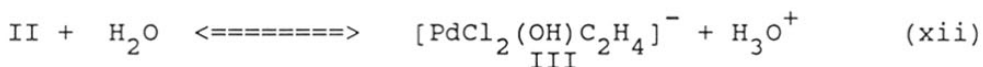
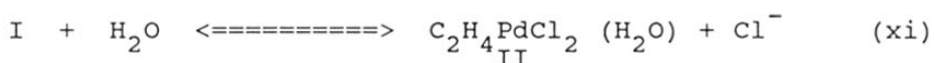
#### 1.2.2.1 Kinetics and mechanism

Both theoretical and experimental studies on Wacker process have been reported in the literature. The kinetics of oxidation of olefins using Pd complex catalysts, has been extensively studied and the relevant literature has been reviewed by Maitlis (1971) and Henry (1980). Oxidation of ethylene, (Wacker Process) using Pd catalysts, has also been studied by several investigators and a summary of kinetic studies and rate equations proposed is presented in Table 1.III.

One of the early reports on the kinetics of oxidation of ethylene was by Vargaftic (1962) and Teramoto (1963). They observed that oxidation of ethylene using homogeneous Pd-Fe catalyst, is first order with

ethylene and Pd ion concentration and inhibited by  $\text{Cl}^-$  and  $\text{H}^+$  ions.

Henry (1964), investigated the kinetics of this reaction in detail, at  $25^\circ\text{C}$ , and 1 atmosphere pressure. The following reaction mechanism was proposed :



Based on the rate data, Henry (1964, 1972) proposed the following rate equation; which is consistent with the mechanism in steps (x - xiv) :

$$\frac{-d[\text{C}_2\text{H}_4]}{dt} = \frac{k' K [\text{PdCl}_4^{2-}] [\text{C}_2\text{H}_4]}{[\text{Cl}^-]^2 [\text{H}^+]} \quad (14)$$

As expected, the rate increased linearly with increase in ethylene and Pd ion concentrations. With  $\text{H}^+$  and  $\text{Cl}^-$  ions, however, a substrate inhibition was observed.

Subsequently, Moiseev, et al. (1966, 1974), proposed a reaction mechanism in which a bimolecular complex of palladium,  $\text{PdCl}_6^{2-}$ , is formed. They proposed the following rate equation :

$$\frac{-d[\text{C}_2\text{H}_4]}{dt} = \frac{k_1[\text{PdCl}_4^{2-}][\text{C}_2\text{H}_4]}{[\text{H}^+][\text{Cl}^-]^2} + \frac{k_2[\text{PdCl}_4^{2-}]^2[\text{C}_2\text{H}_4]}{[\text{H}^+] + [\text{Cl}^-]^3} \quad (15)$$

From the literature reports [see Table 1.III] it can be noted that most of the kinetic and mechanistic studies, have been carried out at room temperature and atmospheric pressure. There is practically no information available on the kinetics in the range of temperatures of practical interest. A modified rate equation, for the oxidation of ethylene, covering the higher temperature range (upto  $90^\circ\text{C}$ ) has also been proposed (Grover 1984) :

$$r_A = \frac{k[\text{PdCl}_2]^m[\text{CuCl}_2]^n[\text{A}^*]}{1 + [k(\text{PdCl}_2)^m(\text{CuCl})^n(k_{La})^{-1}]} \quad (16)$$

Equation (16) was found to represent the rate data at all conditions satisfactorily. It was pointed out that under certain conditions, mass transfer limitations become significant, however, no attempts to develop a

TABLE 1. III : A SUMMARY OF THE KINETICS OF ETHYLENE TO ACETALDEHYDE

Sr. No.	Catalyst System	Reaction Conditions	Rate Equation	Reference
1.	Pd/Cl <sub>2</sub> , p-benzoquinone HClO <sub>4</sub>	25°C Pd(II) < 0.005 mol/l	$r \propto \frac{1}{(Cl^-)^2}$	Moiseev et. al. (1963).
2.	PdCl <sub>2</sub> , p-benzoquinone, HClO <sub>4</sub>	25°C Pd(II) < 0.005 m/l	$r \propto \frac{[PdCl_4]^{2-} [C_2H_4]}{[H^+]}$	Vargafik et.al (1963).
3.	PdCl <sub>2</sub> , HClO <sub>4</sub> - NaClO <sub>4</sub>	25°C No added chloride	$r \propto [PdCl_4]^{2-}$	Vargafik et.al. (1963).
4.	PdCl <sub>2</sub> , HClO <sub>4</sub> - NaClO <sub>4</sub> LiCl - Li ClO <sub>4</sub>	25°C Pd(II) = 0.01-0.2 mol/l I = 4	$r \propto \frac{[PdCl_4]^{2-} [C_2H_4]}{[Cl^-]^2 [H^+]}$	Henry (1964)

5.  $\text{PdCl}_2$ , p-benzoquinone  
 $25^\circ\text{C}$   
 very low  $\text{Cl}^-$  and  $\text{H}^+$   $r \propto$   $\frac{[\text{Pd}] [\text{C}_2\text{H}_4] [\text{H}^+ [\text{Cl}^-]]}{[\text{C}_2\text{H}_4] + [\text{H}^+ [\text{Cl}^-]^3]}$  Jira (1966)
- 
6.  $\text{PdCl}_2$ , p-benzoquinone  
 $\text{LiCl} - \text{LiClO}_4$   
 $25^\circ\text{C}$   
 $\text{Pd(II)} = 0.01-0.2$  mol/l  $r \propto$   $\frac{[\text{PdCl}_4]^{2-} [\text{C}_2\text{H}_4]}{[\text{Cl}^-]^2 [\text{H}^+]}$  Moiseev et.al (1966, 1974).  
 $I = 1.1-4$
- $\frac{[\text{PdCl}_4]^{2-}]^2 [\text{C}_2\text{H}_4]}{[\text{Cl}^-]^3 [\text{H}^+]}$
- 
7.  $\text{PdCl}_2$ , p-benzoquinone  
 $\text{NaClO}_4 - \text{HClO}_4$   
 $25^\circ\text{C}$   
 $\text{Pd(II)} = 0.01-0.2$  mol/l  $r \propto$   $\frac{[\text{PdCl}_4]^{2-}] [\text{C}_2\text{H}_4]}{[\text{Cl}^-]^2 [\text{H}^+]}$  Henry (1972).  
 $I = 2$

mathematical model for the reactor for Wacker Process, has been made so far.

### 1.3 SCOPE AND OBJECTIVE

The literature review on oxidation of ethylene, indicates that further work on reaction engineering aspects of the bubble column reactor, have not been done. Therefore, the aim of the present work was to study the following problems relevant to the Wacker Process.

1. Development of a mathematical model for the conversion of ethylene to acetaldehyde in a bubble column reactor.
2. Critical oxygen concentration at the inlet of the reactor, to ensure that the catalytic system does not deactivate.
3. Experimental studies on conversion in a bubble column reactor, to understand the effect of different parameters involved.
4. Gas hold-up and flow regimes in a bubble column reactor. Effect of surfactants and electrolytes on the gas hold-up.

Such a study would be extremely useful, in understanding the reaction engineering of the Wacker Process.

## REFERENCES

1. Aguilo, A., *Adv. Organomet. Chem.*, **5** (1967), 321.
2. Aguilo, A., and Penrod, J.D., 'Encyclopedia of Chem. Proc. Design', Vol. 1, Eds. J.J.Macketta and W.A. Cunningham, Marcel Dekker, Inc. New York (1977).
3. Bukur, D.B., *Chem. Eng. Sci.*, **38**, (1985), 441.
4. Calderbank, P., Eraus, F., Forby, R., Jepson, G., and Poll, A., 'Catalysis in Practice', Symp. Proceed. (Inst. Chem. Engrs.), (1963).
5. Chaudhari, R.V. and Ramachandran, P.A., *AIChE J*; **26** (1980), 177.
6. Deckwer, W.D., Serpemen, Y, Raleck, M. and Schmidt, B., *Chem. Eng. Sci.*, **36** (1981 a), 765.
7. Deckwer, W.D., Serpemen, Y, Raleck, M. and Schmidt, B., *Chem. Eng. Sci.*, **36** (1981 b), 791.
8. Deckwer, W.D., 'Reaktionstechnik in Blassensaulen', Salle Sawerlander, Frankfurt, (1985).
9. Deckwer, W.D., NATO ASI Series, E Appl. Sci No. 110, Ed. H.I.de Lasa, Martinus Nijhoff Pub. Netherlands, (1986), 411.
10. Evin, A.B., Rab, J.A., and Kasai, P.H., *J. Catal.*, **30** (1973), 109.
11. Faith, W.I., Keyes, D.B. and Clerk, R.L., 'Industrial Chemicals', 2nd ed., John Wiley and Sons Inc., New York, (1957).



12. Fujimoto, K., Negami, Y., and Kunugi, T., *Kogyo Kagaku Zasshi*, **73** (1970), 1822.
13. Fujimoto, K., Negami, Y., Takahashi, T. and Kunugi, T., *Ind. Eng. Chem. Prod. Res. Des. Dev.*, **11** (1972), 303.
14. Goto, S., and Smith, J.M., *AIChE J.* **24**, (1978), 286.
15. Grover, G.S., 'Studies in Transition Metal Complex Catalyzed Reactions : Oxidation of Olefins', Ph. D. Thesis, University of Pune, Pune, India (1984).
16. Hagemeyer, H.J., Kirk - Othmer, *Encycl. Chem. Tech.*, 3rd Ed., John Wiley & Sons Inc., New York, Vol.1 (1978).
17. Henry, P.M., *J. Am. Chem. Soc.*, **86** (1964), 3246.
18. Henry, P.M., *J. Am. Chem. Soc.*, **88** (1968), 1595.
19. Henry, P.M., *Adv. Chem. Ser.*, **70** (1968), 126.
20. Henry, P.M., *J. Am. Chem. Soc.*, **94** (1972), 4437.
21. Henry, P.M., 'Palladium Catalysed Oxidation of Hydrocarbons' D. Reidel Pub. Co., London, (1980).
22. Jaganathan, R., Gholap, R.V., Brahme, P.H. and Chaudhari, R.V., 'Recent Trends in Chemical Reaction Engineering II, Wiley Eastern, (1987), 141.
23. Jira, R., Sedlmeir, J. and Smidt, J., *Ann. Chem.*, **693**, (1966), 99.
24. Jira, R., 'Ethylene and its Industrial Derivatives', Benn, London, (1969).
25. Joshi, J.B., and Shah, Y.T., *Chem. Eng. Commun.* **11** (1981), 165.

26. Kozhevnikov, I.V. and Matveev, K.I., *App. Cat.*, **5**, (1983), 135.
27. Lohse, M., Alper, E. and Deckwer, W.D., *Chem. Eng. Sci.*, **38**, (1983), 1399.
28. Maitlis, P.M., 'The Organic Chemistry of Palladium', Vol. II, Academic Press, New York, (1971).
29. Mashelkar, R.A., *Brit. Chem. Eng.*, **15** (10), (1970), 1297.
30. Matveev, K.I., *Kinet. Katal. Engl. Tran.* **18** (1977), 716.
31. Moiseev, I.I., Vargaftik, M.N. and Syrkin, Ya.K., *Dokl. Akad. Nauk. SSSR*, **153** (1963), 140.
32. Moiseev, I.I., Vargaftik, M.N., Pestrikov, S.V., Levenda, O.G., Romanova, I.N. and Syrkin, Ya. K., *Dokl. Akad. Nauk. SSSR*, **171**, (1966), 1365.
33. Moiseev, I.I., *Kinet. Katal.*, **11** (1970), 342.
34. Moiseev, I.I., Levenda, O.G. and Vargaftik, M.N., *J. Am. Chem. Soc.*, **96** (1974), 1003.
35. Morse, P.L., 'Acetaldehyde', Stanford Research Institute Process Economic Program Report No. 24, 1967, California.
36. Neelay, S.D., U.S. Patent, 3, 284, 170 (1966).
37. Ramachandran, P.A. and Chaudhari, R.V., 'Three Phase Catalytic Reactors', Gordon Breach Science Publishers, New York, (1983).
38. Satterfield, C.N. and Huff, Jr., G.A., *Chem. Eng. Sci.*, **35**, (1980), 195.

39. Shah, Y.T., Kelkar, B.G., Gadbole, S.P., and Deckwer, W.D., *AIChE J.*, **28** (1982), 353.
40. Smidt, J., Hafner, W., Jira, R., Sedlmetier, J., Sieber, R., Ruttenger, R., and Kojer, H., *Angew. Chem.*, **71**, (1959), 176.
41. Stern, E.W., *Catal. Rev.*, **1** (1967), 73.
42. Szoni, G., *Adv. Chem. Ser.*, **70** (1968), 53.
43. Vargaftik, M.N., Moiseev, I.I. and Syrkin, Ya. K., *Izv. Akad. Nauk. SSSR*, (1963), 1147.
44. Weissermel, K., and Arpe, H.J., 'Industrial Organic Chemistry', Verlag Chemie, New York (1978).

## **CHAPTER 2**

### **EXPERIMENTAL**

## 2.1. MATERIALS

Palladium chloride ( $\text{PdCl}_2$ ) was obtained from M/s Arora Matthey Ltd., India, with palladium content equal to 60% Cupric chloride dihydrate ( $\text{CuCl}_2 \cdot 2\text{H}_2\text{O}$ ) was supplied by M/s. Sarabhai Merck, India. Ethylene ( $\text{C}_2\text{H}_4$ ) gas was prepared and compressed in our own laboratory (NCL, Pune, India), with a purity of  $> 99.8\%$ . Oxygen was used from cylinders supplied by Indian Oxygen Limited, Bombay.

Since, palladium chloride was not readily soluble in distilled water, first the desired amount of copper chloride was dissolved in distilled water, the resulting solution had a  $\text{pH} = 1.8 - 1.9$ . Then the weighed amount of  $\text{PdCl}_2$  was added to this solution and the mixture was kept under magnetic stirring at about  $45^\circ\text{C}$ , to make sure that all  $\text{PdCl}_2$  was dissolved.

## 2.2 REACTOR

All the experiments were carried out in a single stage bubble column reactor, operated in a semi-batch manner. A schematic diagram of a typical experimental reactor assembly is shown in figure 2.1. The reactor consisted of a 0.05 m. diameter and 1.50 m. high glass column with an outer jacket, for circulation of water at the desired temperature. The reactor was provided with a

sintered disc at the bottom, as a gas sparging device, having an average hole diameter, in the range of 100-120  $\mu$ m. The gas flow rates were monitored using precalibrated gas rotameters. A provision was also made for sampling the gas and liquid from the reactor for analysis.

### 2.3 EXPERIMENTAL PROCEDURE

In a typical oxidation experiment, the catalyst solution containing known quantities of  $\text{PdCl}_2$  and  $\text{CuCl}_2$ , was charged into the reactor and the reaction mixture was heated to the desired temperature by circulating hot water through the outer jacket, using a thermostat. The premixed gases, (within safety limits of operations) ethylene and oxygen with desired composition were introduced into the reactor, in a continuous manner.

The vapours of water and acetaldehyde along with unreacted gases were passed through a coil condenser, maintained at  $1^\circ\text{C}$ , temperature, using a cryostat. The condensate was collected after every hour. The unreacted gases were scrubbed with water to remove any leftover acetaldehyde. The scrubber solution was changed after every hour and samples were taken for analysis, alongwith the sample of condensate. It was made sure that no trace of acetaldehyde is present in the outlet gas stream after passing through the absorbers. The flow of outlet gas

stream was also measured by a calibrated rotameter and was also analyzed for ethylene content using an orsat apparatus by absorbing it in bromine water solution.

In every experiment, the productivity of acetaldehyde was observed over a period of four hours, after attaining a steady state. All the experiments were carried out, with a large excess of oxygen than that required by stoichiometry. It was observed that after the first hour of the run, the amount of acetaldehyde formed remains constant over a period of time, which indicated that steady state has been achieved. A typical plot of productivity vs. time is presented in Figure 2.2.

#### 2.4 ANALYSIS

It was observed that the quantitative estimation of acetaldehyde, using gas chromatographic method was not reproducible. This might be due to the fact that acetaldehyde is a very volatile compound (b.p. =  $20.8^{\circ}\text{C}$ ) and also very reactive. Therefore, quantitative analysis of acetaldehyde was carried out using sodium sulfite method (Wilson and Wilson 1960). Acetaldehyde samples from condensate and from the scrubbers were taken in stoppered flasks, and the analysis was carried out at temperature  $< 10^{\circ}\text{C}$ , thereby ensuring that there is practically no loss of acetaldehyde by evaporation.

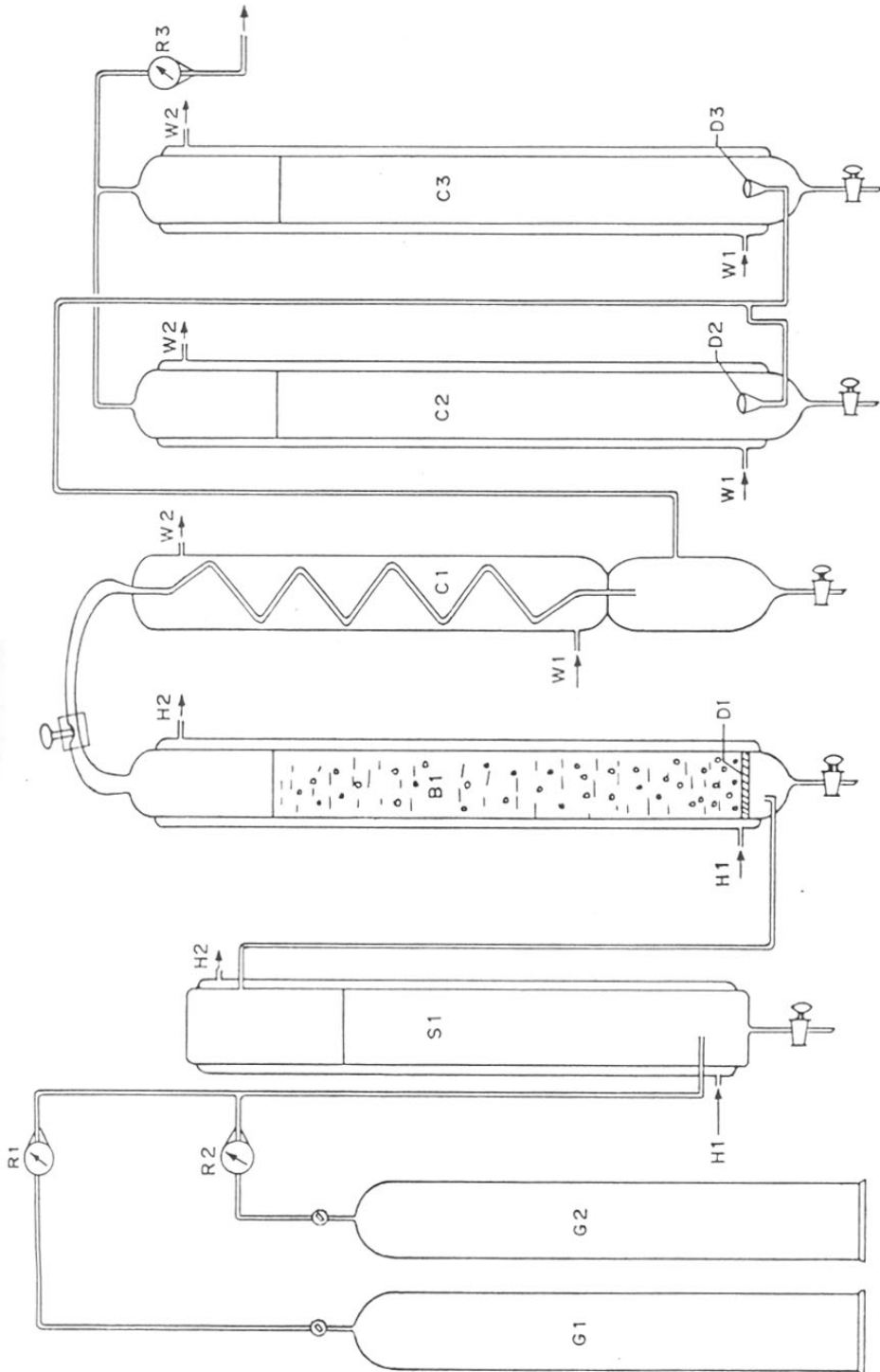


FIGURE 2-1: EXPERIMENTAL SET UP

G1-ETHYLENE CYLINDER, G2-OXYGEN CYLINDER, R1-ROTAMETER FOR ETHYLENE, R2-ROTAMETER FOR OXYGEN, R3-ROTAMETER FOR OUTLET GAS, W1-WATER INLET, W2-WATER OUTLET, S1-PRESATURATOR B1-BUBBLE COLUMN REACTOR, D1-D3-SINTERED DISCS, C1-COIL CONDENSER, C2-C3-ABSORBERS, H1-HOT WATER IN, H2-HOT WATER OUT



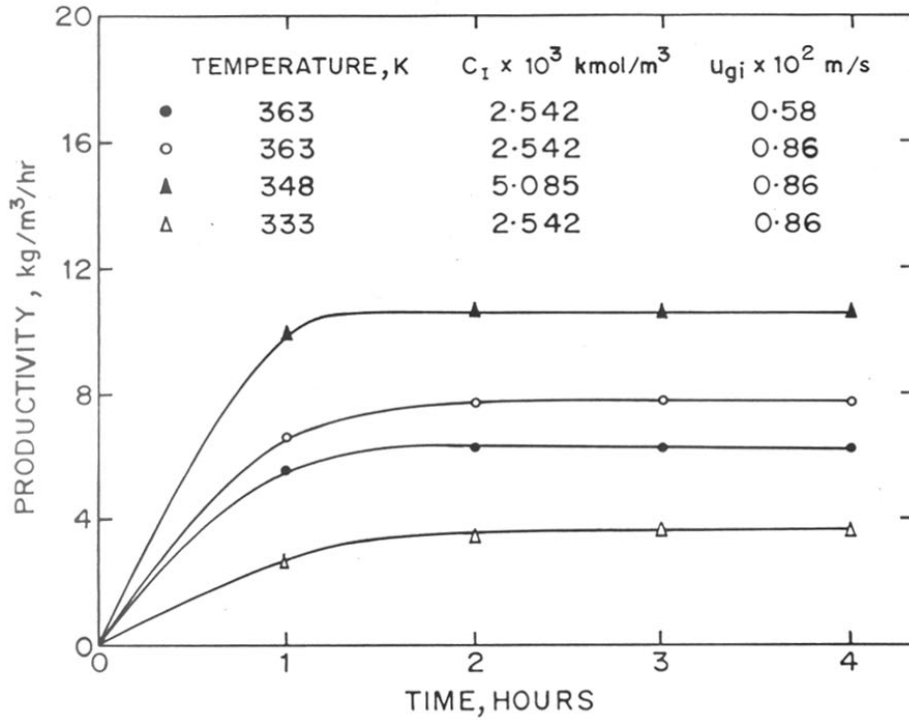


FIGURE 2.2: PRODUCTIVITY Vs TIME PLOTS AT VARIOUS CONDITIONS  
 $[B_{l1} = 0.253 \text{ kmol/m}^3]$

## CHAPTER 3

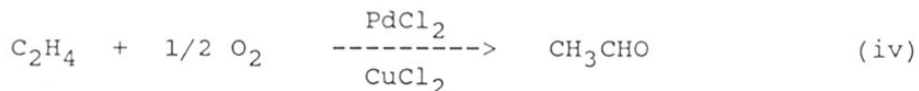
### RESULTS AND DISCUSSION

## 3.1 THEORETICAL MODEL

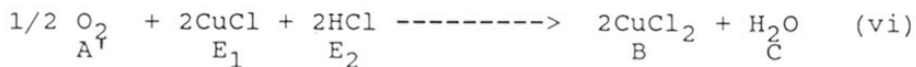
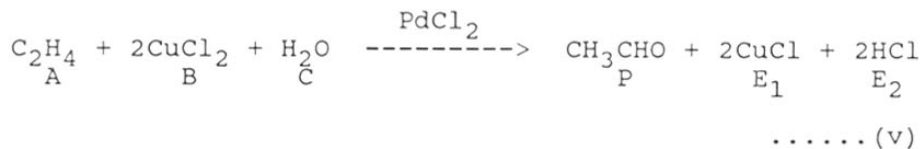
The liquid phase oxidation of ethylene in the presence of PdCl<sub>2</sub>-CuCl<sub>2</sub> catalyst system is described by following reactions ( Smidt et al., 1962 ) :



net reaction :



In practice, this process is carried out such that the concentration of CuCl<sub>2</sub> is several times in excess of PdCl<sub>2</sub>, and therefore, for the purpose of the present study, the reaction scheme was simplified as follows:



The kinetics of both ethylene oxidation to acetaldehyde and the oxidation of cuprous chloride to cupric chloride has been studied previously. The following rate equations have been proposed:

Oxidation of ethylene ( Henry, 1964)

$$r_A = \frac{k_1 A C_I}{E_2 ( E_1 + 2B + E_2 )^2} \quad (1)$$

Here,  $E_1$  and  $E_2$  can be represented in terms of the initial concentrations of  $H^+$  ion ( $E_{2I}$ ) and  $CuCl_2$  ( $B_{1I}$ ) as follows :

$$E_1 = B_{1I} - B_1 \quad (2)$$

$$E_2 = E_{2I} + B_{1I} - B_1 \quad (3)$$

Oxidation of cuprous chloride (Jhaveri and Sharma, 1967)

$$r_{A'} = k_2 A' E_1^2 \quad (4)$$

Following assumptions have been made in the theoretical analysis: (i) the gas phase moves in plug flow and the liquid phase is completely backmixed; (ii) the reactions of dissolved  $C_2H_4$  and  $O_2$  occur in the bulk liquid and the reactions in the film are negligible; (iii) the gas side mass transfer resistance is negligible; (iv) isothermal conditions prevail in the

reactor; and (v) the change in the superficial velocity of the gas phase is considered negligible.

In general, the assumption (v) may appear questionable at the first sight. However, this is expected to be valid in view of the large excess of oxygen in the feed compared to ethylene. Also, this has been verified by solving numerically the full set of mass balance equations along with the equation accounting for the velocity change. The computation clearly showed that the velocity change under the conditions of the present study would be negligible. This would afford a great simplification in the model and as would be demonstrated by comparison with the experimental data, the assumption has been fully justified.

For a semibatch, bubble column reactor operating under steady state conditions, the material balances for the reactant species are given by the following equations:

gas phase

$$- u_g \frac{dA_g}{dx} = k_L a ( A_g/H_A - A_l ) \quad (5)$$

$$- u_g \frac{dA'_g}{dx} = k_L a ( A'_g/H_{A'} - A'_l ) \quad (6)$$

The column inlet conditions provide the necessary initial conditions for the differential equations (5) and (6), as follows :

$$x = 0, A_g = A_{gi}, A'_g = A'_{gi} \quad (7)$$

liquid phase

$$\frac{1}{L} \int k_L a (A_g/H_A - A_l) dx = \frac{k_1 C_I A_1}{(2B_{1I} + E_{2I})^2 (E_{2I} + B_{1I} - B_1)} \dots \dots \dots (8)$$

and

$$\frac{1}{L} \int k_L a (A'_g/H_{A'} - A'_l) dx = k_2 (B_{1I} - B_1)^2 A'_l \quad (9)$$

Under steady state conditions, the material balances of other liquid phase components lead to the following relationships:

$$\frac{2 k_1 C_I A_1}{(2B_{1I} + E_{2I})^2 (E_{2I} + B_{1I} - B_1)} = 4 k_2 (B_{1I} - B_1)^2 A'_l \quad (10)$$

The above set of equations can be analytically solved to give the following equation for the steady state concentration of the cupric chloride in terms of dimensionless quantities defined in the nomenclature:

$$1 + \frac{(1 - e^{-\alpha' 4}) / \alpha_4}{K_2(1 - b_1)^2} - 2\alpha_3 \left[ \frac{1 - e^{-\alpha' 4}}{1 - e^{-\alpha 4}} \right] * \quad (11)$$

$$\left[ 1 + \frac{(1 - e^{-\alpha 4}) / \alpha_4}{\alpha_1 / (1 + e_I - b_1)} \right] \quad (11)$$

The dimensionless ethylene and oxygen concentrations in the liquid phase are given by :

$$a_1 = \frac{(1 - e^{-\alpha 4}) / \alpha_4}{(1 - e^{-\alpha 4}) / \alpha_4 + \alpha_1 / (1 + e_I - b_1)} \quad (12)$$

$$a'_1 = \frac{(1 - e^{-\alpha' 4}) / \alpha'_4}{(1 - e^{-\alpha' 4}) / \alpha'_4 + K_2(1 - b_1)^2} \quad (13)$$

The conversion of ethylene and oxygen are given by

$$X_A = (1 - e^{-\alpha 4}) (1 - a_1) \quad (14)$$

$$X_{A'} = (1 - e^{-\alpha'4}) (1 - a'1) \quad (15)$$

It is to be noted, however, that since in the Wacker process, the stoichiometry of the overall reaction ( reaction iv) is maintained under steady state,  $X_A$  and  $X'_{A'}$  are related as :

$$X_A = 2 \alpha_3 X_{A'} \quad (16)$$

Where,  $\alpha_3$  is the ratio of the concentration of oxygen to that of ethylene in the inlet gas phase.

Thus, for a given set of operating conditions, parameters,  $\alpha_3$ ,  $\alpha_4$ ,  $\alpha'_4$ ,  $\alpha_1$ ,  $K_2$  and  $e_I$  get fixed. Equation (11) is then solved for  $b_1$ . Equations (12), (13), (14) and (15) are then used to determine  $X_A$  and  $X_{A'}$ . In all the cases under study, the computed conversions of ethylene and oxygen bear the relationship given by equation (16) indicating the soundness of the calculation procedure.

### 3.2 PARAMETER ESTIMATION

The use of model equations developed here for the purpose of interpreting the experimental data requires a knowledge of various parameters such as, the physicochemical properties, the intrinsic kinetic constants and the hydrodynamic and mass transfer



parameters. The simulation of the reactor behaviour is therefore strongly dependent on the reliability of these parameters. The details of the parameter estimation is discussed below.

For the present system, the solubility data for ethylene and oxygen in water were obtained from the literature (Wilhelm et al., 1977; and Siedel, 1940). However, the solubility of a gas in a pure solvent is different from that in the presence of an electrolyte in this case,  $\text{CuCl}_2$ , (Long and McDevit, 1952; and Konnik, 1977). A semitheoretical approach suggested by van Krevelen and Hoftizer (1948) was adopted to correct the solubility data for the presence of electrolytes using the following relationship :

$$\log \frac{H_e}{H_e'} = h \cdot I \quad (17)$$

where,  $H_e$  and  $H_e'$  represent the Henry's law coefficient in electrolyte solution and pure solvent respectively and  $I$  is the ionic strength of the solution, given as :

$$I = 1/2 \sum c_i z_i^2 \quad (18)$$

where,  $c_i$  is the concentration of the ions with a valency of  $z_i$ . The salting coefficient  $h$  in the equation is the sum of contributions referring to the species of the gas  $h_G$ , and to the species of the positive and negative ions

present,

$$h = h_G + h_+ + h_- \quad (19)$$

The values of these are given by Onda, et al., (1970). Using this correlation, the solubility of ethylene and oxygen in water was corrected for the presence of  $\text{CuCl}_2$  at different concentrations and the results are given in Table 3.I.

The intrinsic kinetics of oxidation of ethylene to acetaldehyde has been the subject of many investigations (Vargaftik et.al. 1963; Henry 1964; Jira 1969 and Moiseev et al. 1974) in the past. However, most of these studies were carried out at  $25^\circ\text{C}$  and precise values of the rate constants under the conditions of the present work ( $60-90^\circ\text{C}$ ) were not available. These were estimated by simulation of the experimental data as described later.

The reaction rate parameters for the oxidation of cuprous chloride to cupric chloride were reported by Jhaveri and Sharma (1967) and the same were used in this work.

It was also necessary to have a correct value of the gas-liquid mass transfer coefficient ( $k_L a$ ), since this is an important parameter in the reactor modelling. An attempt was made to fit the experimental data by using the values of rate constants reported earlier and the

TABLE 3.1: SOLUBILITY OF ETHYLENE AND OXYGEN IN AQUEOUS CUPRIC CHLORIDE SOLUTION

Temperature K	Concentration of $\text{CuCl}_2$ M	Solubility of ethylene, $\times 10^3$ $\text{kmol} / \text{m}^3 \text{ atm}$	Solubility of oxygen $\times 10^4$ $\text{kmol} / \text{m}^3 \text{ atm}$
333	0.253	2.41	5.03
	0.440	2.13	3.36
	0.600	1.93	2.52
348	0.253	1.901	4.62
	0.440	1.678	3.08
	0.600	1.51	1.95
363	0.253	1.352	4.44
	0.440	1.193	2.96
	0.600	0.987	1.94

values of  $k_{L}a$  obtained by various correlations reported in the literature (Akita and Yoshida 1973; Deckwer et.al. 1974; and Kastaneck 1977). It was found that the match between the predicted values of ethylene conversions and those experimentally observed was not satisfactory (see Figure 3.1). Therefore a part of our own experimental data was used to estimate the values of  $k_1$  and  $k_{L}a$  by the following procedure.

For a given temperature and the gas velocity  $u_{gi}$ , the reactor model given earlier was used to predict the ethylene conversion in the reactor and the values of  $k_1$  and  $k_{L}a$  were estimated so that the predicted and the experimentally observed conversion values matched closely. For the same  $u_{gi}$ , the reaction rate constant ( $k_1$ ) at two other temperatures were estimated by simulating the experimental data at those temperatures. For this purpose, the values of  $k_{L}a$  estimated at the earlier temperature was used, after correcting for the temperature changes, as follows :

$$\frac{(k_{L}a)_2}{(k_{L}a)_1} = \sqrt{\frac{T_2}{T_1}} \quad (20)$$

The parameter  $k_{L}a$  is also a function of  $u_g$  and the dependence of  $u_g$  in most cases is observed as (Deckwer et al., 1974).

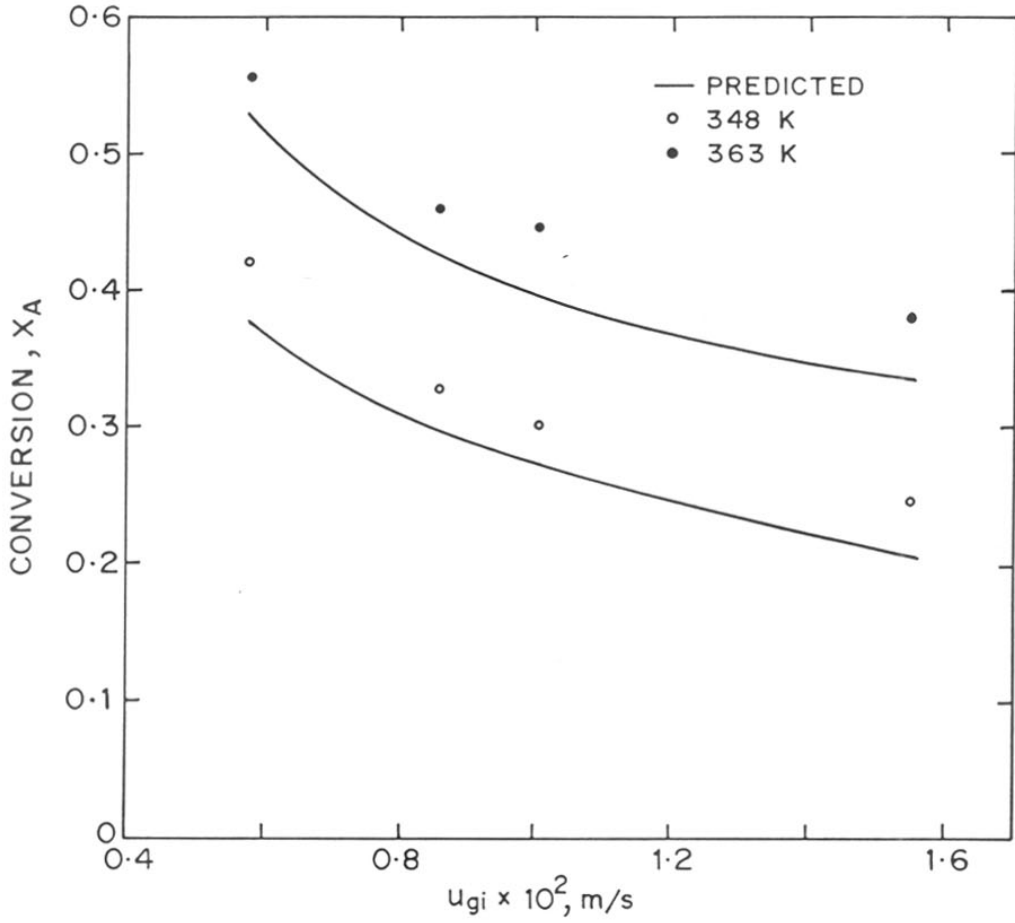


FIGURE 3-1: COMPARISON OF MODEL PREDICTIONS WITH EXPERIMENTAL DATA [USING LITERATURE VALUES OF  $k_1$  AND  $k_L a$ ]

$$k_{L}a = bu_{g}^{n} \quad (21)$$

Since,  $k_{L}a$  at a given  $u_{g}$  was estimated, for other  $u_{g}$  values,  $k_{L}a$  was calculated using the above relationship as :

$$k_{L}a = 1.445 u_{g}^{0.78} \quad (22)$$

At this stage, a brief discussion on the estimation of the gas-liquid mass transfer coefficient ( $k_{L}a$ ) is necessary, since these values were found to be several times higher (Table 3.IV) than those predicted by the literature correlations (Akita and Yoshida 1973; Deckwer et al., 1974; Kastaneck 1977). The higher values of  $k_{L}a$  can be justified for the present case because a) the gas sparger used was a sintered disc, having an average hole diameter in the range of 100-120  $\mu_{m}$ ; b) the liquid medium in the present case was an aqueous solution of a strong electrolyte having a concentration of 0.25M or more, which is highly a non-coalescing medium. For such conditions the bubble diameter is usually in range of  $4 \times 10^{-4}$  to  $10 \times 10^{-4}$  m. (Marrucci and Nicodemo, 1967), and in such a case higher interfacial area and  $k_{L}a$  values are only expected.

### 3.3 COMPARISON OF EXPERIMENTAL DATA WITH THEORY

The experiments carried out for the studies on the reactor performance were under the conditions such that the inlet oxygen concentration was well above the critical level values. (see section 3.4). In these experiments the conversion of ethylene  $X_A$  was observed for various reactor inlet conditions like gas velocity, catalyst concentration etc. The range of various process parameters investigated are given in Table 3.II. For the purpose of theoretical prediction of the ethylene conversion the model equations given in the section 3.1 (equations 12 to 15) were solved numerically. Further, using the estimated values of  $k_1$  and  $k_L a$  as described in section 3.2, the reactor model was used to predict the  $X_A$  at different reactor inlet conditions. The values of the model predictions and the experimental data for all these cases are presented in Table 3.III. The agreement between the model predictions and the experimental data over the wider conditions was excellent indicating the applicability of the estimated values of kinetic and mass transfer parameters. The values of the rate constant  $k_1$  at three different temperatures were correlated by an Arrhenius type equation (see Figure 3.2). The activation energy calculated from this plot was found to be equal to 61.14 kJ/mol. The values of the reaction rate constants

TABLE 3.II: RANGE OF VARIABLES FOR OXIDATION OF ETHYLENE TO ACETALDEHYDE

Palladium chloride concentration	:	$1.2 \times 10^{-3} - 5.085 \times 10^{-3} \text{ kmol/m}^3$
Cupric chloride concentration	:	$0.253 - 0.600 \text{ kmol/m}^3$
Superficial gas velocity	:	$0.58 \times 10^{-2} - 1.55 \times 10^{-2} \text{ m/s}$
Temperature	:	$333 - 363 \text{ K}$



TABLE 3. III : EXPERIMENTAL AND PREDICTED CONVERSION DATA AT VARIOUS REACTION CONDITIONS

Sr. No.	Temperature K	Superficial gas velocity $u_{gi} \times 10^2$ , m/s	PdCl <sub>2</sub> concentration $C_1 \times 10^3$ , kmol / m <sup>3</sup>	CuCl <sub>2</sub> concentration $B_{II}$ , kmol/m <sup>3</sup>	conversion $X_A$ (EXPT)	conversion $X_A$ (PRED)
1.	333	1.01	2.542	0.253	0.173	0.165
2.	333	1.55	2.542	0.253	0.107	0.12
3.	333	0.86	5.085	0.253	0.351	0.346
4.	333	0.86	2.542	0.441	0.0974	0.085
5.	348	1.01	2.542	0.253	0.306	0.296
6.	348	1.55	2.542	0.253	0.247	0.226
7.	348	0.86	1.20	0.253	0.251	0.231
8.	348	0.86	2.542	0.441	0.176	0.154

(Cont.)

9.	348	0.86	2.542	0.582	0.062	0.080
10.	363	1.01	2.542	0.253	0.446	0.430
11.	363	1.55	2.542	0.253	0.380	0.354
12.	363	0.86	1.20	0.253	0.385	0.350
13.	363	0.86	2.542	0.441	0.32	0.342

---

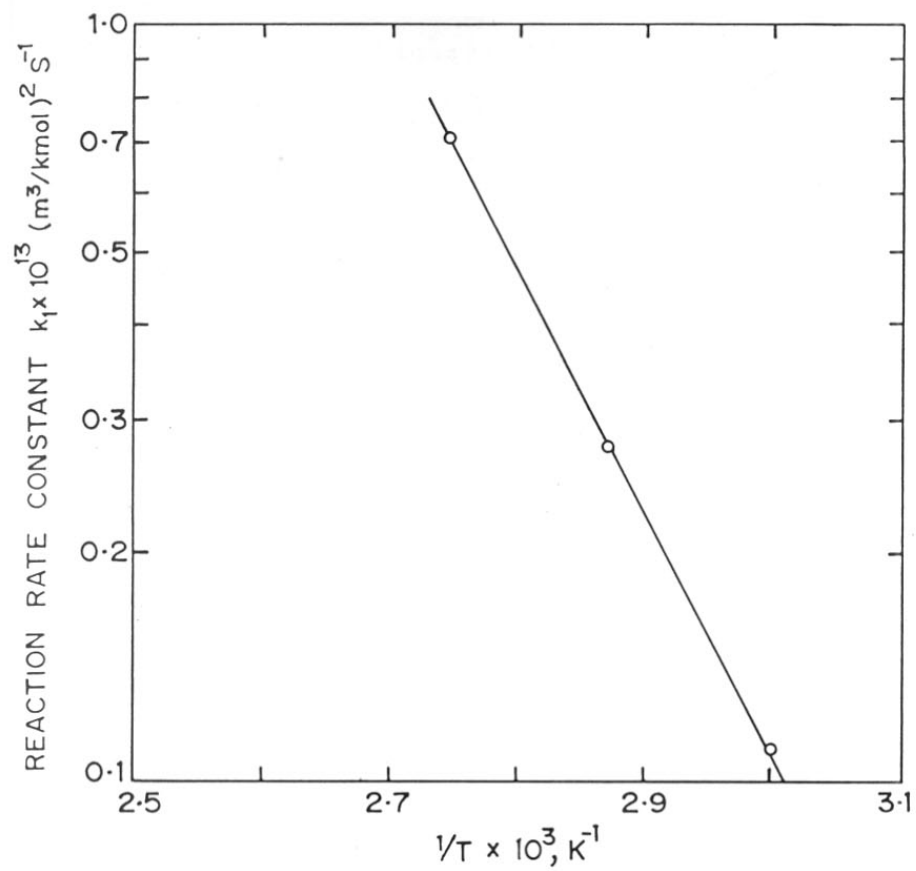


FIGURE 3-2: TEMPERATURE DEPENDENCE OF THE RATE CONSTANT ( $k_1$ )

( $k_1$  and  $k_2$ ) and the gas-liquid mass transfer coefficient ( $k_{La}$ ) are presented in Table 3.IV.

The results showing a comparison of the theoretical predictions with the experimental data, are presented in Figures 3.3 to 3.5, for different gas velocities,  $PdCl_2$  and  $CuCl_2$  concentrations. For a given set of conditions, the conversion of ethylene ( $X_A$ ) falls with increase in total gas velocity ( $u_{gi}$ ), obviously due to decrease in residence time with increase in ( $u_{gi}$ ). The conversion of ethylene ( $X_A$ ) increases with an increase in  $PdCl_2$  concentration ( $C_I$ ), while it decreases with an increase in  $CuCl_2$  concentration ( $B_{1I}$ ). The decrease in conversion with increase in  $B_{1I}$ , is a result of chloride ion inhibition on the rate of the reaction, which is also consistent with the rate expression (1). The excellent agreement between the model predictions and the experimental results (Figures 3.3 - 3.5) at all temperatures covering wide range of operating conditions indicates the internal consistency of the experimental data and also the possible use of the reactor model proposed here for the design purposes.

TABLE 3. IV : VALUES OF THE GAS-LIQUID MASS TRANSFER COEFFICIENT ( $k_{L,a}$ )<sup>\*</sup> AND THE RATE CONSTANTS ( $k_1$ ) AND ( $k_2$ )<sup>\*\*</sup>

Temperature K	$k_{L,a}$ , s <sup>-1</sup>	Reaction rate constant, $k_1 \times 10^{13}$ , (m <sup>3</sup> / kmol) <sup>2</sup> /s	Reaction rate constant, $k_2 \times 10^{-2}$ , (m <sup>3</sup> / kmol) <sup>2</sup> /s
333	0.301	0.110	10.41
348	0.312	0.281	17.76
363	0.318	0.716	29.30

\*  $u_{gi} = 0.86 \times 10^{-2}$  m/s.

\*\* From Zhaveri and Sharma (1967).

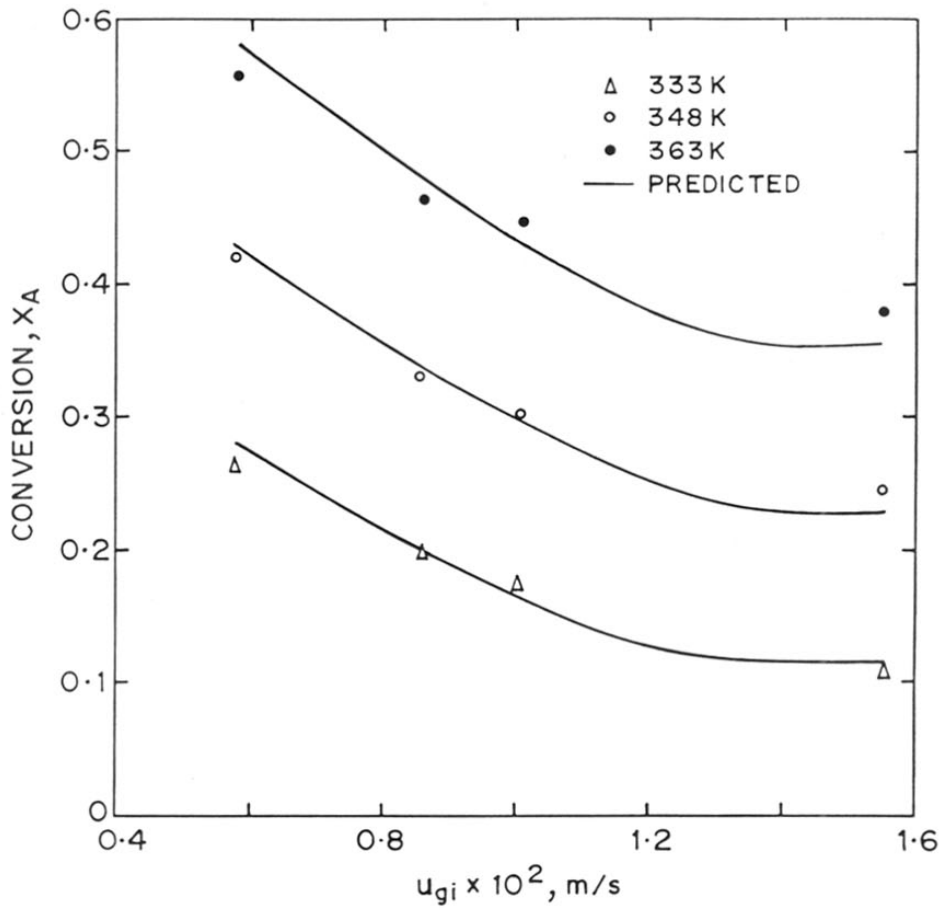


FIGURE 3-3: EFFECT OF SUPERFICIAL GAS VELOCITY ON CONVERSION.

$$[C_I = 2.542 \times 10^{-3} \text{ kmol/m}^3, B_{lI} = 0.253 \text{ kmol/m}^3]$$

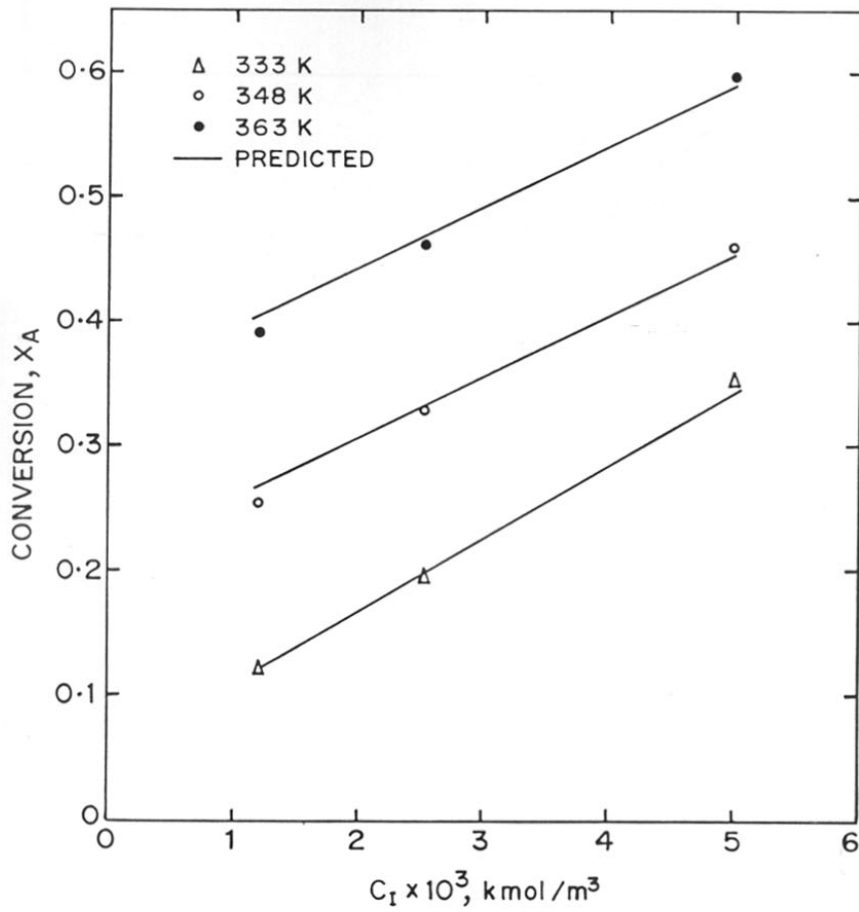


FIGURE 3-4: EFFECT OF CATALYST CONCENTRATION ON CONVERSION  
[ $u_{gi} = 0.86 \times 10^{-2}$  m/s,  $B_{L1} = 0.253$  kmol/m<sup>3</sup>]

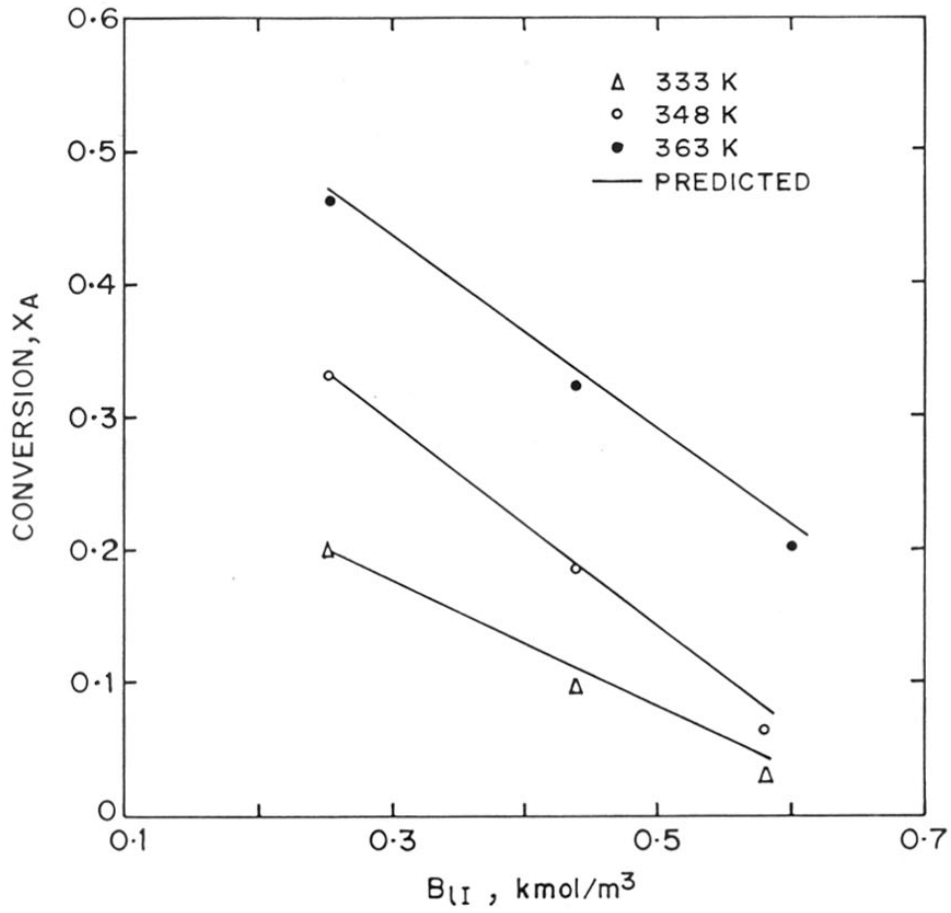


FIGURE 3.5: EFFECT OF  $\text{CuCl}_2$  CONCENTRATION ON CONVERSION  
 $[u_{gi} = 0.86 \times 10^{-2} \text{ m/s}$  AND  $C_I = 2.542 \times 10^{-3} \text{ kmol/m}^3]$



### 3.4 CRITICAL CONCENTRATION OF OXYGEN

#### 3.4.1 Introduction

There are several industrially operated catalytic oxidation processes, in which redox type homogeneous catalysts are being used. In these reactions, the reactant is oxidized by a transition metal complex catalyst, with the result that the metal itself gets reduced to a lower valence state. This reduced species is again re-oxidized insitu to the active form, by using a cocatalyst and molecular oxygen, thus continuing the cycle. One of such important reactions is the oxidation of ethylene to acetaldehyde, which has already been discussed in the previous section 3.1. Another example is the removal of  $H_2S$  from natural gas by catalytic oxidation using iron chelate catalyst, (Locat process, Hardison, 1985).

Usually such oxidation processes are carried out under conditions of excess oxygen than required by the stoichiometry. An important practical problem encountered in the design and operation of such a process is to estimate the excess oxygen requirement at the inlet of the reactor. This is expected to be a nontrivial exercise and not very obvious in view of the involvement of mass transfer and the possibility of a very undesirable performance with an arbitrary choice of the excess oxygen

concentration. Also, the large excess of oxygen concentration may decrease the effective concentration of the reacting species, such as ethylene, in case of single stage Wacker process, consequently leading to poor productivity. Therefore, it is an important practical problem to estimate the excess oxygen requirement at the inlet of the reactor. For such a reaction, a critical concentration of oxygen would exist below which the catalytic cycle will operate with very poor efficiency.

Let us consider the specific case of Wacker process. According to the reaction stoichiometry, (described in section 3.1) ethylene oxidation actually involves catalytic species whose concentration determines the ethylene conversion. Since, this catalytic species itself gets reduced, the rate of its re-oxidation, that is the regeneration of the catalyst should be much faster than the ethylene oxidation step, for a smooth steady state operation of the catalytic cycle. In order to have such a high rate of reoxidation, concentration of dissolved oxygen at all points in the reactor should be high enough. Thus, under a given set of operating conditions, the achievable steady state conversion of ethylene will be attained, only if the oxygen concentration at the reactor inlet is higher than a certain level, which, can be called as a critical concentration of oxygen.

## **CHAPTER 2**

### **EXPERIMENTAL**

Below this critical level of oxygen concentration, the rate of re-oxidation step is slowed down, giving rise to the increase in accumulation of the reduced species. As a consequence, rate of ethylene oxidation would slow down producing less and less acetaldehyde. Under these circumstances, steady states would be more difficult to achieve and the catalytic cycle would operate at a poor efficiency. In extreme cases, if degree of the reoxidation is too low, precipitation of palladium and cuprous chloride may occur leading to operational problems.

In order to operate the process with maximum efficiency, the estimation of this critical  $O_2$  concentration at the reactor inlet is highly essential based on which the excess  $O_2$  requirement should be calculated.

No attempts to analyze such a problem seem to have been made in the past. The objective of the present work is to make a theoretical prediction of the critical inlet  $O_2$  concentration by way of a steady state analysis of the above reactor configuration and to study the effect of other operating parameters on this important variable. Also, the predicted ethylene conversions under various set of conditions, have been compared with the experimental results. The present analysis is expected to be very useful for practical design and optimum operation

of the Wacker process and this approach can also be extended to evaluate the critical oxygen concentration for other reactions based on redox catalysts. The theoretical model developed here allows estimation of the excess oxygen requirement for achieving optimum conversion of ethylene. This has been demonstrated experimentally.

#### 3.4.2 EXPERIMENTAL

Materials and the reactor set up used were the same as have been described in section 2.1 and 2.2 respectively. For determining the critical concentration of oxygen, the following procedure was followed.

First, under a given set of constant reaction parameters, a run was carried out where oxygen was in excess ( $\alpha_3 = 2$ ) than required by the stoichiometry. Then for the same set of reaction conditions only the concentration of oxygen was lowered, step by step and the effect was observed on the productivity of acetaldehyde. The total gas flow rate was maintained constant by compensating with nitrogen gas. At a certain oxygen concentration, a drop in productivity of acetaldehyde was observed, immediately after the second hour of the run, and palladium black was also observed along the walls of the reactor. This observation clearly indicates

that the oxygen concentration went down below the minimum level of oxygen, required for the smooth oxidation of ethylene, which is defined as the critical concentration of oxygen.

The critical oxygen concentration was observed for different ratios of inlet concentrations ( $\alpha_3$ ), inlet gas velocity ( $u_{gi}$ ), catalyst concentration ( $C_I$ ), the concentration of cupric chloride ( $B_{II}$ ) and temperature.

#### 3.4.3 Results and discussion

Several experiments were carried out in which the ratio of the concentration of oxygen to that of ethylene ( $\alpha_3$ ) in the reactor inlet was varied, keeping other conditions constant and the conversion of ethylene ( $X_A$ ) was observed. The effect of various process parameters like gas velocity,  $PdCl_2$  concentration,  $CuCl_2$  concentration for different  $\alpha_3$  values, on the conversion ( $X_A$ ) was also studied. For a particular value of  $\alpha_3$ , under a given set of reactor inlet conditions, the productivity of acetaldehyde was observed over a period of 4 hours and these results are presented in Figures 3.6 and 3.7. It can be seen from these figures, that at  $\alpha_3 = 2$ , a steady state is attained by the first hour of the reaction, indicated by the constant productivity obtained thereafter. For  $\alpha_3 = 1$ , the steady state is attained,

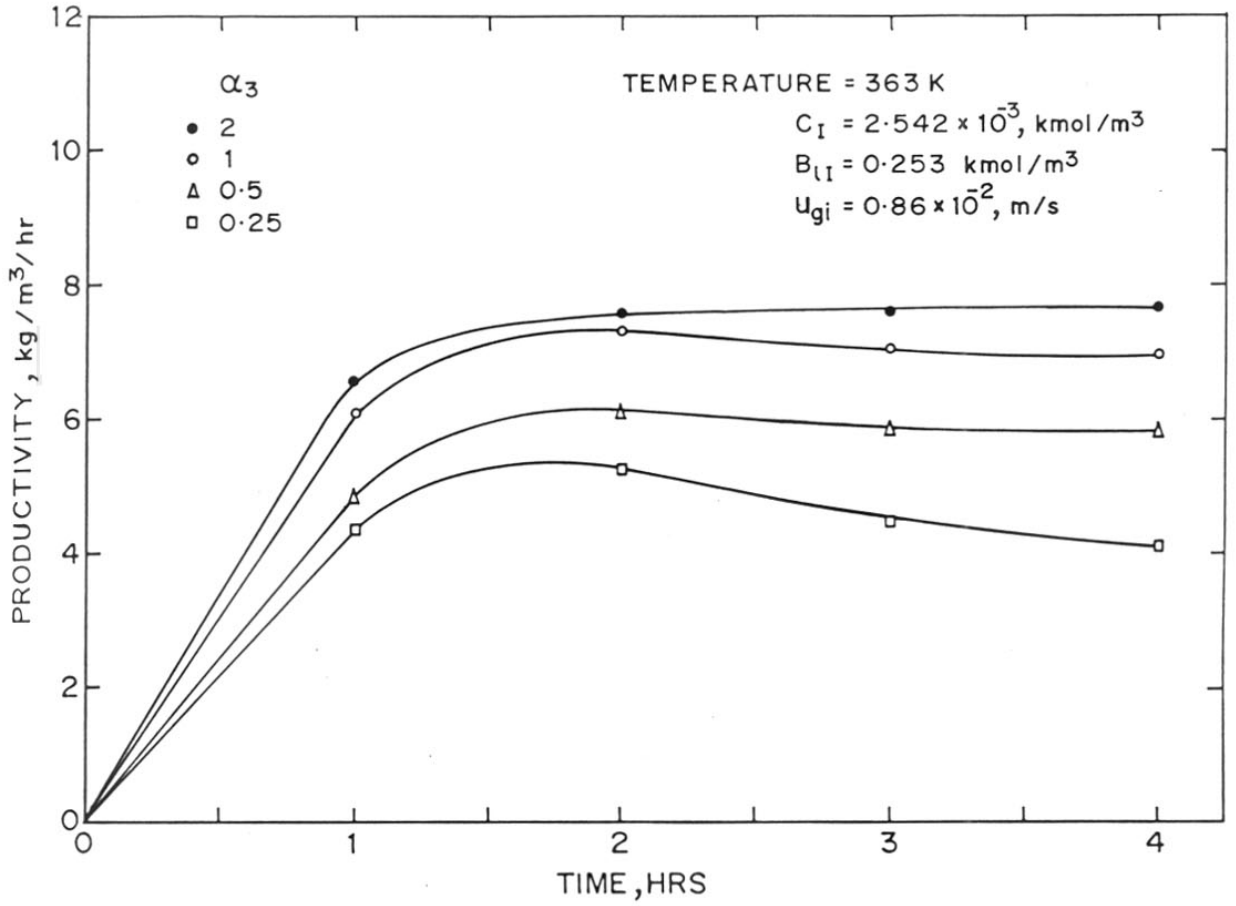


FIGURE 3.6: A PLOT OF PRODUCTIVITY Vs TIME AT VARIOUS RATIOS INLET GAS PHASE CONCENTRATIONS ( $\alpha_3$ )

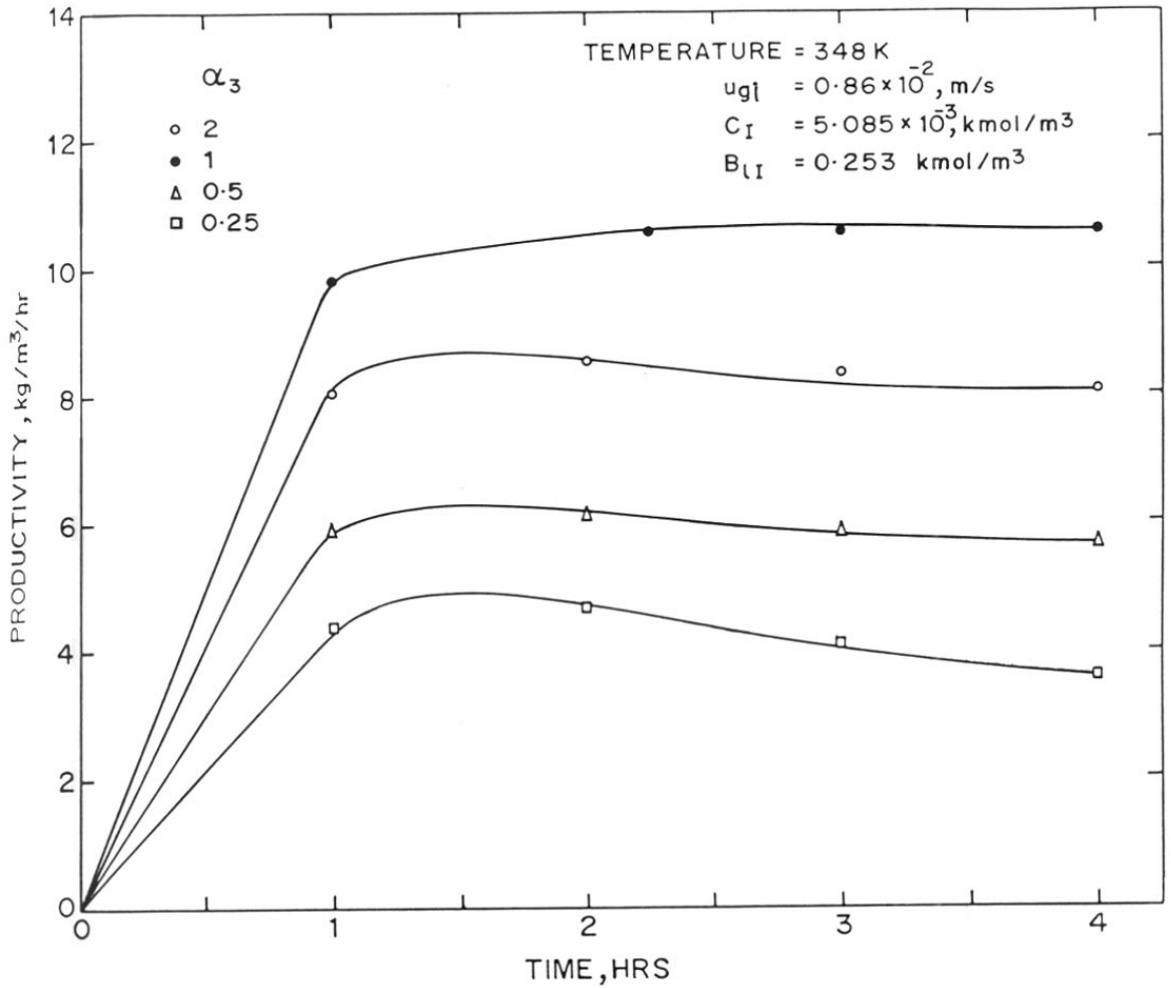


FIGURE 3-7 : A PLOT OF PRODUCTIVITY Vs TIME AT VARIOUS RATIOS OF INLET GAS PHASE CONCENTRATION ( $\alpha_3$ )



though, with less productivity of acetaldehyde, than that obtained for the previous case ( $\alpha_3 = 2$ ). For  $\alpha_3 < 0.5$ , the steady state itself is very difficult to achieve and the process operates with less and less efficiency as indicated by the deterioration of the productivity values.

The results of effect of process parameters at various  $\alpha_3$  values, on the reactor performance, are presented as  $X_A$  vs.  $\alpha_3$  plots in Figures 3.8 - 3.11. Following the numerical procedure given in the previous section (3.1, 3.2) conversions of ethylene and oxygen were predicted for different ratios of inlet concentrations ( $\alpha_3$ ), inlet gas velocity ( $u_{gi}$ ), catalyst concentration ( $C_I$ ), and the concentration of cupric chloride ( $B_{1I}$ ). These results are also presented in Figures 3.8-3.11 by thick lines. These plots indicate that for a set of specific values of  $u_{gi}$ ,  $C_I$ ,  $B_{1I}$  and  $E_{2I}$ , all of which can be independently set, at the steady state, a certain  $O_2$  concentration is required to be maintained at the reactor inlet in order to obtain a specified ethylene conversion in the reactor. These figures clearly show an excellent agreement between the model prediction and the experimental results. The practical implications of such results are discussed below.

The stoichiometry of the overall reaction

(reaction iv) merely stipulates that the molar conversions of ethylene and oxygen are related to each other by the stoichiometric factor, which is expressed by equation (16). For 100% conversion of oxygen (i.e.  $X_{A'} = 1$ ), the  $\alpha_3$  required for a given ethylene conversion ( $X_A$ ) is  $X_A/2$ . This is represented in Figures 3.8 - 3.10 by full line A. But under practical operating conditions, where the reoxidation steps are much faster than ethylene oxidation step (i) and where the redox catalytic process is in smooth operation, oxygen conversion can hardly reach 100% , as the process is limited by the rate of ethylene oxidation. This gives rise to a definite value of  $\alpha_3$  for obtaining a specified ethylene conversion ( $X_A$ ) given the other operating parameter values. And, in general, this value of  $\alpha_3$  may be far in excess of that given by curve A. It is interesting to note that, in each of the three figures, the region enclosed between line A and any particular  $X_A - \alpha_3$  plot for a particular parameter set ( $u_{gi}$ ,  $C_I$  and  $B_{1I}$ ) is unfeasible as far as that particular parameter set is concerned. For instance, in Figure 3.8, for  $u_{gi} = 0.86 \times 10^{-2}$  m/s, the maximum conversion achievable is 0.47 no matter what value of  $\alpha_3$  is used. On the other hand, even this maximum permissible conversion level cannot be achieved, if  $\alpha_3$  falls from 1.5 to 1.0. Thus, the computed steady-state values of  $X_A - \alpha_3$  as plotted, become a critical curve, to the left and above which

would lie an unfeasible region. This fact has actually been demonstrated experimentally and the data are presented in Figures 3.8-3.11.

The second observation made from this analysis that deserves discussion is that, as  $\alpha_3$  was lowered for any given set of reactor inlet conditions,  $X_A$  started decreasing (see figures 3.8-3.10). This implies slower reoxidation steps, so much so that below certain  $\alpha_3$  levels steady states were increasingly difficult to achieve, (see Figures 3.6 and 3.7 also) and if achieved, this would result in very high CuCl concentrations. The latter was evidenced by the Pd metal precipitation (black) along the walls of the reactor and this would be highly undesirable from practical operational considerations. Under such conditions, the redox catalytic nature of the system is said to be operating with lower efficiency. The dotted portions in all these figures thus indicated a region where steady state was difficult to reach and CuCl accumulation was likely to take place and was an undesirable region to operate the reactor. Thus, it was substantially to the right of dotted curve B that the practical operating zone should lie. This curve thus indicates a locus of the critical  $\alpha_3$  and, hence, the critical  $O_2$  concentration at the reactor inlet, below which it is impractical to operate the reactor. Hence, the choice of excess oxygen

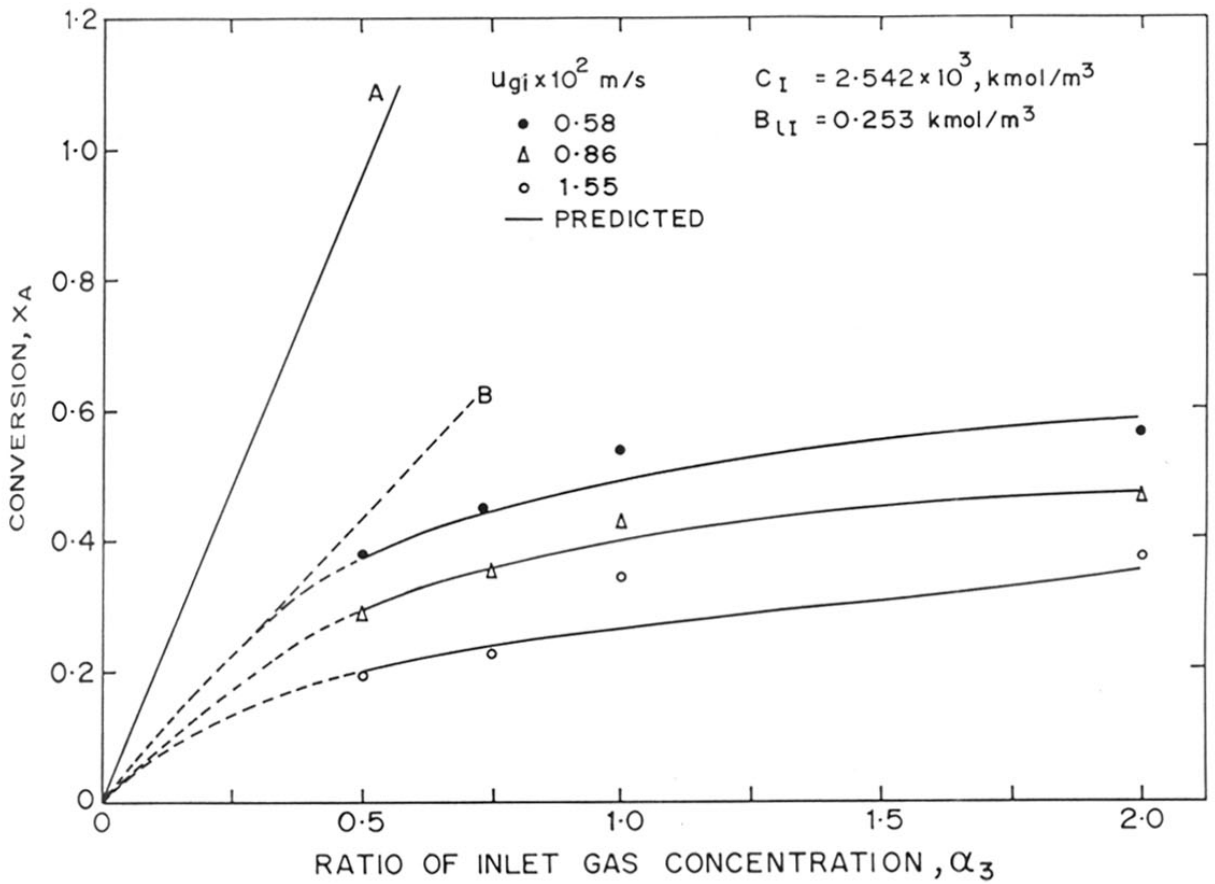


FIGURE 3-8:  $X_A$  Vs  $\alpha_3$  PLOTS : EFFECT GAS VELOCITY ( $u_{gi}$ ) AT TEMPERATURE = 363 K

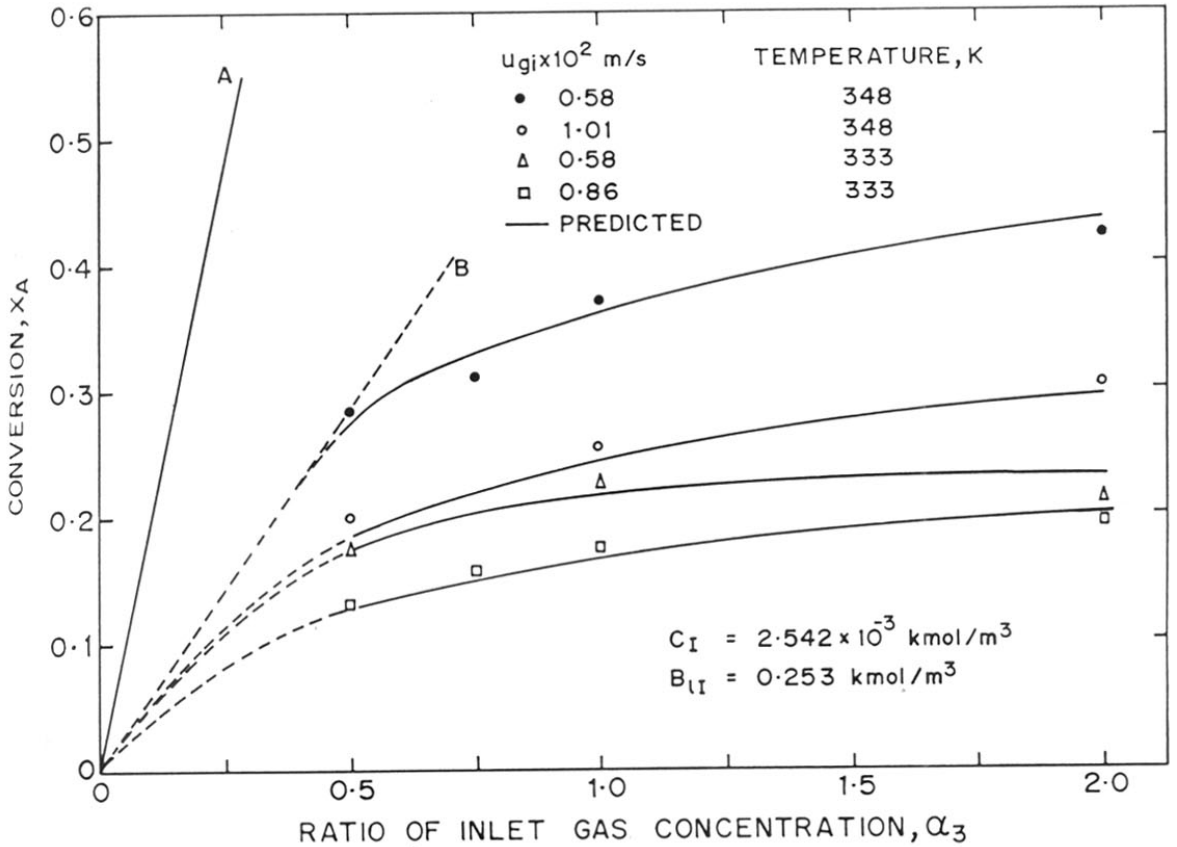


FIGURE 3-9:  $X_A$  Vs  $\alpha_3$  PLOTS: EFFECT OF GAS VELOCITY ( $u_{gj}$ ) FOR TEMPERATURE 348K AND 333K

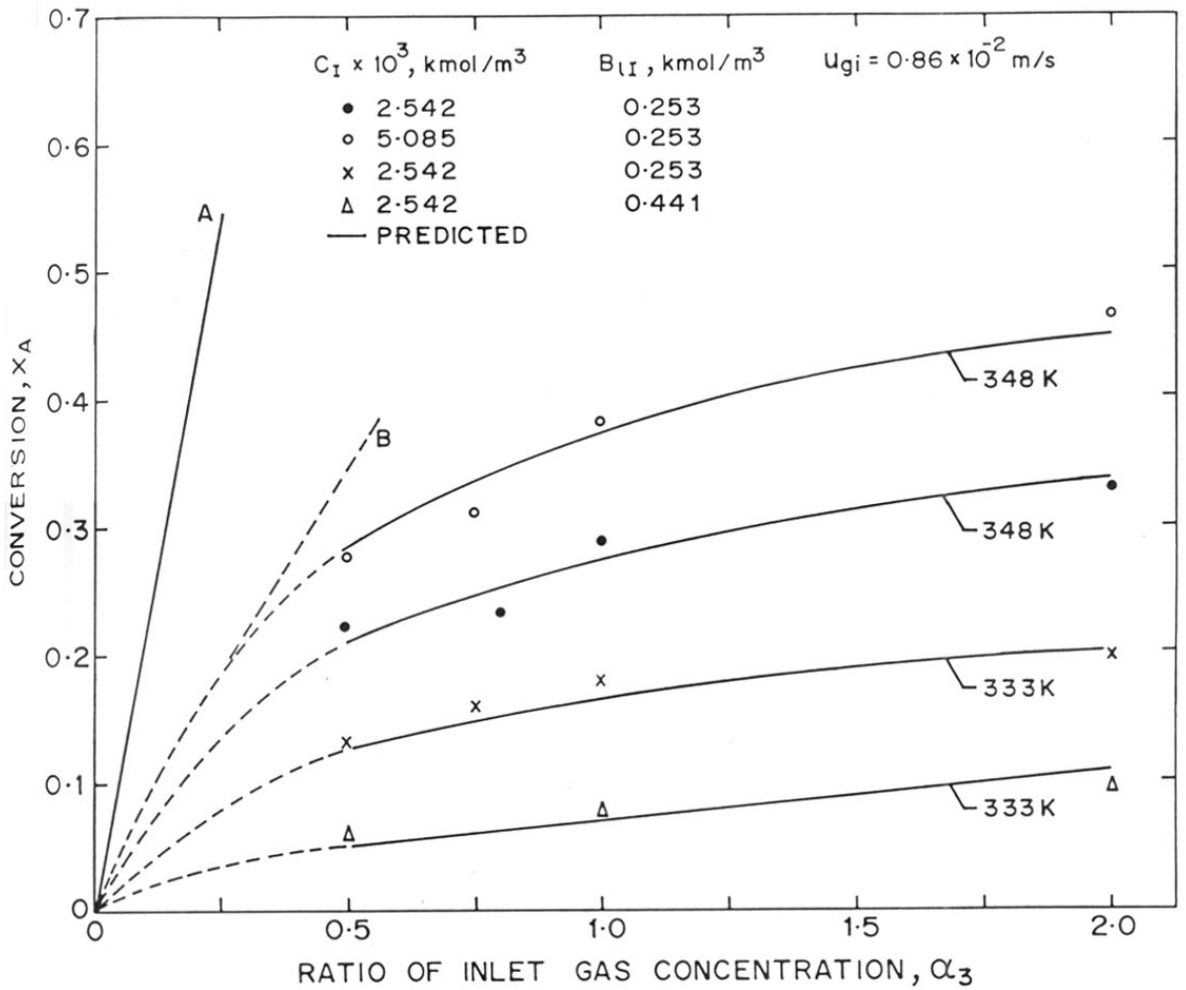


FIGURE 3.10:  $X_A$  Vs  $\alpha_3$  PLOTS: EFFECT OF  $\text{PdCl}_2$  ( $C_I$ ) AND  $\text{CuCl}_2$  ( $B_{I1}$ ) CONCENTRATION

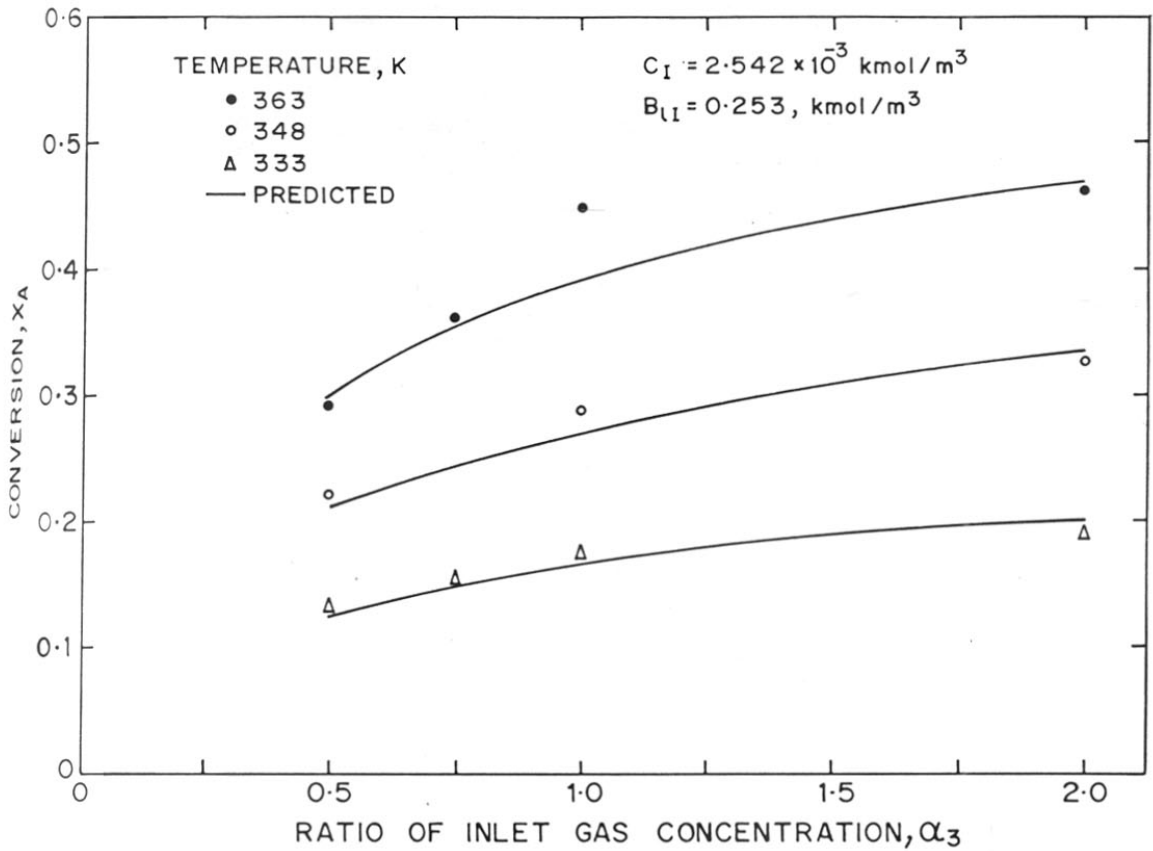


FIGURE 3.11:  $X_A$  Vs  $\alpha_3$  PLOTS: EFFECT OF TEMPERATURE AT  $u_g = 0.86 \times 10^{-2} \text{ m/s}$

requirement in such redox type catalytic processes should be based on the critical concentration of oxygen rather than on the stoichiometric requirement. Also, the theoretical model presented here can be used for an a priori estimation of the excess oxygen requirement under a given set of operating conditions.

### 3.5 CONCLUSIONS

The performance of a bubble column reactor for the Wacker process was studied experimentally at various reactor inlet conditions. A theoretical model was also developed to predict the conversion of ethylene, assuming gas in a plug flow manner and a backmixed liquid phase. The reaction rate constants and the gas-liquid mass transfer coefficient  $k_{La}$ , were estimated by simulation of a few experimental data. Using these parameters, reactor performance was predicted theoretically and results were compared with experimental data. The agreement between the theory and experiments was found to be excellent for a wide range of conditions. This indicates that the model developed here can be reliably used for design purposes.

For an industrially important redox catalytic process such as the Wacker process, being carried out in a semi-batch bubble reactor, it was found that a critical concentration of oxygen at the reactor inlet exists below



which the redox catalytic system operates with low efficiency and may lead to the operational problems. It is suggested that the choice of excess oxygen requirement should be based on the critical concentration of oxygen rather than on the stoichiometry. Furthermore, the above approach also produces the design charts which can be used to read the minimum required  $\lambda_3$  under the given operating conditions in order to obtain a specified ethylene conversion. This has been demonstrated experimentally also.

## NOMENCLATURE

A	:	species A (ethylene) or concentration of ethylene, kmol/m <sup>3</sup>
a	:	gas-liquid interfacial area, m <sup>-1</sup>
a <sub>1</sub>	:	A <sub>1</sub> H <sub>A</sub> /A <sub>gi</sub>
A'	:	species A' (oxygen) or concentration of oxygen, kmol/m <sup>3</sup>
a' <sub>1</sub>	:	A' <sub>1</sub> H <sub>A</sub> '/A' <sub>gi</sub>
B	:	species B (cupric chloride) or concentration of cupric chloride, kmol/m <sup>3</sup>
b	:	B/B <sub>II</sub>
C	:	species C (palladium chloride) or concentration of palladium chloride, kmol/m <sup>3</sup>
E <sub>1</sub>	:	species E <sub>1</sub> (cuprous chloride) or concentration of cuprous chloride, kmol/m <sup>3</sup>
E <sub>2</sub>	:	species E <sub>2</sub> (hydrochloric acid) or concentration of hydrochloric acid, kmol/m <sup>3</sup>
e <sub>1</sub>	:	E <sub>21</sub> / B <sub>II</sub>
H <sub>A</sub> , H <sub>A</sub> '	:	Henry's constant for ethylene and oxygen, respectively, m <sup>3</sup> (1)/m <sup>3</sup> (g)
K <sub>1</sub>	:	(k <sub>1</sub> × C <sub>l</sub> ) / B <sub>II</sub> ) / (2 × B <sub>II</sub> + E <sub>21</sub> ) <sup>2</sup> , s <sup>-1</sup>
K <sub>2</sub>	:	(k <sub>2</sub> × B <sub>II</sub> <sup>2</sup> ) / (k <sub>L</sub> a)
k <sub>1</sub>	:	rate constant, (m <sup>3</sup> / kmol) <sup>2</sup> /s
k <sub>2</sub>	:	rate constant, (m <sup>3</sup> / kmol) <sup>2</sup> /s
k <sub>L</sub>	:	liquid-side mass transfer coefficient, m/s
L	:	liquid height, m

Q	:	volumetric flow rate, m <sup>3</sup> /s
r	:	rate of reaction, kmol/m <sup>3</sup> /s
u <sub>g</sub>	:	superficial gas velocity, m/s
u	:	u <sub>g</sub> /u <sub>gi</sub>
X	:	conversion
x	:	axial distance, m
z	:	dimensionless axial distance, x/L

#### Greek symbols

$\alpha_1$	:	$K_1 / (k_L a)$
$\alpha_3$	:	$A'_{gi} / (A_{gi})$
$\alpha_4'$	:	$(k_L a) \times L / u_{gi} \times (H_A)$
$\alpha_4$	:	$(k_L a) \times L / u_{gi} \times (H_A')$

#### Subscripts

i	:	inlet of reactor
I	:	initial
o	:	outlet of reactor
g	:	gas phase
l	:	liquid phase

## REFERENCES

1. Aguilo, A., and Penrod, J. D., "Acetaldehyde", in Encycl. Chem. Proc. Design, vol. 1, Eds. Mcketta, J. J., and W.A. Cunningham, Marcel Dekker, Inc., New York (1977).
2. Akita, K., and Yoshida, F., Ind. Eng. Chem. Proc. Des. Dev., **12**, (1973), 76.
3. Danckwerts, P. V., "Gas-Liquid Reactions", McGraw-Hill, (1970).
4. Deckwer, W. D., Burckhart, R., and Zoll, G., Chem. Eng. Sci., **29**, (1974), 2177.
5. Deckwer, W. D., "Reaktionstechnik in Blassensaulen", Salle Sawerlandes, Frankfurt, (1985).
6. Hardison, L.C., Hydrocarbon Process. (1985), 70.
7. Henry, P. M., J. Am. Chem. Soc., **86**, (1964), 3246.
8. Jhaveri, A. S., and Sharma, M. M., Chem. Eng. Sci., **22**, (1967), 1.
9. Jira, R., "Ethylene and Its Industrial Derivatives", Benn, London, (1969).
10. Kastaneck, F., Coll. Czechoslov. Chem., **42**, (1977), 2491.
11. Konnik, E. I., Russ. Chem. Rev., **46**, (1977), 577.
12. Long, F.A., and McDevit, W. F., Chem. Rev., **51**, (1952), 119.
13. Marrucci, G., and Nicodemo, L., Chem. Eng. Sci., **22**, (1967), 1257.

14. Mashelkar, R. A., Brit. Chem. Eng., **15**, (1970), 1297.
15. Moiseev, I. I., Levanda, O.G., and Vargaftik, M.N., J. Am. Chem. Soc., **96**, (1974), 1003.
16. Onda, K., Sada, E., Kobayashi, T., Kito, S., and Ito, K., J. Chem. Eng. Japan, **3**, (1970), 18.
17. Ramachandran, P. A., and Chaudhari, R.V., "Three Phase Catalytic Reactors", Gordon and Breach Sci. Pub., New York, (1983).
18. Shah, Y. T., Kelkar, B.G., Godbole, S.P., and Deckwer, W.D., AIChE. J., **28**, (1982), 353.
19. Siedel, A. D., "Solubilities of Inorganic and organic Compounds", Van Nostrand Co. Inc., New York, (1970).
20. Smidt, J., Hafner, W., Jira, R., Sedlmetier, J., Sieber, R., Ruttenger, R., and Kojer, H., Agnew. Chem., Int. Ed. Engl. **1**, (1962), 80.
21. Vargaftik, M. N., Moiseev, I.I., and Syrkin, Ya. K. Izv. Akad. Nauk, SSR, Khim. Nauk, **6**, (1963), 1147.
22. Wilhelm, E., Battino, R. and Wilcock, R.J., Chem. Rev., **77**, (1977), 219.
23. Wilson, C. L. and Wilson, D.H., "Comprehensive Analytical Chemistry", vol. I B, Elsevier, Amsterdam, (1960).

## **CHAPTER 4**

# **GAS HOLD - UP AND FLOW REGIMES IN A BUBBLE COLUMN REACTOR**

#### 4.1 GENERAL BACKGROUND AND LITERATURE SURVEY

Bubble columns have wide ranging applications in different fields of chemical industry. They are commonly used as gas-liquid reactors, bio-reactors, and gas absorbers and some of the important examples are found in hydrogenation, oxidation, polymerization, carbonylation and fermentation processes ( see also Table 4.I). Because of the simple construction and less operational costs they are considered to be commercially viable reactors. Bubble columns can be operated in a semi-batch mode (static liquid phase) or in a continuous manner in which gas and liquid phases are introduced in a co-current or a counter-current manner. For a particular application, bubble columns have been modified suitably. Sectionalized bubble column reactor is used where low backmixing is desired, in most of the biotechnological processes. Loop reactors are used in the ICI pressure cycle fermenter (Hines, 1978). For some reactions, where high gas component conversion is not necessary and low pressure drop is required, a horizontally sparged bubble column reactor can be used (Joshi and Sharma, 1976). When high gas residence time is desired, for complete conversion of gas phase, downflow bubble columns can be used. A special design for continuous operation with facilities for separation of catalyst has been proposed by Ohorodnik et al. (1975).

TABLE 4.I : SOME EXAMPLES OF THE PROCESSES CARRIED OUT IN BUBBLE COLUMN REACTORS\*

Sr. No.	Reaction system	Reference
1.	Partial oxidation of ethylene to acetaldehyde	Smidt et al. (1959), Jira et al. (1976).
2.	Oxidation of ethylene in acetic acid solution to vinyl acetate	Krekeler and Schmitz (1968).
3.	Oxidation of acetaldehyde to acetic acid	Sittig (1967); Kostyak et al. (1962).
4.	Oxidation of sec butanol to acitic acid	Sittig (1967).
5.	Oxidation of butanes to acetic acid and methyl ethyl ketone	Hofermann (1964); Saunby and Kiff (1976).
6.	Oxidation of toluene to benzoic acid	Kaeding et al. (1965).

(Cont.)



7. Carbonylation of methanol to acetic acid  
Hjortkjaer and Jensen (1976).
8. Hydroformylation of olefins to aldehydes and alcohols  
Oliver and Booth (1970).
9. Coal liquefaction  
Frank and Knop (1979); Shah (1981).
10. Polymerization of olefins  
Albright (1967a); Gates et al. (1979).
11. Hydrogenation of unsaturated fatty acids  
Albright (1967b); Baltes et al. (1975).
12. Hydrogenation of adipic acid dinitrile to hexamethylene diamine  
Weissermel and Arpe (1976).
13. Hydrogenation of nitroaromatics to amines  
Albright et al. (1967c).
14. Methanol from synthesis gas  
Sherwin and Frank (1976).
15. Fischer-Tropsch synthesis  
Kolbel and Ralek (1977, 1980).
16. Production of single cell protein  
Schugert et al. (1978); Moo-Young (1975).

(Cont.)

17. Production of primary and secondary metabolites Smith and Greenshields (1974).
18. Production of animal cells Katinger et al. (1979).
19. Waste water treatment Bayer (1977); Zlokarnik (1978).

---

\* Shah et al. (1982).

In order to understand the design aspects of bubble column reactors a knowledge of hydrodynamics, mass transfer and kinetic parameters is essential. It is well known that the bubble columns operate in different flow regimes depending on the gas velocity and dimensions of the equipment. The flow regimes are also dependent on the properties of liquid and gas phases as well as the type of distributor used. Similarly, the interfacial area for mass transfer is strongly dependent on the gas hold-up which again depends on the reactor configuration and system properties. Extensive studies have been reported in the literature on flow regimes and gas hold-up in bubble column reactors and these have been reviewed by Mashelkar (1970), Shah et al. (1982), Ramachandran and Chaudhari (1983) and Deckwer (1985).

The flow regimes in a bubble column reactor can be classified as :

1. Homogeneous bubbly flow : This is characterized by almost uniformly sized bubble distribution, and occurs, at superficial gas velocities less than 0.05 m/s (Fair, 1967).
2. Heterogeneous bubble flow : At higher gas velocities ( $> 0.07$  m/s) sufficient number of bubbles coalesce, forming large bubbles. Large bubbles move in the presence of small bubbles (Hills and Darton, 1976).

3. Churn turbulent slug flow : This regime occurs at large gas velocities in small-diameter reactors. Large bubbles are stabilized by the column wall and move as slugs. Various flow regimes are schematically shown in Figure 4.1.

It has been shown (Kawagoe et al., 1976; Kelkar et al., 1983a, and 1983b) that the presence of electrolytes, traces of alcohols and impurities substantially influence the conditions at which the transition in flow regime occurs. The type of sparger used, physico-chemical properties of liquid, and the liquid velocity can affect the transition between flow regimes (Shah and Deckwer, 1981). Bach and Pilhofer (1978) have suggested the churn turbulent regime is most commonly encountered in industrially operated bubble column reactors. Knowledge of the transition from the bubble flow to the churn turbulent and slug flow regimes is important because the conversion depends strongly on the flow regime (Deckwer and Schumpe, 1979 and Schumpe, et al. 1979).

Similarly, the role of electrolytes and surfactants on the gas hold-up in bubble columns has been investigated (Akita and Yoshida, 1973; Deckwer et al., 1974; Hikita et al., 1980; and Kelkar et al., 1983a, 1983b). It has been observed that the changes in physical properties of the systems alone do not explain the

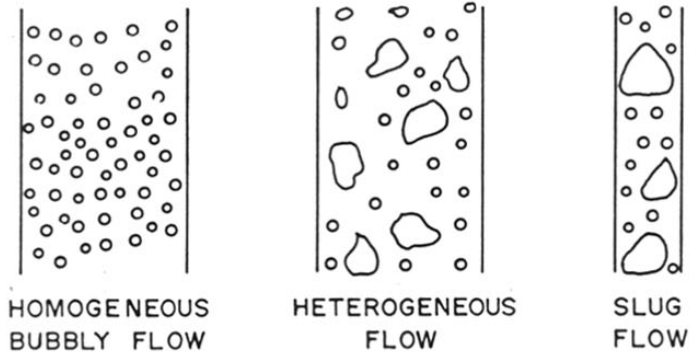


FIGURE 4-1: FLOW REGIMES IN BUBBLE COLUMNS

observed variations in the gas hold-up and the flow regimes in the presence of electrolytes and trace impurities (Shah et al., 1982). It is believed that the major influence is due to change in the coalescence behaviour of the gas bubbles, caused by changes in the hydrodynamics of the gas-liquid interface. More recently, there have been a few reports on the role of surfactants and electrolytes on the gas hold-up and flow regimes. (Posarac and Tekic, 1987; Zheng et al., 1988; Renjun et al., 1988; Ozturk et al., 1987; and Kulkarni et al., 1987). The observed trends in changes in gas hold-up and flow regimes have been reasonably understood qualitatively but no quantitative approach has yet emerged which could represent data of several investigators. Obviously, to achieve this, extensive data on gas hold-up and flow regimes is necessary. The aim of the present work was to study these parameters in a semi-batch bubble column reactor for different types and concentrations of electrolytes and surfactants. Most of the previous studies have been reported at ambient conditions though the industrial bubble column reactors are often operated at elevated temperatures. Therefore, it was also the aim of this work to obtain data on gas hold-up and flow regimes as a function of temperature. The observed data has been compared with the literature correlations and an attempt has been made to discuss the results based on the theory of coalescence. Finally,

correlations have been proposed and their applicability to the data obtained has been examined.

## 4.2 EXPERIMENTAL

### 4.2.1 Materials

In all the experiments, air was used as the gas phase, and the aqueous solutions were prepared using deionized water. The electrolytes used were : NaCl,  $\text{CuCl}_2$ ,  $\text{Al}_2(\text{SO}_4)_3$ ,  $\text{FeCl}_3$ . All salts used in this work were of laboratory reagent grade, supplied by m/s. S.D. fine chemicals, Bombay. Other liquid phases used were : Aqueous solutions of methanol, n-butanol, formic acid, acetic acid and propionic acid.

### 4.2.2 Apparatus

A glass bubble column with an i.d. of 0.1 m and a height of 1.5m was used in a semibatch mode for investigation of the flow regimes and the gas hold-up. The bubble column reactor was provided with an outer jacket, through which hot water could be circulated at a desired temperature. The gas distributor used was a sintered glass disc of 0.1m diameter and a mean pore size of 100-200  $\mu\text{m}$ .

#### 4.2.3 Experimental procedure

A number of methods are known for the estimation of gas hold-up in a bubble column, e.g. pressure difference method, conductivity measurements using probes, X-ray absorption and rising method (Deckwer, 1985). In the present work, the rising method was used mainly because (1) It does not need any further apparatus, etc. atleast in case of transparent and pressureless reactors; (2) It is easy to operate for determination of the gas hold-up, the height of an expanded bed in the presence of a gas ( $H_E$ ) and that without a gas ( $H_O$ ) were observed. It was ensured that a desired uniform temperature was achieved throughout the column. The gas was presaturated with the liquid under study at the temperature of the experiment before introducing it into the column. The gas hold-up was calculated as :

$$\epsilon_g = \frac{H_E - H_O}{H_E} \quad (1)$$

The gas flow rates were monitored by a calibrated rotameter and were varied over a range of  $5.31 \times 10^{-3}$  to  $5.83 \times 10^{-2}$ ,  $\text{ms}^{-1}$ , while the temperature range studied was 303-358 K.



The flow regimes were observed visually in each experiment. Particularly, the gas velocity at which the transition from the bubble flow to the churn turbulent flow regime occurs was noted for different conditions. The flow regime transition was also characterized using the drift flux theory (Wallis, 1969).

#### 4.3 RESULTS AND DISCUSSIONS

The objective of this work was to obtain experimental data on gas hold-up and flow regimes in a bubble column with the aim of understanding the role of electrolytes, surfactants and temperature effect. Following the procedure described above the effect of gas velocity, temperature, types and concentration of electrolytes and surfactants was investigated. The range of parameters covered is given in Table 4.II.

##### 4.3.1 Gas Hold-up in air-water system

A plot of gas hold-up vs. superficial gas velocity for air-water system is shown in Figure 4.2, which indicates that similar trends were observed for both tap water as well as distilled water, with the only difference that the gas hold-up values for distilled water system were marginally lower (~ 5%) than those for the tap water system. The effect of

TABLE 4.II : RANGE OF PARAMETERS STUDIED

1.	Superficial gas velocity $u_g$	$0.53 \times 10^2$ - $5.86 \times 10^{-2}$ m/s
2.	Temperature	303 - 358 K
3.	Types of electrolytes	1,1; 2,1; 3,1 and 3,2
4.	Concentration of electrolytes	0.1 M to 0.5 M
5.	Types of surfactants	C <sub>1</sub> - C <sub>4</sub> , alcohols and carboxylic acids
6.	Concentration of surfactants	0.001 % - 0.5 %

temperature on the gas hold-up for air water system is also shown in Figure 4.2, which indicates that the gas hold-up decreases with increase in temperature. In contrast to this, the gas hold-up was found to increase with increase in temperature, for air water system, in a recent work by Renjun et al.(1988). However, the reverse trends observed could be due to the different type of gas distributor used. The lowest gas hold-up obtained in the present work was at 343K while , the gas hold-up observed at 358K was higher than that observed at 323K. A comparison of experimental results with those predicted by different correlations, for air-water system, at 303K ,is shown in Figure 4.3. The gas hold-up values predicted by all the correlations considered here, were lower than those observed in the present work. However, the prediction of gas hold-up using the correlation of Hikita et al. (1980) was found to be in reasonable agreement with the experimental data for the air-water system.

#### 4.3.2 Effect of electrolytes on the gas hold-up

The effect of different types of electrolytes on the gas hold up was studied and the results for 303 K and 0.1M concentration are shown in Figure 4.4. The

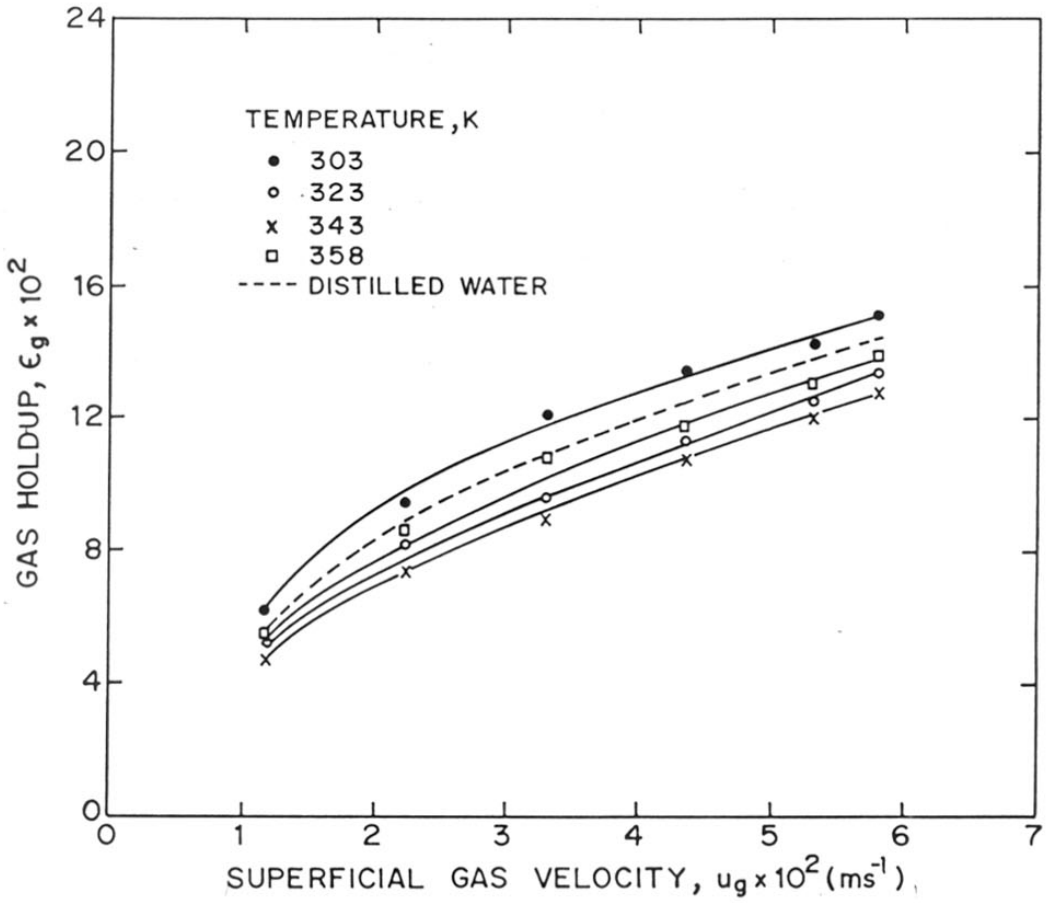


FIGURE 4·2: GAS HOLDUP Vs SUPERFICIAL GAS VELOCITY FOR AIR-WATER SYSTEM

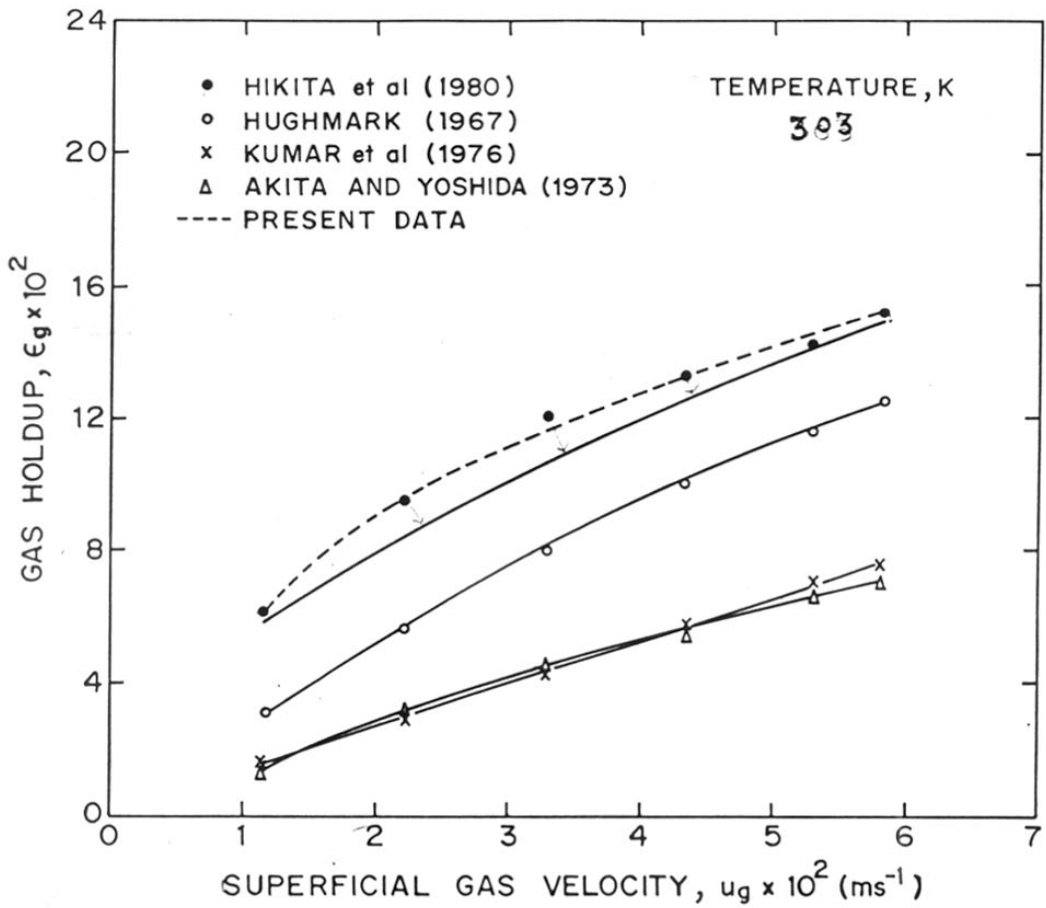


FIGURE 4-3: COMPARISON OF EXPERIMENTAL DATA WITH PREDICTIONS OF DIFFERENT CORRELATIONS FOR AIR WATER SYSTEM

gas hold-up for air-aq.-electrolyte system was found to be substantially higher than that for air-water system, being highest for air- aq.  $\text{FeCl}_3$  solution and lowest for air- aq.  $\text{NaCl}$  system.

The effect of temperature on the gas hold-up for different types of electrolytes is shown in Figures 4.5 - 4.7. It was observed that, in general, the gas hold-up increased with increase in temperature for all the electrolytes. The effect of temperature was however, more pronounced for  $\text{CuCl}_2$  solution. For air-aq.  $\text{Al}_2(\text{SO}_4)_3$  system, it was observed (see Figure 4.7) that at higher temperatures the gas hold-up vs. gas velocity plot passed through a maxima. This observation could be due to a change in the flow regime. The transition of flow regime for this case occurred at lower gas velocities as the temperature was increased.

The effect of concentration of the electrolytes on the gas hold-up was also studied. The results are presented in Figure 4.8 for air-aqueous  $\text{NaCl}$  system at 303 K. The gas hold-up was found to be a mild function of concentration of electrolyte and the similar observation was obtained for other electrolytes also. This was probably due to the fact that the concentrations of electrolytes under study were already beyond the critical concentration above which there is practically no enhancement of the gas hold-up (Kelkar, et al., 1983a).

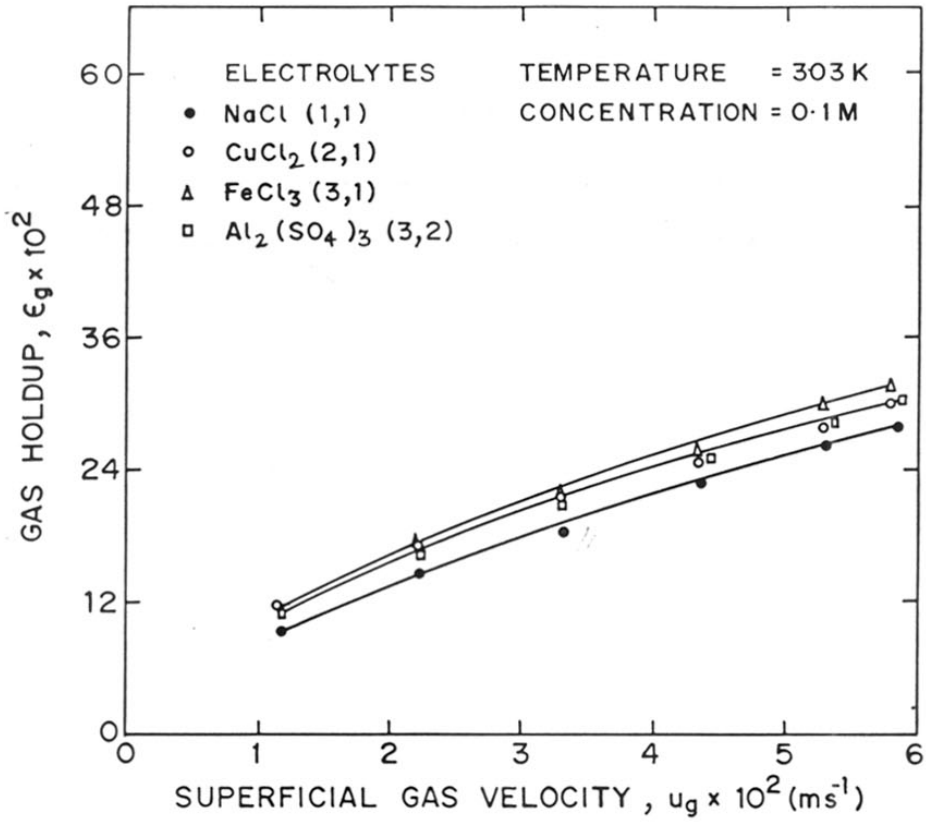


FIGURE 4.4: GAS HOLDUP Vs  $u_g$  FOR DIFFERENT TYPES OF ELECTROLYTES

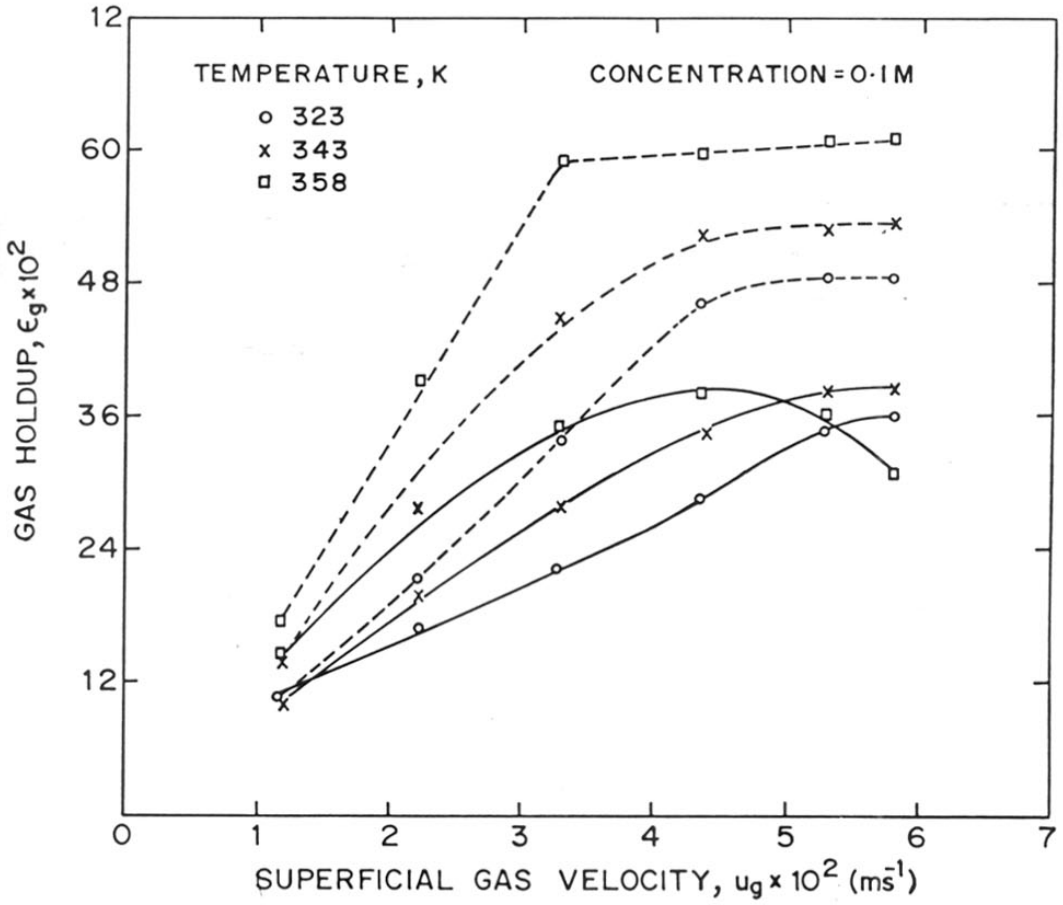


FIGURE 4.5: GAS HOLDUP Vs  $u_g$  AT DIFFERENT TEMPERATURES FOR NaCl (—) AND  $\text{CuCl}_2$  (----)



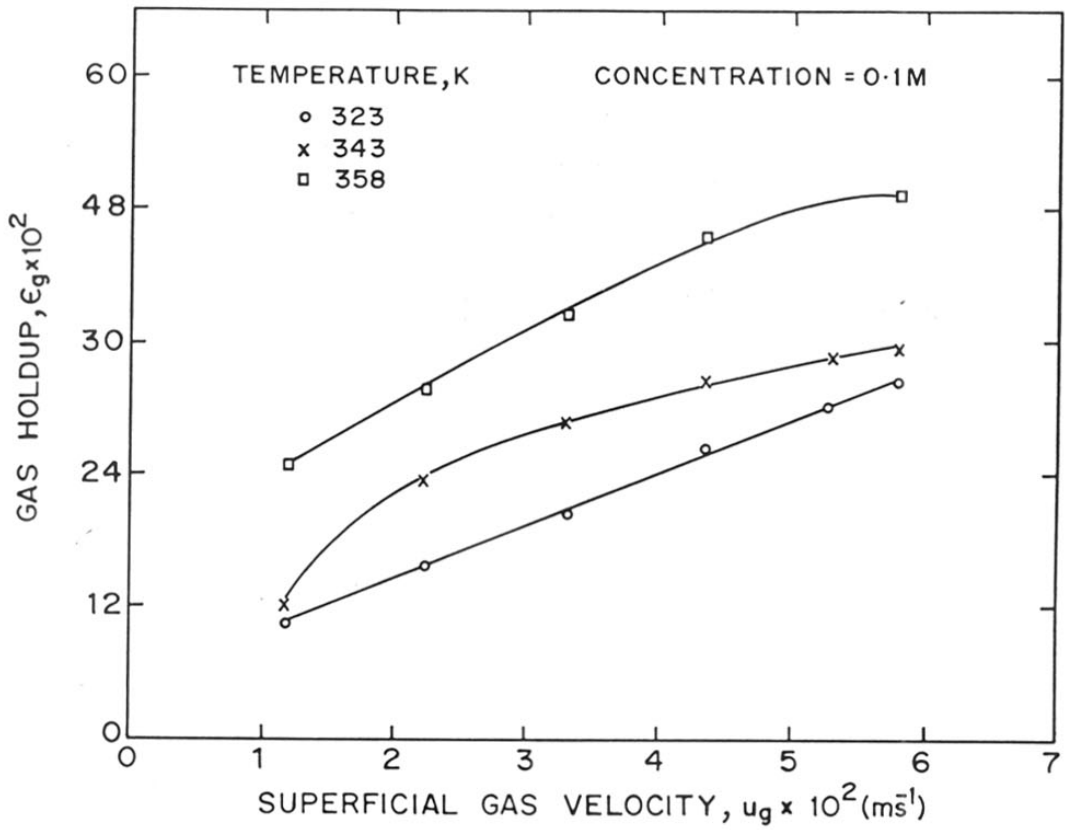


FIGURE 4.6: GAS HOLDUP Vs  $u_g$  AT DIFFERENT TEMPERATURES FOR  $\text{FeCl}_3$

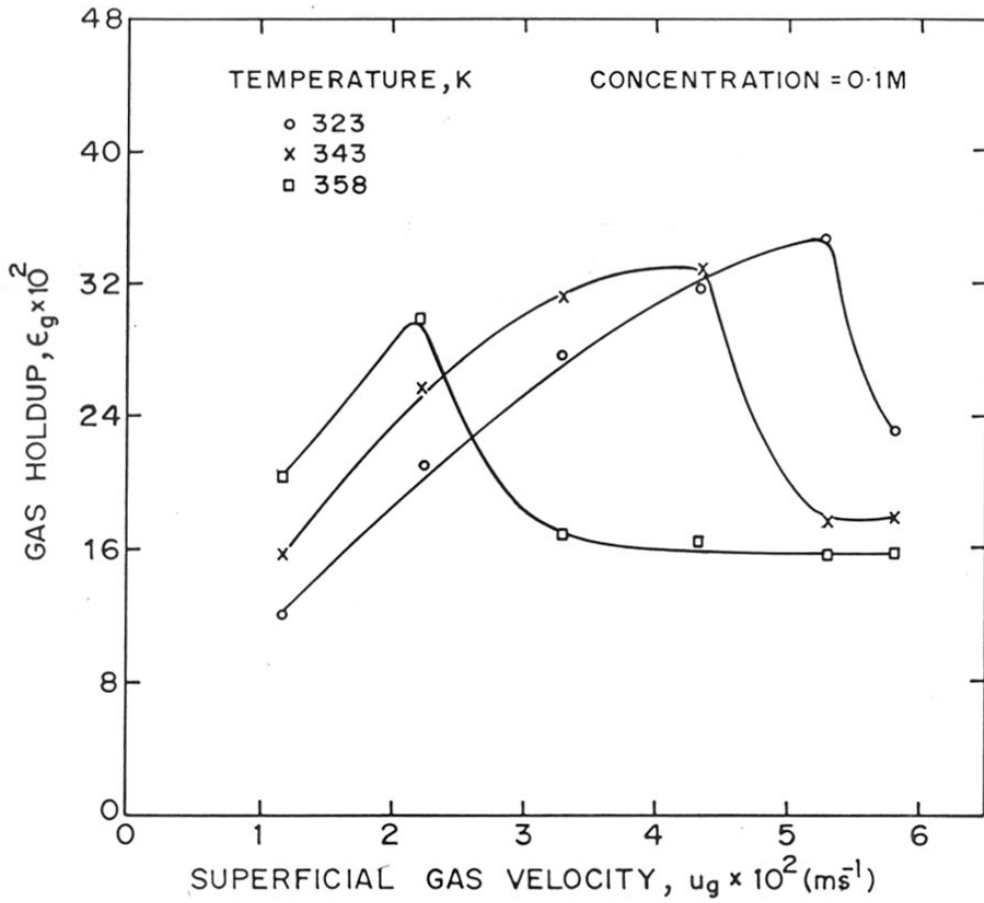


FIGURE 4.7: GAS HOLDUP Vs  $u_g$ , AT DIFFERENT TEMPERATURES FOR  $\text{Al}_2(\text{SO}_4)_3$

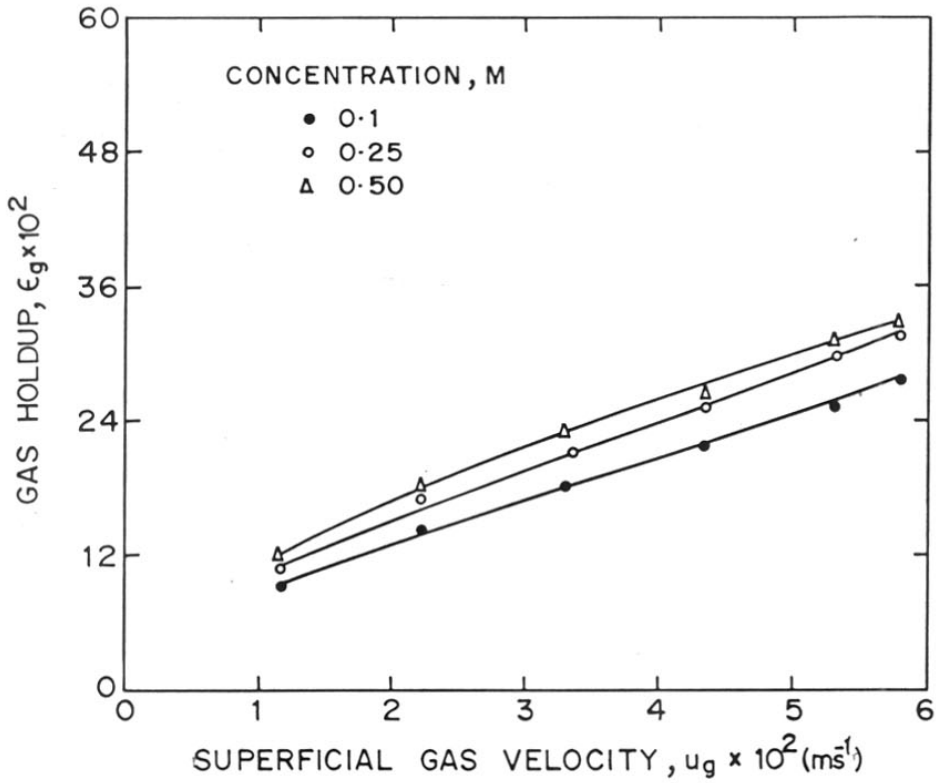


FIGURE 4·8: EFFECT OF CONCENTRATION OF NaCl ON GAS HOLDUP

The experimental results on gas hold-up in the presence of different electrolytes obtained in the present work were compared with the predictions of various correlations. A typical plot showing a comparison of the gas hold-up predicted by various literature correlations with the experimental one, for aqueous NaCl (0.1M) system is presented in Figure 4.9. It can be seen from this figure that the predictions by none of the correlations match with the experimental data, indicating that accounting for physical properties alone does not explain the high gas hold-up observed for electrolytic solutions. Further details on the approach for correlating these data has been discussed in section 4.3.4.

#### 4.3.3 Effect of surfactants

The effect of surfactants such as alcohols and carboxylic acids on the gas hold-up was also studied. For dilute aqueous solutions of both alcohols and carboxylic acids, the gas hold-up was very much higher than that of air-water system. Several experiments were carried out at various concentrations of surfactants and it was found that in case of n-butanol, only a trace quantity of n-BuOH (0.001 %) is enough to obtain the gas hold-up as high as 45%. (See Figure 4.11). The comparison of the

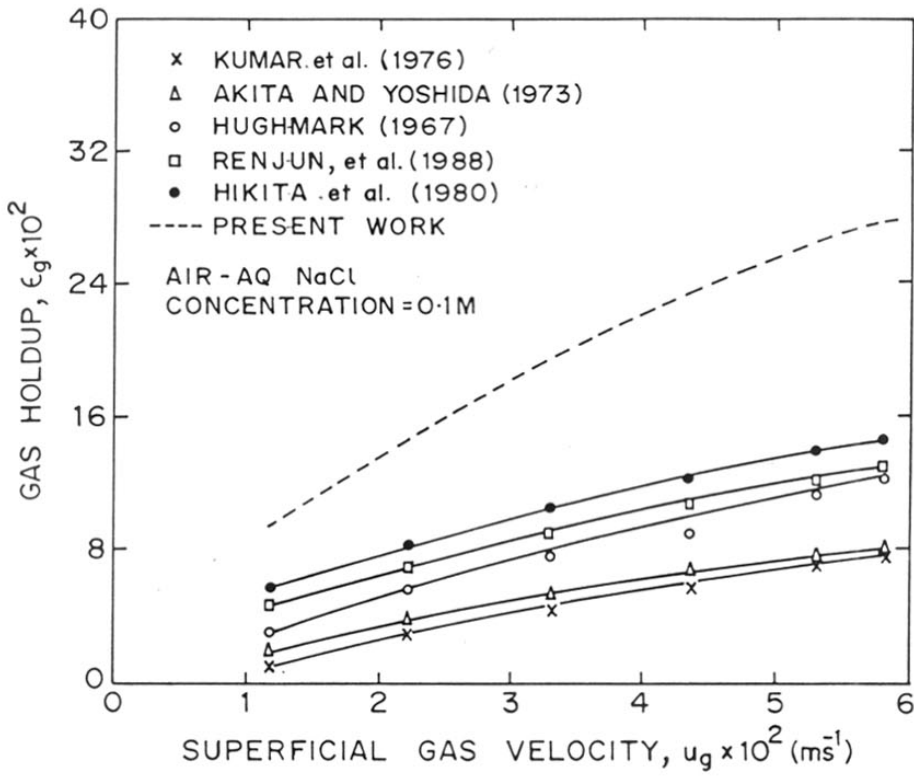


FIGURE 4.9: COMPARISON OF EXPERIMENTAL DATA WITH VARIOUS LITERATURE CORRELATIONS

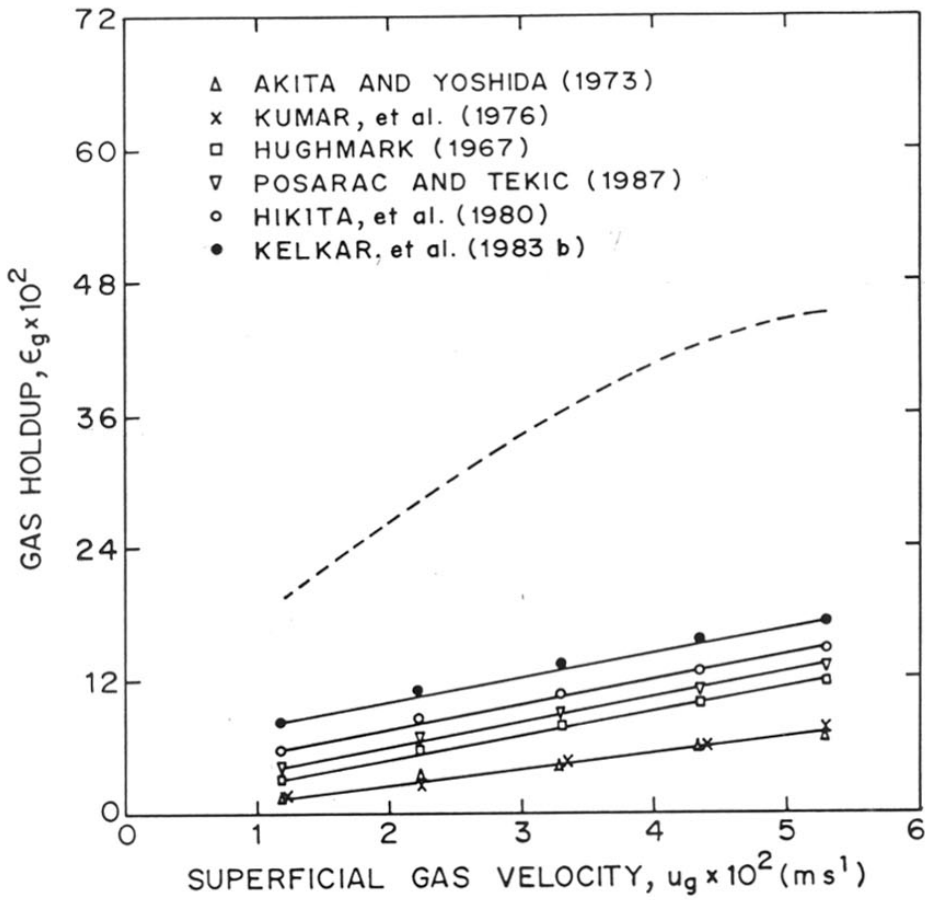


FIGURE 4-10: COMPARISON OF EXPERIMENTAL DATA (---) WITH VARIOUS LITERATURE CORRELATIONS (—) FOR AIR-AQUEOUS METHANOL SYSTEM (METHANOL-0.3%)

experimental results for these system with different correlations is shown in Figures 4.10 - 4.12.

The gas hold-up was found to increase substantially with increase in temperature, for the surfactants also. This has been demonstrated in Figures 4.13 and 4.14, for aqueous n-butanol and aqueous acetic acid, system. Similar trends were observed for other surfactants in the present study. However, in case of methanol the increase in gas hold-up was not uniform, which could be due to the its volatility at higher gas velocities and temperatures.

#### 4.3.4 Correlation of data

The differences observed with electrolytic solutions are mainly due to the non-coalescence behaviour of these system. Due to this phenomenon smaller bubble size and higher gas hold-up is generally observed. The theory of coalescence has been described by Marrucci (1969) [ liquid-phase diffusion model] and Sagert and Quinn (1978) [Dynamic surface tension model of Andrew, 1960]. On careful examination of these models it was noticed that one of the important dimensionless groups  $N_{CO}$ , describing the process of bubble coalescence is defined as :

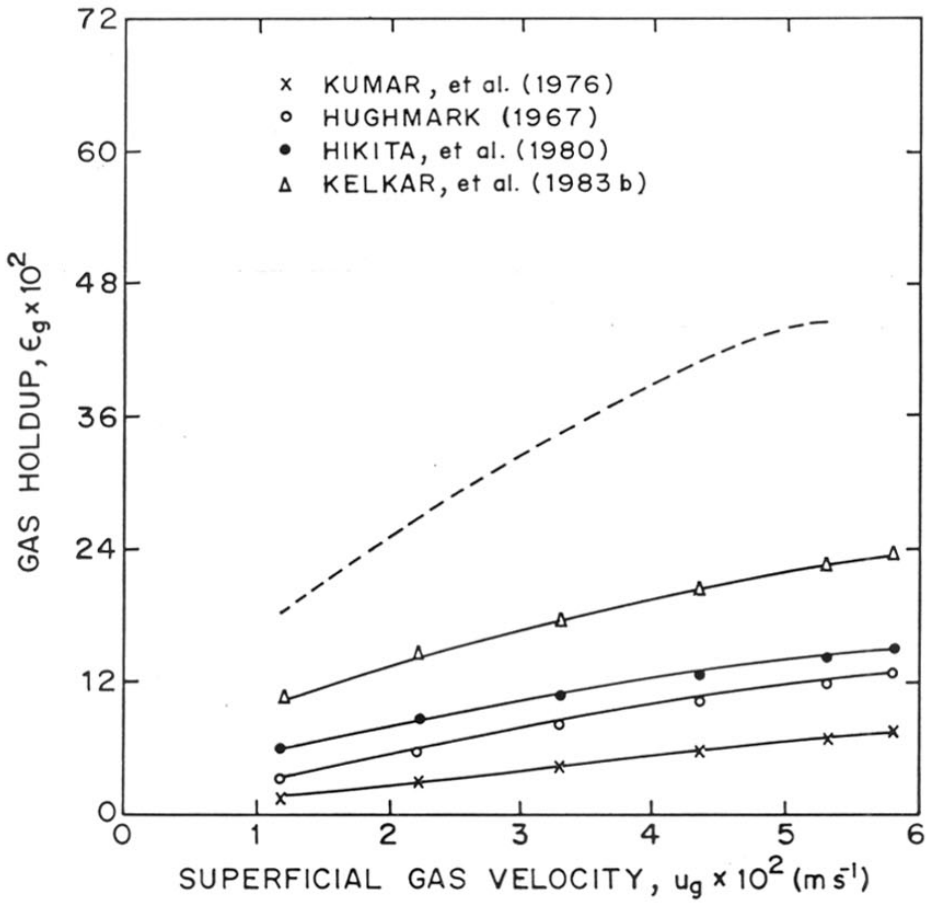


FIGURE 4-11: COMPARISON OF EXPERIMENTAL DATA (----) WITH VARIOUS LITERATURE CORRELATIONS (—) FOR AIR-AQUEOUS *n*-BUTANOL SYSTEM (*n*-BUTANOL = 0.001%)



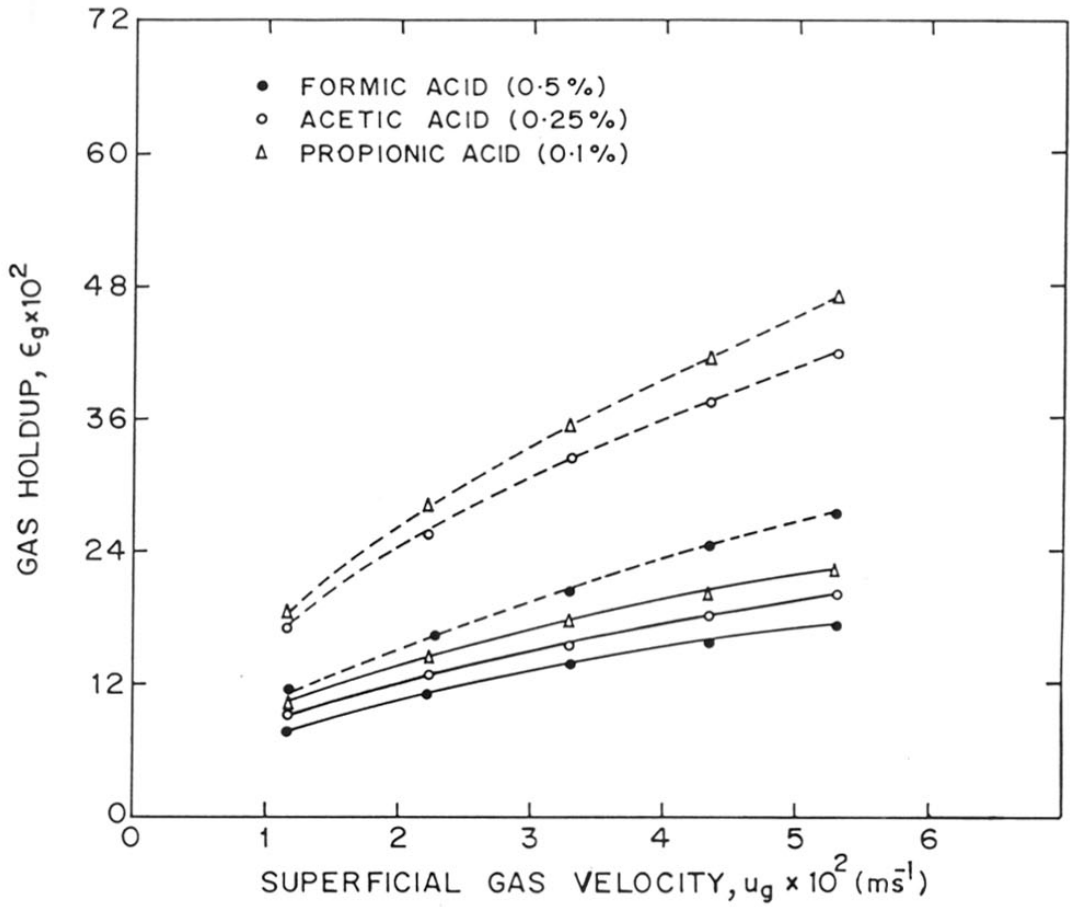


FIGURE 4.12 : COMPARISON OF EXPERIMENTAL DATA (---) WITH THE CORRELATION OF KELKAR et al (1983 b) (—) FOR CARBOXYLIC ACIDS

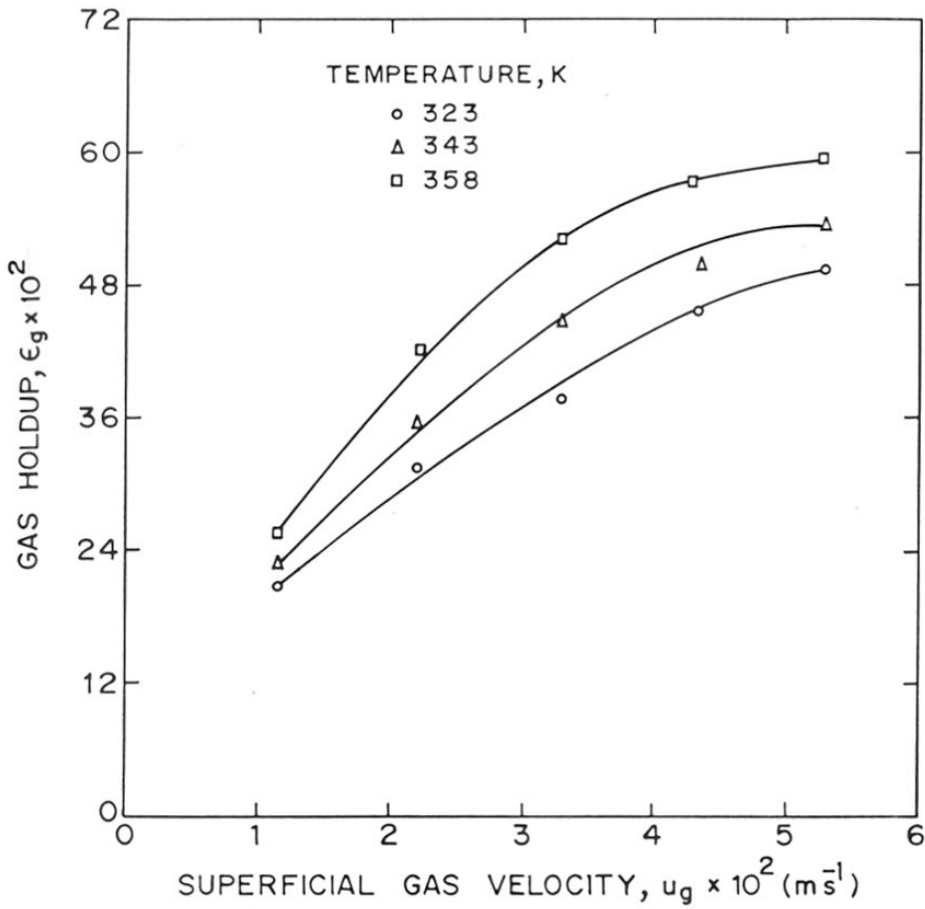


FIGURE 4.13 : GAS HOLDUP Vs  $u_g$  , AT DIFFERENT TEMPERATURES FOR AIR - AQUEOUS n-BUTANOL SYSTEM ( $n\text{-BuOH} = 0.001\%$ )

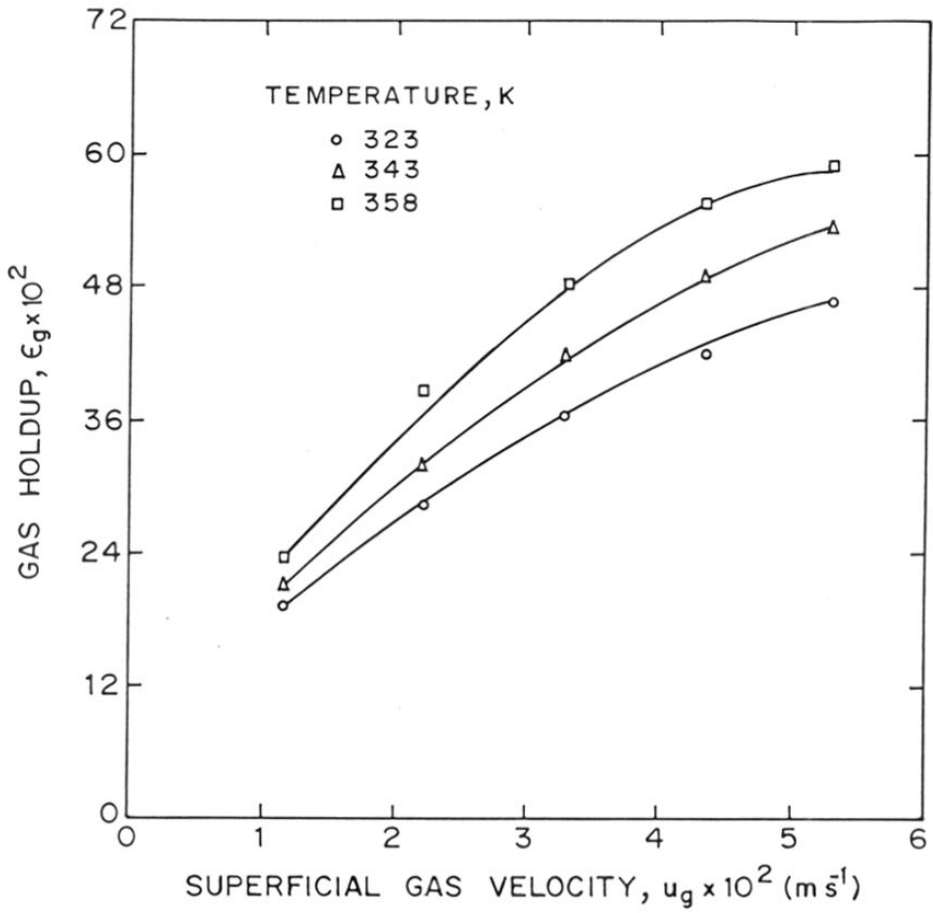


FIGURE 4-14: GAS HOLDUP Vs  $u_g$ , AT DIFFERENT TEMPERATURES FOR AIR-AQUEOUS ACETIC ACID SYSTEM (ACETIC ACID = 0.25%)

$$N_{CO} = \frac{Crk^2}{\gamma} \quad (2)$$

$$\text{where } c = \frac{2c}{\nu RT} \left( \frac{d\gamma}{dc} \right)^2 \quad (3)$$

and

$$k = \left( \frac{12\pi\gamma}{Ar} \right)^{1/3} \quad (4)$$

Sagert and Quinn (1978) have evaluated the significance of this parameter and concluded that for  $Crk^2/\gamma > 28-30$ , the coalescence is almost completely suppressed. Whereas for a value of  $Crk^2/\gamma < 2$ , the system tends to be a coalescing system. In between region of  $N_{CO}$  (2-30) would depend on the concentrations of the electrolytes and the surfactants. Based on this observation, a modified correlation for gas hold-up was used to represent the data :

$$\epsilon_g = 1.145 \left( \frac{u_g \mu_L}{\gamma} \right)^{0.578} \left( \frac{\mu_L^4 g}{\rho_L \gamma^3} \right)^{-0.131} \left( \frac{\rho_G}{\rho_L} \right)^{0.062} \times \left( \frac{\mu_G}{\mu_L} \right)^{0.107} \left( \frac{Crk^2}{\gamma} \right)^{0.0917} \quad (5)$$

Since, Hikita's correlation (1980) represented the data for air-water system in the present work satisfactorily, it was used as the basis for modification. Using the gas hold-up data for various types and concentration of electrolytes, the above correlation was evaluated. A comparison of the predicted and the observed gas hold-up is shown in Figure 4.15, which shows an excellent agreement. Figures 4.16 and 4.17 show  $\epsilon_g$  vs.  $u_g$  data for some electrolytes alongwith those predicted by previous correlations and equation (5). It is clear from Figures (4.16 and 4.17), that the correlation proposed in this work suitably accounts for the coalescence effect and explains the enhancement of the gas hold-up in the presence of electrolytes. It may be noted here, that the parameter  $Crk^2/\gamma$  is a function of  $d\gamma/dc$ , suggesting that  $d\gamma/dc$  is more important than the  $\gamma$  (surface tension) itself, in deciding the coalescence behaviour of the gas-liquid system. The data for changes in surface tension with the concentrations for some electrolytes were obtained directly from the literature (Marrucci and Nicodemo, 1967) and for others were evaluated from the literature correlations (Robinson and Stokes, 1959; and Horvath 1985). The values of  $d\gamma/dc$ , for various electrolytes are given in Table 4.III.

Following a similar approach, the hold-up data obtained for aqueous surfactants solution were also

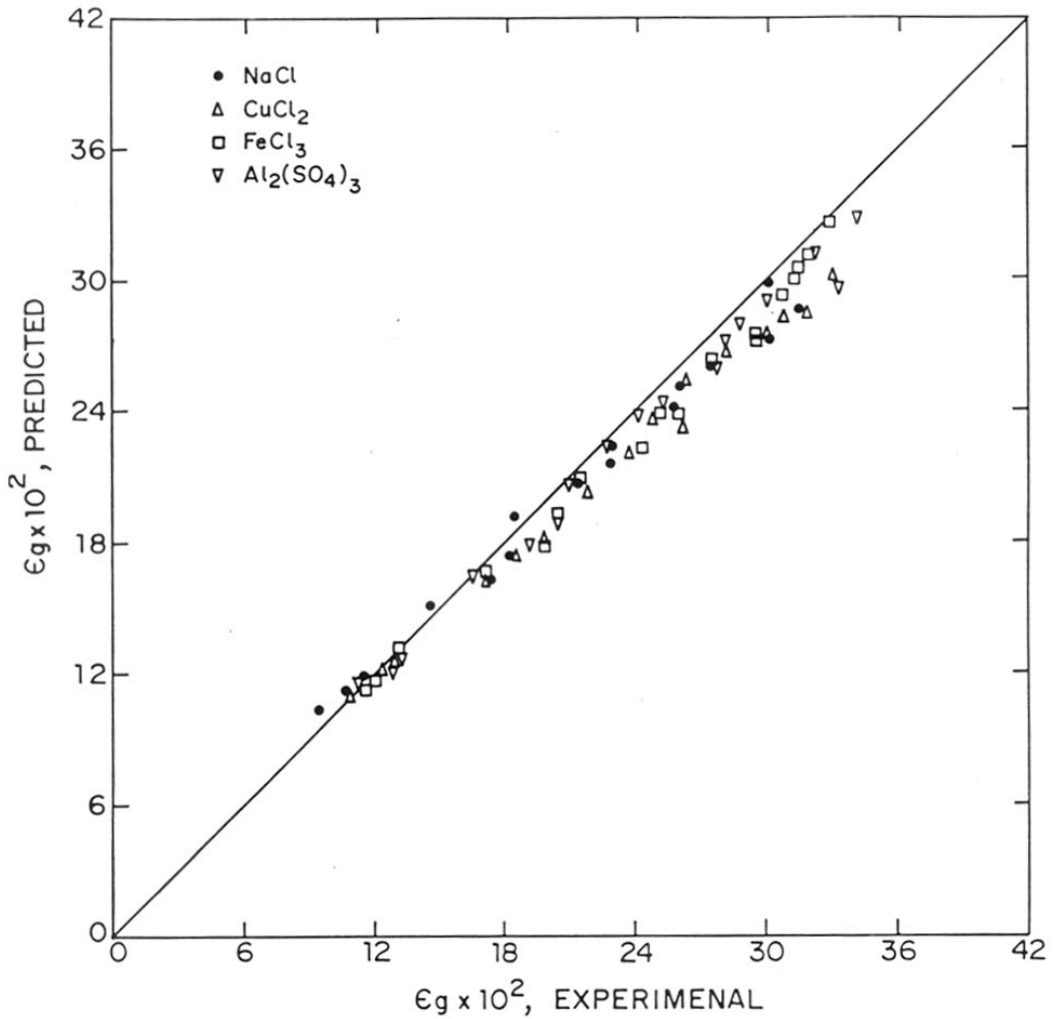


FIGURE 4.15 : COMPARISON OF THE PRESENT DATA WITH THE PROPOSED CORRELATION FOR GAS HOLDUP FOR ELECTROLYTIC SOLUTIONS (Eq.(5)) (CONCENTRATION RANGE: 0.1 M-0.5 M)

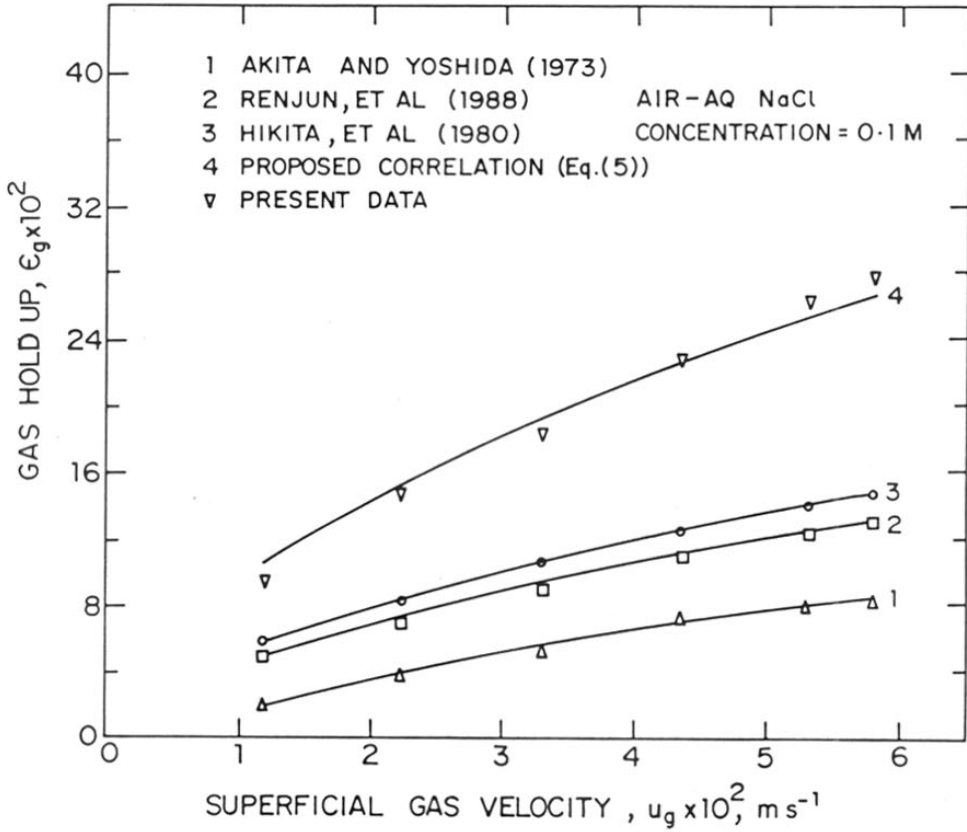


FIGURE 4.16 : COMPARISON OF EXPERIMENTAL DATA WITH VARIOUS LITERATURE CORRELATIONS AND THE PROPOSED CORRELATION (Eq.(5))

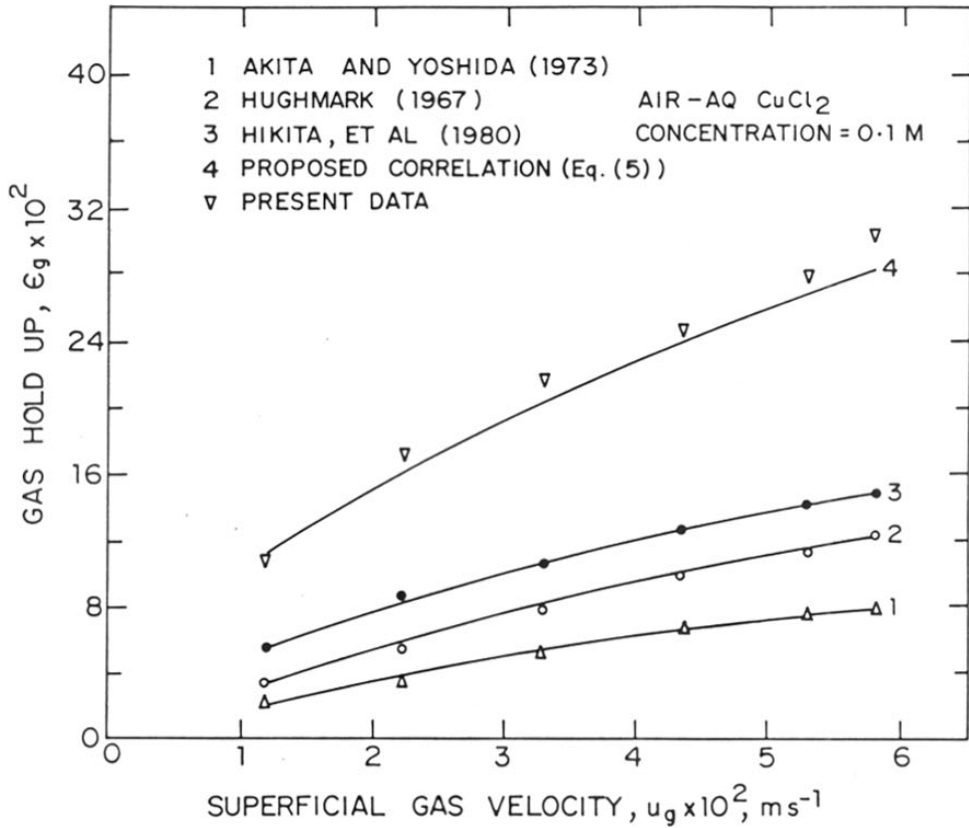


FIGURE 4.17 : COMPARISON OF EXPERIMENTAL DATA WITH VARIOUS LITERATURE CORRELATIONS AND THE PROPOSED CORRELATION



TABLE 4. III : VALUES OF  $d\gamma/dc$  FOR ELECTROLYTES

Electrolyte	$d\gamma/dc \times 10^6,$ Nm <sup>2</sup> /mol
NaCl	1.40
CuCl <sub>2</sub>	1.83
FeCl <sub>3</sub>	2.1
Al <sub>2</sub> (SO <sub>4</sub> ) <sub>3</sub>	2.16

TABLE 4. IV : VALUES OF  $d\gamma/dc$  AND  $Crk^2/\gamma$  FOR SURFACTANTS

Surfactant	$d\gamma/dc \times 10^6,$ $Nm^2/mol$	$Crk^2/\gamma$
Methanol	3.30	31.22
n-butanol	86.67	275.00
Formic acid	1.90	7.1
Acetic acid	4.56	50.75
Propionic acid	5.17	100.00

evaluated. For the system investigated in this work, the values of the parameter,  $Crk^2/\gamma$ , were evaluated and these are presented in Table 4.IV. For the purpose of estimating  $d\gamma/dc$ , the literature data (Reid and Sherwood, 1966; and Tamura et al., 1955) on change in surface tension with concentration of surfactants were fitted using polynomial regression method. These values indicate that except in the case of formic acid, the systems represent an asymptotic regime of the non coalescence behaviour where the coalescence is almost entirely suppressed. The observations of gas hold-up is consistent with change in  $Crk^2/\gamma$ . Using the gas hold-up data for various types and concentrations of surfactants the following correlation was evaluated :

$$\epsilon_g = 0.672 \left( \frac{u_g \mu_L}{\gamma} \right)^{0.578} \left( \frac{\mu_L^4 g}{\rho_L \gamma^3} \right)^{-0.131} \left( \frac{\rho_G}{\rho_L} \right)^{0.062} \left( \frac{\mu_G}{\mu_L} \right)^{0.107} \left( \frac{0.82 Crk^2/\gamma}{1 + 0.154 Crk^2/\gamma} \right) \quad (6)$$

A comparison of the predicted and observed gas hold-up is shown in Figure 4.18. Figure 4.19 shows  $\epsilon_g$  vs.  $u_g$  data for methanol and n-butanol systems alongwith

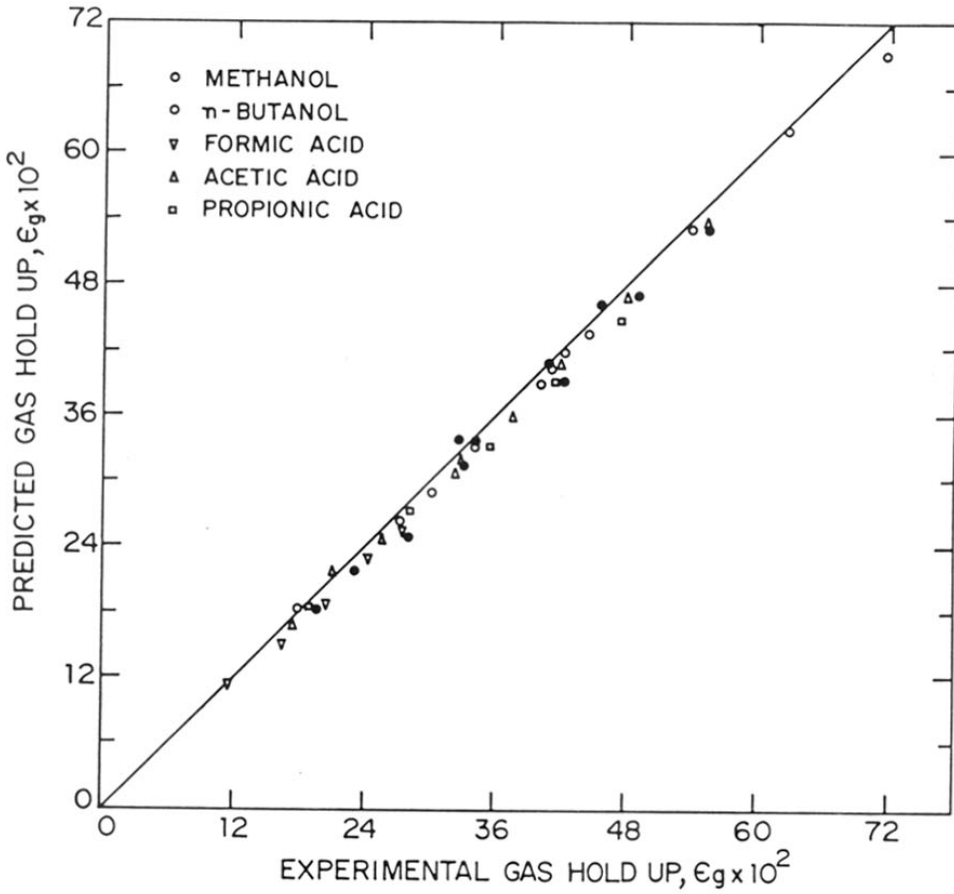


FIGURE 4.18: COMPARISON OF THE EXPERIMENTAL DATA WITH THE PROPOSED CORRELATION FOR VARIOUS SURFACTANTS (Eq.(6))

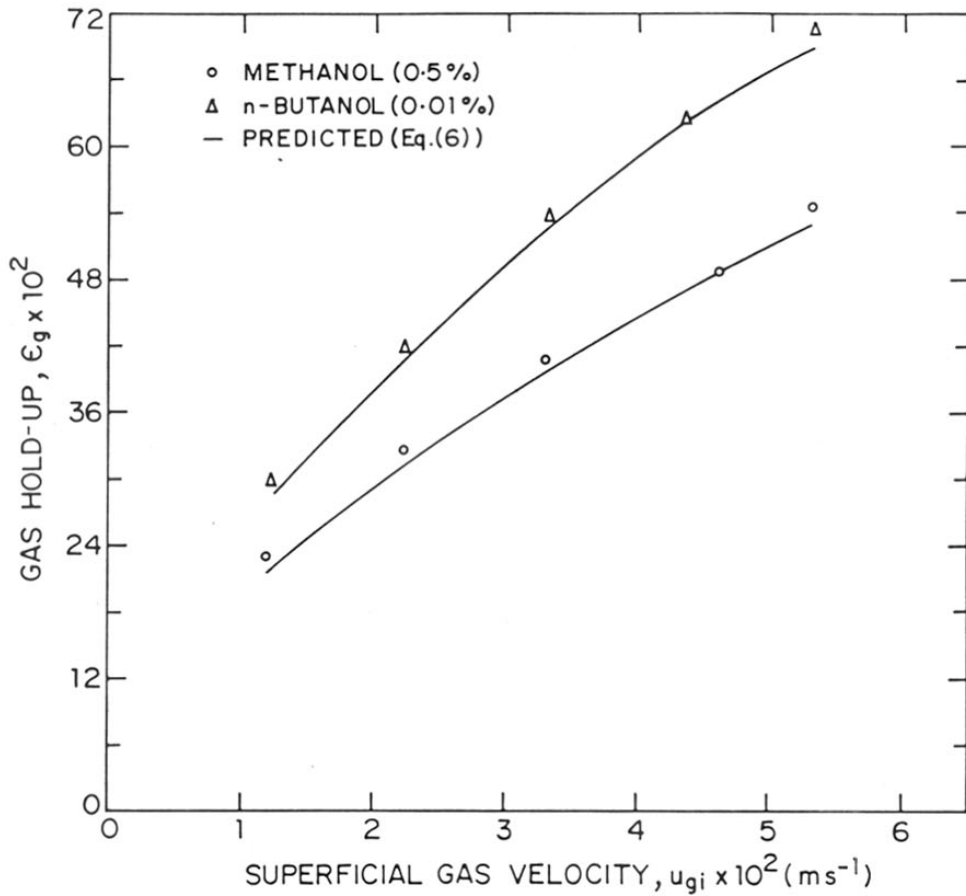


FIGURE 4.19: COMPARISON OF THE EXPERIMENTAL DATA WITH THE PROPOSED CORRELATION (—), FOR AIR-AQ METHANOL AND AIR-AQ n-BUTANOL, SYSTEMS

the predictions by the equation (6). Both these figures show an excellent agreement of experimental data with the prediction of the proposed correlation, indicating a significant contribution of the parameter,  $Crk^2/\gamma$ , to the non-coalescing tendency of the surfactants.

It may be noted that the correlation proposed here, both for electrolytes and surfactants were used to represent the data at ambient temperature (303K). However, these can be modified for higher temperatures by incorporating the vapour pressure of the solvent and the surface tension gradient at those temperatures.

#### 4.3.5 Flow regimes

The effect of temperature on the flow regime characteristics of a bubble column was studied for air-water, air-electrolyte and air-surfactant systems. For this purpose, the drift flux theory described by Wallis (1969) was used. The drift flux of the gas for a semibatch operation is defined as

$$j_{GL} = u_g (1 - \epsilon_g) \quad (7)$$

The drift flux charts were prepared based on the observed gas hold-up vs. superficial gas velocity data and some typical results are shown in Figures 4.20 -

4.23. From the flow regime charts of the drift flux vs. gas hold-up, the condition of the transition from bubble flow to churn turbulent flow regime is indicated by a change in the slope of the curve. In the present work, it was found that the visually observed transition gas velocity was in reasonable agreement with that obtained from the drift flux charts.

The effect of temperature on the flow regime transition for the air-water system was found to be most interesting (see Figure 4.24). At lower temperature (303K), the bubble flow regime was operating over a wide range of gas velocity, while with increase in the temperature the degree of coalescence was also increased substantially, causing a change in the operating flow regime. The gas velocity, at which the transition from the bubble flow to churn turbulent flow regime occurs, as a function of temperature, is shown in Figure 4.24, which clearly indicates that increase in temperature results a decrease in the transition gas velocity ( $u_{gT}$ ). The influence of temperature on the flow regime characteristics in the presence of NaCl, CuCl<sub>2</sub> and n-butanol is shown in Figures 4.21 to 4.23. Here, it was observed that due to non-coalescing tendency of the solutions, the gas velocity for the transition from bubble flow to churn turbulent flow regime was found to be higher than in the air-water system. Nevertheless,  $u_{gT}$  was found to decrease with

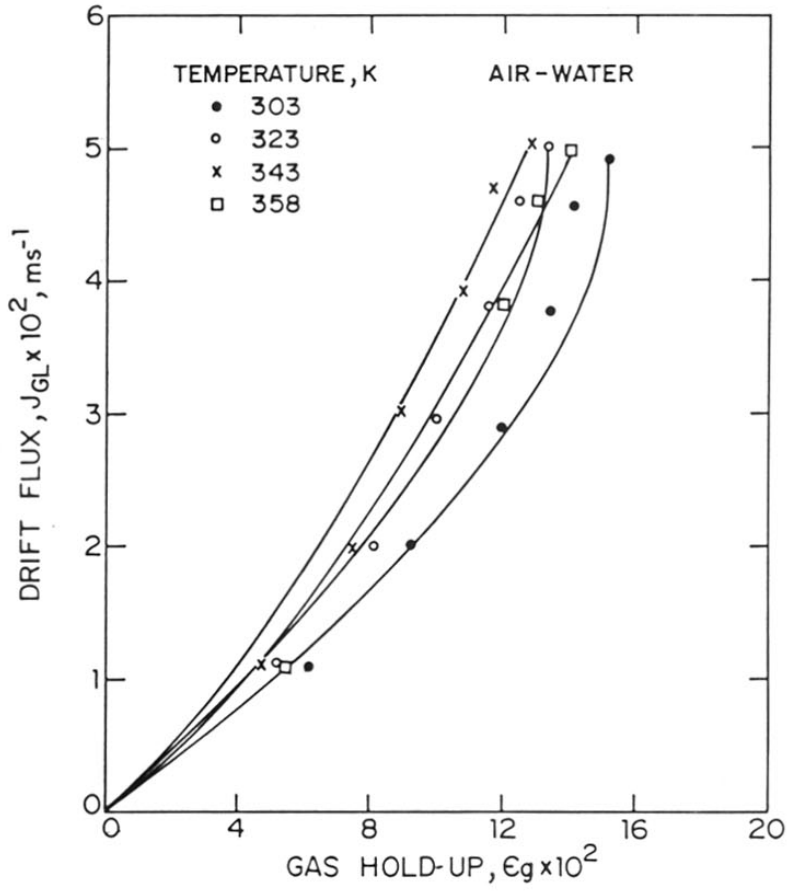


FIGURE 4.20: DRIFT FLUX Vs GAS HOLD UP FOR AIR-WATER AT DIFFERENT TEMPERATURES



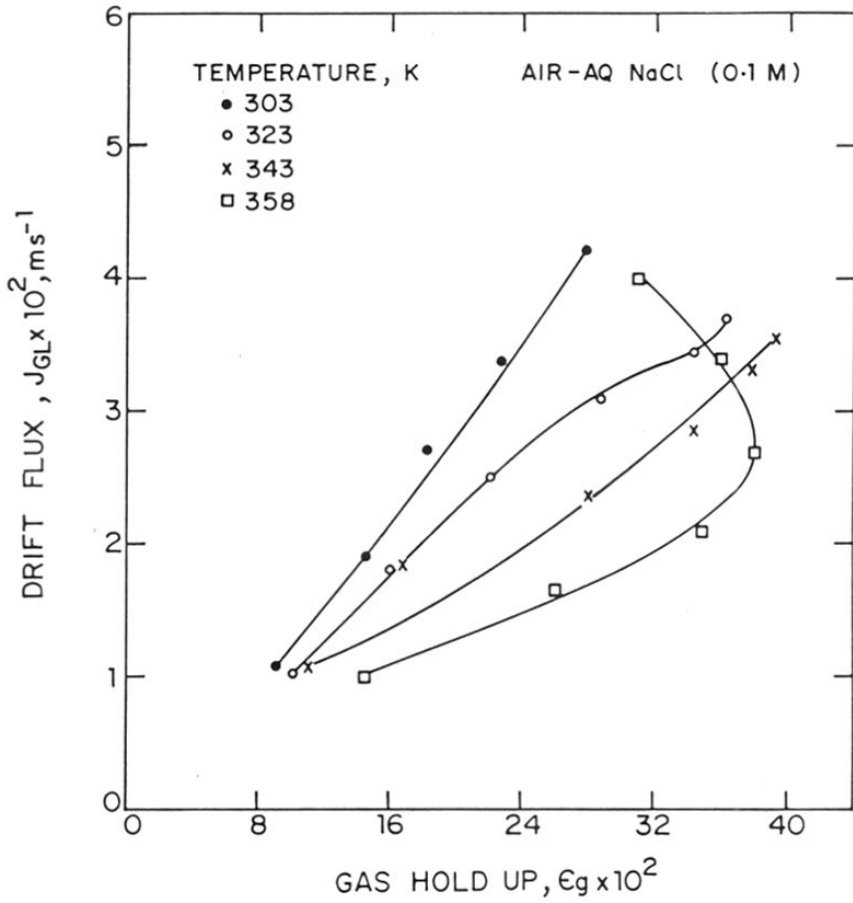


FIGURE 4.21: DRIFT FLUX Vs GAS HOLD UP FOR AIR-AQUEOUS NaCl AT DIFFERENT TEMPERATURES

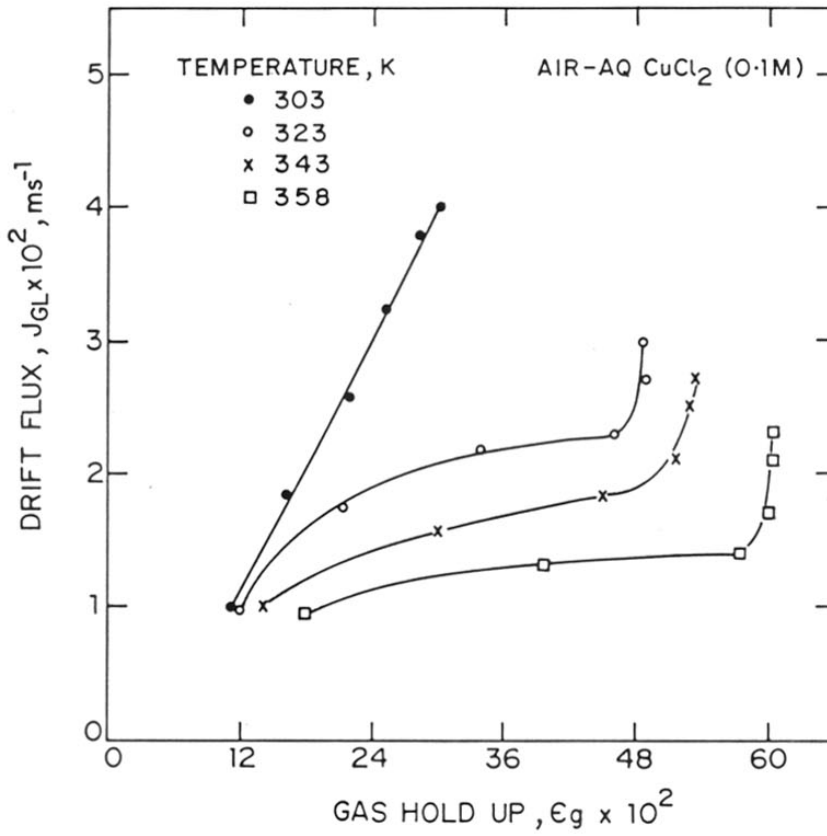


FIGURE 4.22: DRIFT FLUX VS GAS HOLD UP FOR AQUEOUS  $\text{CuCl}_2$  AT DIFFERENT TEMPERATURES

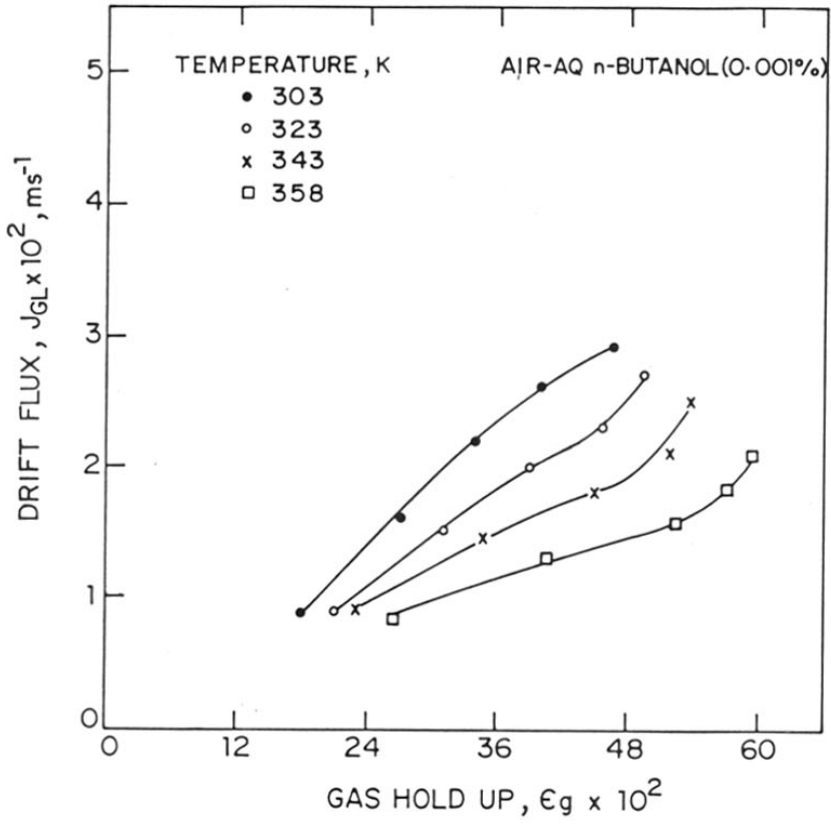


FIGURE 4.23: DRIFT FLUX Vs GAS HOLD UP FOR AQUEOUS n-BUTANOL AT DIFFERENT TEMPERATURES

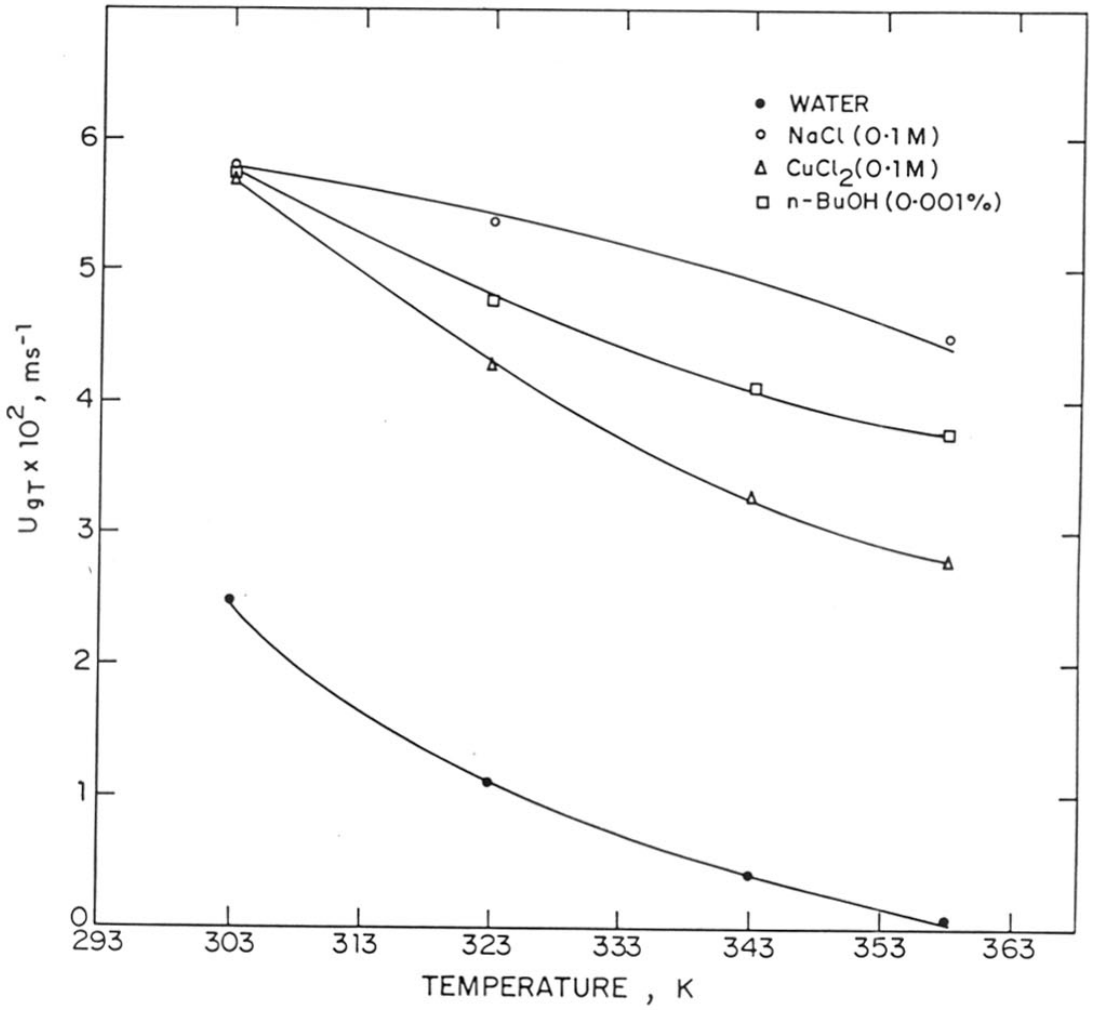


FIGURE 4.24 : TRANSITION GAS VELOCITY Vs TEMPERATURE FOR DIFFERENT SYSTEMS

temperature even for electrolytes and surfactants [ see Figure 4.24 ].

#### 4.4 CONCLUSIONS

Extensive experimental data on gas hold-up, in presence of different types of electrolytes and surfactants have been collected, in a bubble column reactor. Effect of concentrations and temperature on the gas hold-up was also studied. Experimental data were compared with various literature correlation for gas hold-up. It was found that none of the correlations could predict the higher gas hold-up observed in case of non coalescing systems such as electrolytes and surfactants. Two different correlations have been proposed to represent the gas hold-up for aqueous electrolytes and aqueous surfactants systems. A parameter  $N_{CO}$ , has been incorporated in both these correlations, which basically is a function of surface tension gradient ( $d\gamma/dc$ ) indicating that  $d\gamma/dc$  is more important than the surface tension itself, in suppressing the coalescence.

It was also found that increase in temperature has considerable effect on the gas hold-up and flow regime characteristics in a bubble column reactor. In case of both electrolytes and surfactants, the gas hold-up was found to increase with increase in temperature. The

transition gas velocity ( $u_{gT}$ ) at which the flow regime changes was found to decrease with increase in temperature. However,  $u_{gT}$  in case of non coalescing systems was always more than that of air-water system.

## NOMENCLATURE :

A	:	Hamaker - London constant for water, $3.5 \times 10^{-20}$ J
C	:	as defined by equation (3)
c	:	concentration of solute, kmol/m <sup>3</sup>
g	:	acceleration due to gravity, m/s <sup>2</sup>
H <sub>E</sub>	:	height of expanded bed, m
H <sub>o</sub>	:	height of non-aerated bed, m
J <sub>GL</sub>	:	drift flux, as defined by equation, (7)
N <sub>co</sub>	:	dimensionless group defined by equation (2)
R	:	gas constant, 8.314 J/mol/K
r	:	bubble radius, m
U <sub>gT</sub>	:	transition gas velocity, m/s
u <sub>g</sub>	:	superficial gas velocity, m/s

## Greek symbols

ε <sub>g</sub>	:	fractional gas holdup
γ	:	surface tension, N/m
ρ <sub>G</sub>	:	gas density, kg/m <sup>3</sup>
ρ <sub>L</sub>	:	liquid density, kg/m <sup>3</sup>
μ <sub>G</sub>	:	gas viscosity, Pa.s
μ <sub>L</sub>	:	liquid viscosity, Pa.s

## REFERENCES

1. Akita, A. and Yoshida, F., Ind. Eng. Chem. Proc. Des. Dev. **12** (1973) 76.
2. Albright, L.F., Chem. Eng., (Jan. 16, 1967a), 169.
3. Albright, L.F., Chem. Eng., (Oct. 6, 1967), 249.
4. Albright, L.F., Chem. Eng., (Nov. 6, 1967), 251.
5. Andrew, S.P.S., 'Int. Symp. on distillation', Ed. P.A. Rottenburg, Inst. of Chem. Engrs., London, (1960).
6. Bach, H.F., Pilhofer, T., Germ. Chem. Eng., **1**, (1978), 270.
7. Baltes, J.B., Cornils, B. and Frohning, C.D., Chem. Ing. Tech., **47**, (1975), 522.
8. Bayer Turmbiologie, Bayer Prospects D. 991-7127/89 77797.
9. Deckwer W. D., Burckhart, R. and Zoll G., Chem. Eng. Sci. **29** (1974) 2177.
10. Deckwer W. D., and Schumpe, A., "Two-phase Momentum, Heat and Mass Transfer in Chemical Process and Engineering Systems", Ed. F. Durst, G.V. Tskilauri, and N.H. Afgan, **2**, Hemisphere Pub. Corp., Washington, D.C. (1970).
11. Deckwer, W.D., 'Reaktionsterchnik in Blassensaulen', Salle + Sauerlander, Frankfurt, (1985).
12. Fair, J.R., Chem. Eng., **74**, (1967), 67.



13. Franck, H.G., and Knop, A., "Kohleveredelung-  
Chemie and Technologie", Springer Verlag,  
New York (1979).
14. Gates, B.C., Katzer, J.R., and Schiut, C.G.A.,  
"Chemistry of Catalytic Processes", Mc Graw-Hill,  
New York (1979).
15. Hikita, H., Asai, S., Tanigawa, K., Segawa, K.,  
and Kitao, M., Chem. Eng. J., **20**, (1980), 59.
16. Hills, J.H., and Darton, R.C., Trans. Inst. Chem.  
Engrs., **54**, (1976), 258.
17. Hines, D.A., Proc. 1st Eur. Congr. Biotechn. CH-  
Interlaken, Sept. 1978, Dechem. Monographs, **82**,  
Verlag Chemie, Weinheim, (1978).
18. Hjortkjaer, J., and Jensen, V.W., Ind. Eng. Chem.  
Proc. Des. Dev., **15**, (1976), 46.
19. Hofermann, H., Chem. - Ing. - Tech., **36**, (1964),  
422.
20. Horvath, A.L., 'Handbook of Aqueous Electrolyte  
Solutions', Ellis Horwood Ltd., U.K. (1985).
21. Hughmark, G.A., Ind. Eng. Chem. Proc. Des. Dev.,  
**6**, (1967), 218.
22. Jira, R., Balu, W., and Grimm, D., Hydrocarbon  
Process., (March, 1976), 97.
23. Joshi, J.B., and Sharma, M.M., Trans. Inst. Chem.  
Engrs., **54**, (1976), 42.

24. Kaeding, W.W., Lindblom, R.O., Temple, R.G., and Mahon, H.I., *Ind. Eng. Chem. Proc. Des. Dev.*, **4**, (1963), 97.
25. Katinger, H.W.D., Scheirer, W., and Kromer, E., *Ger. Chem. Eng.* **2**, (1979), 31.
26. Kawagoe, K., Inove, T., Nakao, K., and Otake, T., *Int. Chem. Eng.*, **16**, (1976), 176.
27. Kelkar, B.G., Phulgaonkar, S.R., and Shah, Y.T., *Chem. Eng. J.*, **27**, (1983a), 125.
28. Kelkar, B.G., Godbole, S.P., Honath, M.F., Shah, Y.T., Carr, N.L., and Deckwer, W.D., *AIChE. J.*, **29**, (1983b), 361.
29. Kolbel, H. and Ralek, M., "Chemierohstoffe aus Kohle", Ed. J. Falbe and G. Jhieme Verlag, Stuttgart, (1977).
30. Kolbel, H., and Ralek, M., *Catal. Rev. Sci. Eng.*, **27** (2) (1980). 225.
31. Kostyak, N.G., Lov, S.V., Falkorski, V.B., Starkov, A.V., and Levina, N.M., *J. Appl. Chem. USSR*, **35**, (1962), 1939.
32. Krekeler, H., and Schmitz, H., *Chem. - Ing.-Tech.*, **40**, (1968), 785.
33. Kulkarni, A., Shah, Y.T., and Kelkar, B.G., *AIChE. J.* **33**, (1987), 690.
34. Kumar, A., Dagalaesan, T., Laddha, G.S., and Hoelscher, H.E., *Can. J. Chem. Eng.*, **54**, (1976), 503.

35. Marrucci, G., Chem. Eng. Sci., **24**, (1969), 975.
36. Marrucci, G., and Nicodemo, L., Chem. Eng. Sci., **22**, (1967), 1257.
37. Mashelkar, R.A., Brit. Chem. Eng., **15** (10), (1970), 1297.
38. Moo - Young, M., Can. J. Chem. Eng., **53** (1975), 113.
39. Ohorodnik, A., Sennewald, K., Hindeck, J., and Statzke, P., U.S. Pat., 3, 901, 660 (1975).
40. Oliver, K.L., and Booth, B., Hydrocarbon Process, **49**, (1970), 112.
41. Ozturk, S.S., Schumpe, A., and Deckwer, W.D., AIChE. J. **33**, (1987), 1473.
42. Posarac, D., and Tekic, M.N., AIChE. J. **33**, (1987), 497.
43. Ramachandran, P.A., and Chaudhari, R.V., 'Three Phase Catalytic Reactors', Gordon and Breach Sci. Pub., N.Y. (1983).
44. Reid, R.C., and Sherwood, T.K., 'The Properties of Gases and Liquids', 2nd Ed., McGraw-Hill, New York, (1966).
45. Renjun, Z., Xinzhen, J., Baozhang, L., Yong, Z., and Laigio, Z., Ind. Eng. Chem. Res. **27**, (1988), 1910.
46. Robinson, R.A. and Stokes, R.H., 'Electrolyte Solutions', Butterworths, London, (1959).

47. Sagert, N.H. and Quinn, M.J., Chem. Eng. Sci., 33, (1978), 1087.
48. Saunby, J.B., and Kiff, B.W., Hydrocarbon Process., (1976), 247.
47. Schugerl, K., Lucke, J., Lehmann, I., and Wagner, F., Adv. Biochem. Eng., 8, (1978), 63.
48. Schumpe, A., Serpemen, Y., and Deckwer, W.D., Ger. Chem. Eng., 2, (1979), 234.
49. Shah, Y.T., Kelkar, B.G., Godbole, S.P., and Deckwer, W.D., AIChE. J., 28 (1982), 353.
50. Shah, Y.T., and Deckwer, W.D., 'Scale-up in Chemical Process Industries', Ed. R. Kabel and A. Bisio, John Wiley, (1981).
51. Shah, Y.T. "Reaction Engineering in Direct Coal Liquefaction", Addison - Weiley Pub. Co., Reading, MA (1981).
52. Sherwin, M.B., and Frak, M.E., Hydrocarbon Process, 55, (1976), 122.
53. Sittig, M., "Organic Chemical Process Encyclopedia", Noyer Develop. Corp. U.S.A. (1967).
54. Smidt, J., Hofner, W., Jira, R., Sedimeior, J. Sieler, R., Ruttinger, R., and Kojer, H., Angew. Chem. 71, (1959), 176.
55. Smith, E.L., and Greenshielch, R.M., Chem. Eng. 81, (1974), 28.
56. Tamura, M., Kurata, M., and Odani, H., Bull. Chem. Soc. Japan, 28, (1955), 83.

57. Wallis, G.B., 'One Dimensional two Phase Flow', McGraw - Hill, Pub., N.Y. (1969).
58. Weissermel, K., and Arpe, H.J., "Industrielle Organische Chemie", Verlag Chemie, Weinheim, New York (1976).
59. Zheng, C., Yao, B., and Feng, Y., Chem. Eng. Sci., **43**, (1988), 2195.
60. Zlokarnik, M., Adv. Biochem. Eng. **8**, (1978), 133.

**PART II**

**HYDROGENATION OF  
META-NITROCHLOROBENZENE  
TO META-CHLOROANILINE IN  
A SLURRY REACTOR**

# **CHAPTER 1**

## **INTRODUCTION**

## 1.1 GENERAL BACKGROUND

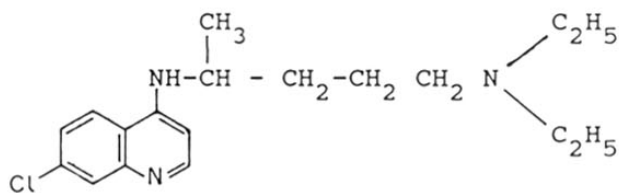
Slurry reactors have extensive applications in chemical industries, particularly in the liquid phase catalytic hydrogenation of organic compounds. Due to the presence of three phases (gas, liquid and solid), mass transfer, mixing and surface chemical reaction, play important roles in the overall performance of slurry reactors. These aspects need to be studied critically, while designing the slurry reactors. For any specific system of practical importance, a knowledge of intrinsic kinetics of the reaction is most essential in order to develop suitable reactor models. Such a study is also important, in providing a design basis and scale up of large scale reactors. The aim of the present work was to study the reaction engineering aspects of hydrogenation of meta-nitrochlorobenzene (MNCB) to meta-chloroaniline (MCA) in the liquid phase, using 1% Pt-S/C, as a catalyst. Aromatic amines are important intermediates in the manufacture of dyestuffs, agricultural products, polymers, rubber chemicals, drugs and photographic chemicals.

m-Chloroaniline is extensively used as an intermediate with diverse applications in dyes, drugs and pesticides. Azoic, azo, mordant and even vat dyes and pigments are derived from m-chloroaniline. Permanent



orange GTR pigment, obtained from m-chloroaniline is used in the printing inks which have very good fastness to water, oil and heat. Azo dyes derived from m-chloroaniline are useful for dyeing variety of fabrics like cotton, viscose rayon, wool, silk and fur, in various shades of bright orange, red, khaki and brown with very good light and washing fastness properties. (Venkataraman, 1952).

The established drugs derived from m-chloroaniline are mainly antimalarials, diuretics and tranquilizers. Among the antimalarials, chloroquine (1) (Surrey and Hammer, 1946) and amodiaquin (Blicke, 1942) are well known examples. A number of thiazide diuretic

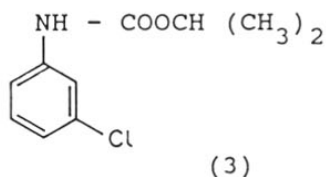
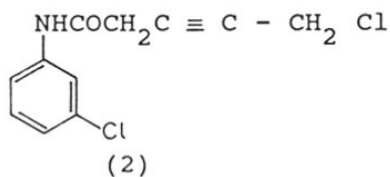


(1)

and hypertensive drugs are prepared from 3-chloroaniline-4,6-disulphonamide, which is a valuable intermediate, obtained by the chlorosulphonation of MCA followed by reaction with ammonia. Chlorpromazine hydrochloride, derived from MCA, is an important tranquilizer drug.

Among the herbicides, derived from MCA, carbyne

(barban) (2) (Hopkins, et al., 1959), is selective for pre- and post - emergence control of grasses in crops such as wheat, mustard, peas and sunflower. While the



other one, chloro IPC (chloroproham) is used for the control of weeds in fruits and vegetables.

m-chloroaniline acts as a solvent and plasticizer for polyesters (Ger. offen. 1956). It is also being used as an excellent corrosion inhibitor for steel and aluminium alloys in acids at different concentrations. (Every and Riggs, 1964; and Talati and Pandya, 1976).

In view of the importance of m-chloroaniline in industry it was thought necessary to study the engineering aspects of this process. The following aspects of this problem were studied :

- o Kinetic modelling of hydrogenation of MNCB using a

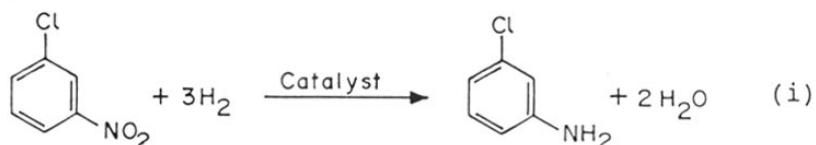
Pt-S/C catalyst.

- o Modelling of a batch slurry hydrogenation reactor to compare the theory and experiments under isothermal and non-isothermal conditions.

In this chapter, a detailed survey of literature on the above reaction system and status of development in analysis of slurry reactors has been summarized.

### 1.1.1 Reaction

Hydrogenation of m-nitrochlorobenzene can be represented as :



In the reduction of the nitro group the oxygen is progressively replaced by hydrogen. The reaction is a highly exothermic process, the heat of reaction being about 545 kJ/mol (Mcnab, 1981). The catalytic hydrogenation of nitro group is believed to proceed sequentially through the nitroso and hydroxylamine intermediates. The widely accepted reaction mechanism is shown in Figure 1.1, which was deduced by Haber (1898), from his work on the electrochemical reduction of

nitrobenzene.

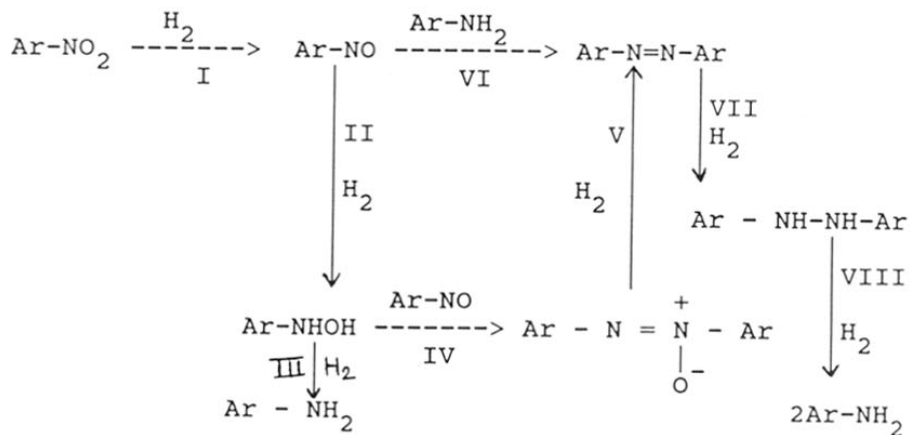


Figure : 1.1 Haber reduction scheme

### 1.1.2 Literature Survey

The reduction of nitro compounds was carried out in earlier days using iron and acid reagent system (Bechamp 1854a; 1854b; Meldola 1908). Subsequently, many other reduction methods using reagents like sulfides, zinc in neutral or acid solutions, stannous chloride in HCl, metal hydrides or amalgams, were developed. Stratz (1984), has reviewed this chronological development of reduction methods of nitro compounds to amines. After 1950, a new era started in this field, with the development of catalytic vapour phase hydrogenation processes for reduction of nitro compounds (U.S. Pat.,

1955). Catalytic hydrogenation, gives a purer product at a lower cost and has major advantages with respect to environmental pollution and waste disposal. At the same time liquid phase hydrogenation processes using suspended catalysts were also developed and commercialized by Du Pont (U.S. Pats., 1952 and 1958), G.A.F. Corp. (U.S. Pat., 1963) and Tolochemie (Belg. Pat., 1977) for reduction of nitrobenzene to aniline. Presently, the processes via liquid phase catalytic hydrogenation are preferred for reduction of aromatic nitro compounds to amines using supported metal catalysts and some important examples of this class are presented in Table (1.I).

Catalytic hydrogenation of halo nitrocompounds is an industrially important reaction in the manufacture of chloroanilines such as o-,m- and p- chloroanilines. During this process dehalogenation is also encountered which is not desirable. However, recently catalysts and processes have been developed, which can be applied commercially, for the selective reduction of halo nitro compounds. A summary of catalysts used in these processes is presented in Table (1.II). However, most of the processes given in this table were accompanied by the formation of dehalogenated products to some extent. Further developments in achieving selective hydrogenation of halo nitrocompounds were the use of specially modified platinum on carbon catalysts. Three types of modifications

of such platinum catalysts exist. These are :

- 1) platinum catalyst with triphenyl phosphite
- 2) sulfided platinum catalyst and
- 3) platinum catalyst with morpholine

Table 1.III shows a comparison of performance of these catalysts for the hydrogenation of 3,4-dichloronitrobenzene under the same temperature and pressure conditions. It can be seen from this table that sulfided Pt catalyst yielded the highest purity product. Other investigators also have obtained high selectivities over sulfided platinum on carbon (Ger. Offen. 1971, 1973). Dovell and Greenfield (1967) obtained chloroanilines from corresponding nitrochloro benzenes, practically without any dehalogenation by using sulfides of platinum, rhodium and ruthenium.

Excellent results have been reported by using newly developed, improved sulfided platinum on carbon catalyst F -103-RSH, 5 % Pt (Degussa 1980). Various halonitro aromatics such as o-,m-,p- nitrochlorobenzene, p -nitrobromo benzene, were hydrogenated using this catalyst with a selectivity in the range of 99.8-100 % (Stratz 1984).

TABLE I. I : EXAMPLES OF LIQUID PHASE CATALYTIC HYDROGENATION  
OF NITROCOMPOUNDS

Sr. No.	Nitro Compounds	Catalyst	Process	Company	Reference
1.	Nitroxylene	Ni on kieselguhr	Liquid phase continuous	Shell	U.S. Pat. (1949).
2.	Nitroarenes	PtO <sub>2</sub>	Liquid phase batch	Shell	Brit. Pat. (1975).
3.	dinitro chlorobenzene	activated Ni	Liquid phase batch	Boyle Midway	U.S. Pat. (1949).
4.	Various	Various	Liquid phase batch	UOP	U.S. Pat. (1954).
5.	Nitro benzene	Ni on kieselguhr	Liquid phase continuous	ICI	Belg. Pat. (1965).
6.	Nitrobenzene	Ni on kieselguhr	Liquid phase batch	ICI	Brit. Pat. (1965) Brit. Pat. (1968).
7.	1-nitroanthra-quinone	Pd on carbon	Liquid phase batch	BASF	Ger. Pat. (1974).

TABLE 1. II : SELECTIVE LIQUID PHASE HYDROGENATION OF HALONITRO-AROMATICS

Sr. No.	Nitro Compounds	Catalyst	Reference
1.	m-nitrochloro benzene	Rh/Al <sub>2</sub> O <sub>3</sub>	U.S. Pat. (1956).
2.	m-nitrochloro benzene	CaO / Cr <sub>2</sub> O <sub>3</sub>	U.S. Pat. (1957).
3.	o- and p-nitro chlorobenzene	Ru, Pd / C	Bavin (1958)
4.	m-nitrobromo benzene	Rh + Ca(OH) <sub>2</sub>	U.S. Pat. (1962).
5.	p-nitrochloro benzene	Pt-BaCO <sub>3</sub> or Pt - SrCO <sub>3</sub>	Fr. Pat. (1966).
6.	dichloronitro benzene	Pt / Al <sub>2</sub> O <sub>3</sub>	Fr. Pat. (1967).
7.	halonitro benzene	Ru + S	Dovell and Greengfield (1967).
8.	halo-nitro benzene	Pt / Al <sub>2</sub> O <sub>3</sub>	Fr. Pat. (1967).
9.	o-nitro chloro benzene	Ni + Zr on kieselguhr	U.S. Pat. (1972).
10.	halo nitro arenes	Rh	Fr. Pat. (1974).



TABLE 1. III      COMPARISON OF MODIFIED Pt CATALYSTS FOR SELECTIVE HYDROGENATION OF 3,4 DINITROCHLOROBENZENE

Catalyst	Inhibitor	Dehalogenation %	Product Purity %
5 % Pt / Carbon	Triphenyl phosphite	< 0.01	98.52
5 % Pt / Carbon sulfided		0.09	99.82
5 % Pt / Carbon	Morpholine	0.18	99.50

\* Kosak (1980)

### 1.1.3 Kinetics and Mechanism

Kinetics of liquid phase hydrogenation of nitro aromatic compounds has been studied by several investigators using the suspended metal catalysts (Yao and Emmett 1959; 1961a,1961b,1962; Dovell et al. 1970; Metcalfe and Rowden 1971; Burge and Collins 1980; Wisniak and Klein 1984; and Rajadhyaksha and Karwa 1986). Most of these studies have been carried out using nitro benzene, and/or nitrophenol as substrates and Raney Ni, Pd, Rh and Pt as catalysts. Overall reaction rate was found to be dependent on mass transfer while studying the liquid phase hydrogenation of nitrobenzene using noble metal catalysts (Acres and Cooper 1972). Also, the reaction rate was found to be first order with respect to hydrogen and zero order with respect to the substrate but increased to first order with increase in catalyst concentration and agitation speed (Baltzly 1976; Burge and Collins 1980; Meschke and Hastung 1960).

Pascoe (1988) has studied the selective hydrogenation of bromonitro benzene isomers using four commercially available catalysts. He investigated the effect of solvents, ethanol and tetra hydro furan and pressure on selectivity of the reaction. The hydrogenation runs were carried out at room temperatures. He found that the effect of pressure on the rates was

greater than the solvent effect. Also, the rate of reaction was found to be greater over the noble metal catalysts than the raney Ni catalyst.

It was noted from the survey of the literature that most of the work on the selective hydrogenation of halo nitro compounds is in the form of patents. For the system chosen in the present work, which is one of the important industrial processes, there have been no studies on the kinetics.

## 1.2 ANALYSIS OF SLURRY REACTORS

### 1.2.1 General

Slurry reactors are commonly used in the hydrogenation of aromatic nitro compounds to anilines and therefore the relevant information and the literature on this subject has been summarized in this section.

Slurry reactor is a type of three phase reactor, in which the solid particles are suspended by means of mechanical or gas induced agitation. Slurry reactors have many diverse applications in chemical industries and particularly in catalytic processes. Some of the well known examples are : hydrogenation and oxidation of a variety of organic compounds, Fischer-Tropsch reaction

for hydrocarbon synthesis, ethynylation of aldehydes and polymerization reactions. Recent applications of slurry reactors are in the field of pollution control and in the field of heterogenized homogeneous catalysis.

Depending on the mode by which the catalyst particles are suspended, slurry reactors are classified into three categories. Schematic of all these reactors are shown in Figure 1.2.

- i) Mechanically agitated slurry reactors : In this case, the catalyst particles are kept in suspension by means of mechanical agitation
- ii) Bubble columns slurry reactors : In this type, the particles are suspended by means of gas-induced agitation, and
- iii) Three phase fluidized-bed reactors : Here, the particles are kept in suspension by means of the combined action of bubble movement and cocurrent liquid flow. The main difference in this type and bubble column slurry reactor is that in the fluidized bed reactor, the particles are suspended mainly due to liquid flow.

Mechanically agitated reactors offer advantages like higher heat and mass transfer efficiencies compared with bubble column reactor, while they have drawbacks

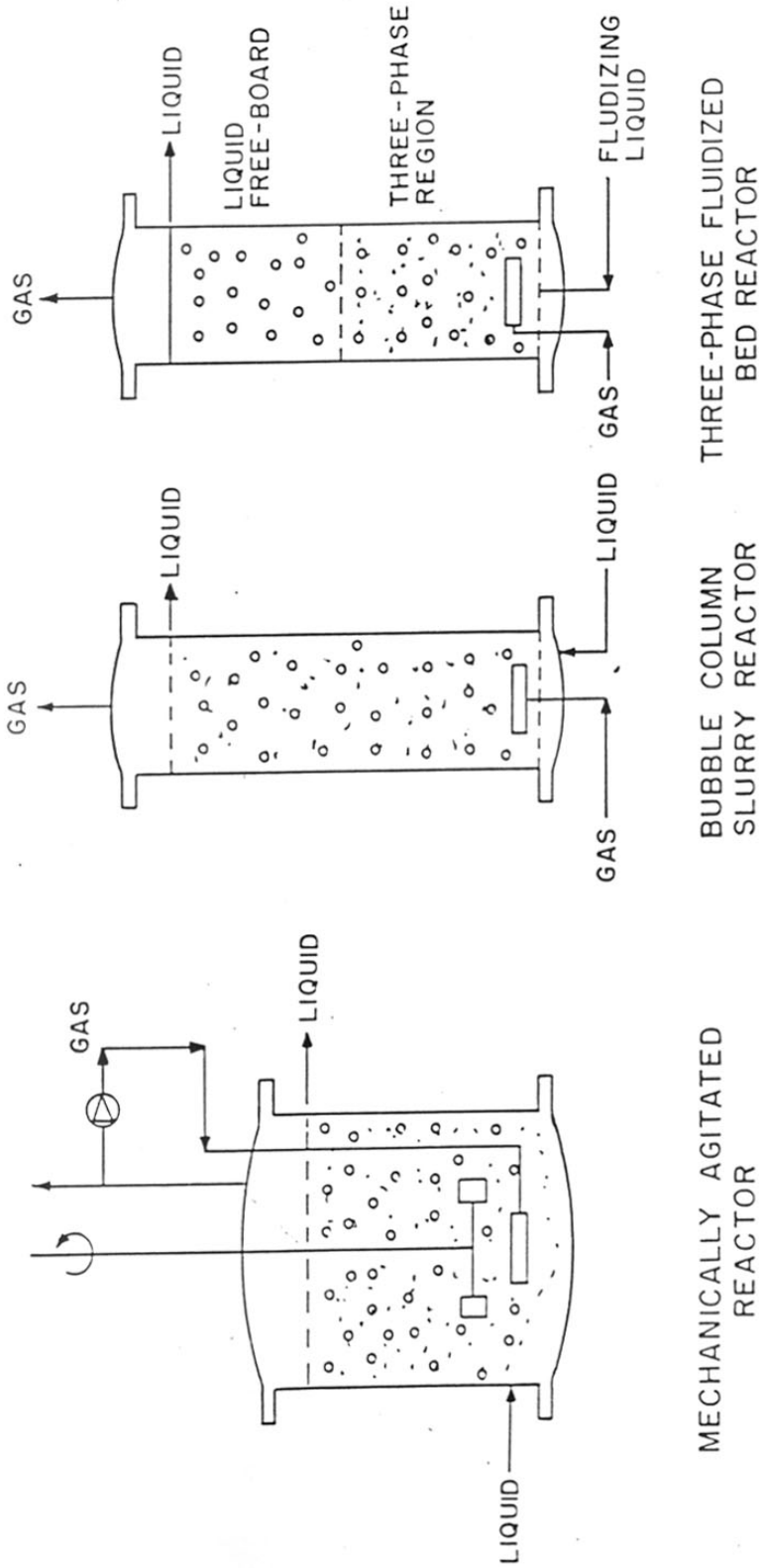


FIGURE 1.2: DIFFERENT TYPES OF THREE-PHASE SLURRY REACTORS

like catalyst attrition and complete backmixing of the liquid phase. Bubble column reactors have advantages like low power consumption simple design for construction and less maintenance.

The slurry reactors have many advantages over the other three phase reactors, such as trickle bed or packed bubble bed reactors, and these are given below :

- 1) Since small size of catalyst particles can be used in a slurry reactor, the intraparticle diffusional resistance is less in comparison to that in a trickle or packed bubble bed reactor. In trickle bed reactors, normally larger catalyst particle size is used, for which intraparticle diffusion effects are significant.
- 2) External mass transfer coefficients in slurry reactors are higher than those in trickle or packed beds, leading to better utilization of the catalyst.
- 3) Usually exothermic reactions are carried out in slurry reactors, since temperature control is better due to higher heat capacities and higher heat transfer coefficients of the slurries. Slurry reactors are relatively safer for reactions with temperature run away. Due to large liquid volumes, isothermal conditions can be maintained easily.
- 4) In slurry reactors, the problem of partial wetting

of catalyst particles, does not arise. This situation is often encountered in trickle bed reactors, for a certain range of liquid flow rates and in such cases the entire catalyst may not be utilized.

5) Due to the pelletizing difficulties and the high cost involved in pelletizing, slurry reactors may prove to be a better choice, in some applications.

In spite of these several advantages of slurry reactors, they pose some practical problems like separation of the catalyst from the products and handling of the slurry. Therefore, the application of slurry reactors in continuous processes has been limited. However, such problems can be overcome by modifying the slurry reactors to suit a certain specific application. The loop recycle reactor is one such example (Figure 1.3), which is widely used in hydrogenation of castor oil and fatty acids. Other novel gas-liquid-solid reactors have been critically reviewed by Chaudhari et al., (1986).

#### 1.2.2 Literature survey

Sherwood and Farkes (1966) and Satterfield (1970) were the first to describe the analysis of the transport phenomena in slurry reactors for the case of a

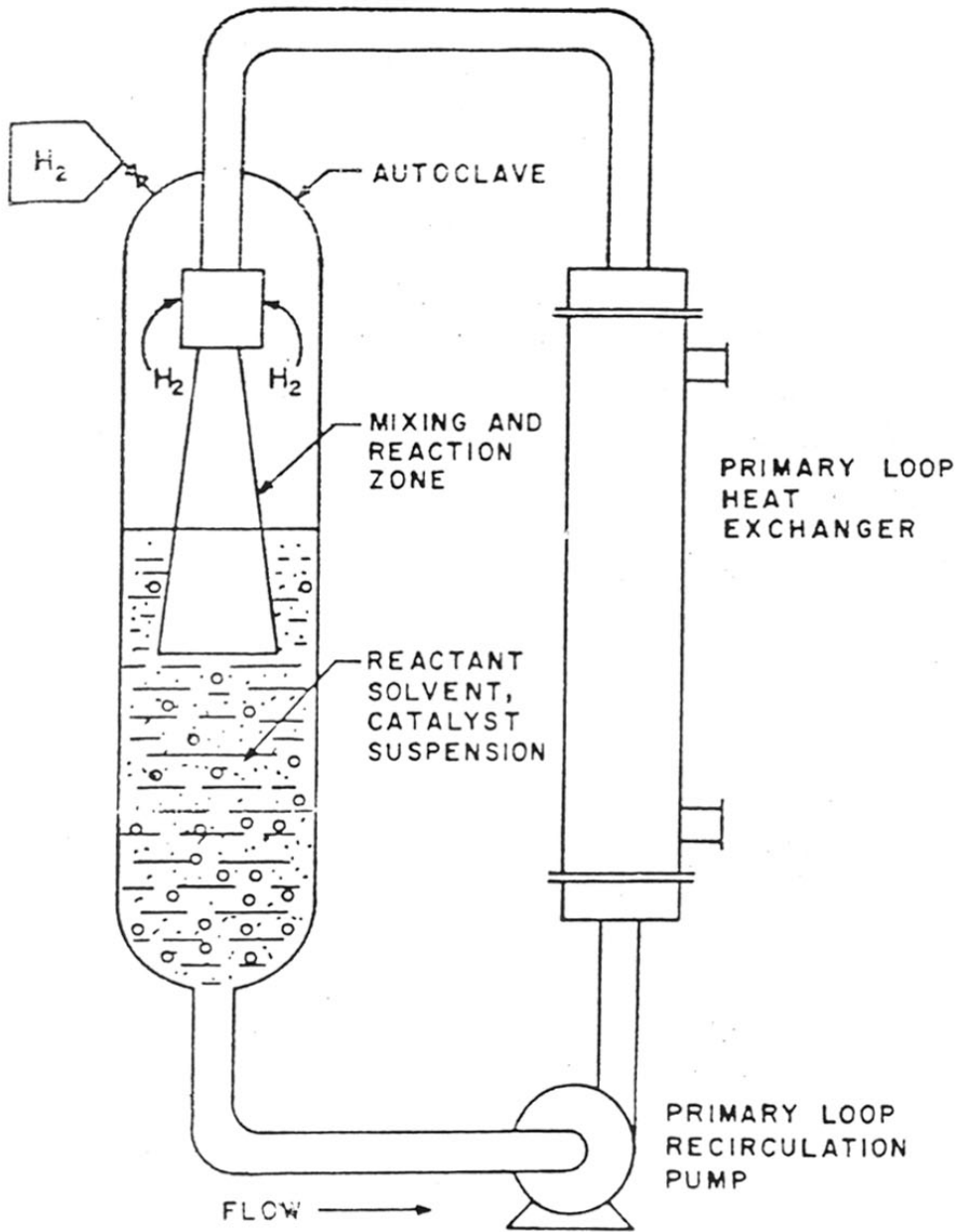


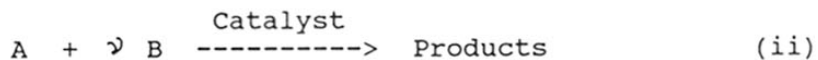
FIGURE 1-3: SCHEMATIC OF A JET LOOP REACTOR



simple first order reaction. Later on, Chaudhari and Ramachandran (1980), have dealt with the various aspects of the analysis of complex reactions, concept of overall effectiveness factor, modelling of semibatch reactors and also the hydrodynamics, of slurry reactors. The advances on the methods of designing and predicting the parameters required for design purposes, have been discussed by Ramachandran and Chaudhari (1983) and Shah (1979). They have critically evaluated the applicability of literature correlations for design purposes.

### 1.2.3 Theory

A simple form of three phase slurry system can be represented by the following reaction scheme :



Here, the species A is generally a reactant in the gas phase and B is a non-volatile reactant present in the liquid phase,  $\nu$  is the stoichiometric coefficient of B. A number of steps are involved for the reaction to take place, between A and B, at the catalyst surface.

1. Transport of A from bulk gas phase to the gas-liquid interface.
2. Transport of A from gas-liquid interface to the

bulk liquid.

3. Transport of A and B from bulk liquid to the catalyst surface.
4. Intraparticle diffusion of the reactants in the pores of the catalyst.
5. Adsorption of the reactants on the active sites of the catalyst.
6. Surface reaction between A and B to give products.

The concentration profiles of species A as it diffuses from the bulk gas to the interior of the catalyst is shown in Figure 1.4, wherein B is in large excess. In the case of reversible reactions and volatile products, additional steps such as desorption of products and transport from catalyst surface to the bulk liquid, and to the bulk gas phase for volatile products, will have to be taken into consideration.

Generally, all of these steps may not be important in every reaction. For example, in most three phase systems, gas side mass transfer resistance is negligible, if pure gas or high concentration of the gas phase reactant is used. In slurry reactors, the intraparticle diffusional resistance can be neglected, since very fine catalyst particles are generally used. However, to interpret the laboratory data correctly and apply them for designing purposes an understanding of all the transport phenomena is essential.

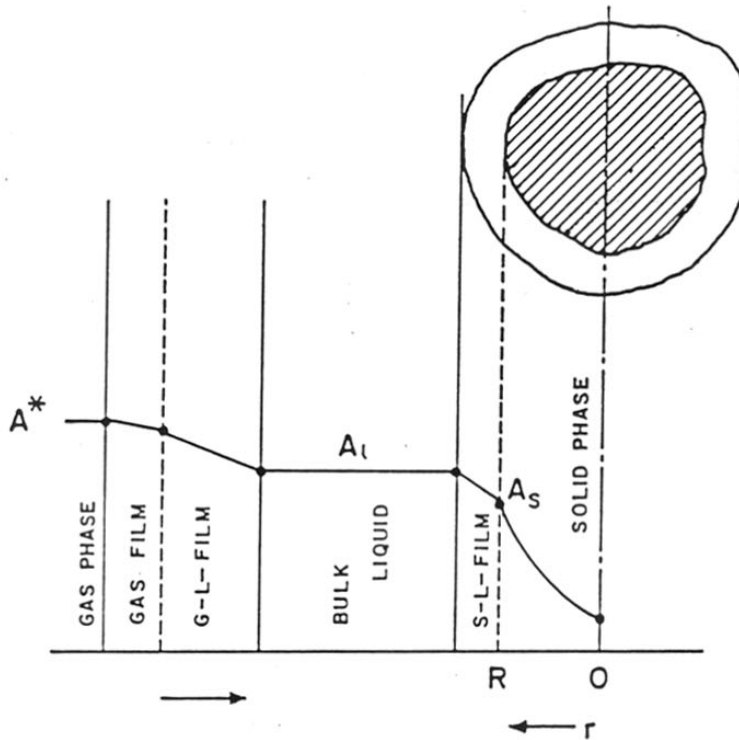


FIGURE 1-4 : CONCENTRATION PROFILE FOR  
A SLURRY CATALYSED REACTION

The analysis can be done first for a differential reactor in which concentration of A and B can be assumed to be more or less constant throughout the reactor. This assumption simplifies the theoretical analysis. Also, laboratory reactors are often operated in a differential manner, and the analysis can be directly useful in the interpretation of experimental data from such reactors.

#### 1.2.3.1 Analysis of differential reactors

Consider the reaction scheme represented by Eq. (ii), for which the concentration of reactant B is far in excess than that of gas A. The rate of reaction based on power law model is then given as,

$$r_A = k_m A^m \quad (2)$$

Where,  $k_m$  is the pseudo  $m^{\text{th}}$  order rate constant,  $\text{m}^3/\text{kg} (\text{m}^3/\text{kmol})^{m-1} \text{s}^{-1}$  and is defined as,

$$k_m = k_{mn} B_1^n \quad (3)$$

Where,  $B_1$  is the concentration of B in the bulk liquid  $\text{kmol}/\text{m}^3$ .

The number of steps necessary for the reaction to occur can be divided grossly into two : (a) overall

mass transfer from fluid phase to the catalyst surface and (b) intraparticle diffusion with surface reaction.

### 1.2.3.2 Overall rate of mass transfer

The rate of mass transfer of species A from the gas phase to the surface of the catalyst can be derived from the relevant equation for steps (1) to (3). The rate of gas-liquid mass transfer in a differential reactor is given by :

$$r_A = k_L a (A^* - A_1) \quad (4)$$

The term  $k_L a$  in Eq. (4), represents the overall gas-liquid mass transfer coefficient and can be related to the individual gas side and liquid side mass transfer coefficients as :

$$\frac{1}{K_L a} = \frac{1}{H_A k_g a} + \frac{1}{k_L a} \quad (5)$$

For sparingly soluble gases, like hydrogen, and for pure gas feeds (i.e. not inert diluents) the term  $K_L a$  can be approximated to  $k_L a$ .

The rate of mass transfer from the bulk liquid to the surface of the catalyst, is given as :

$$r_A = k_s a_p (A_l - A_s) \quad (6)$$

The term  $a_p$  for spherical particles is given as :

$$a_p = \frac{6w}{\rho_p d_p} \quad (7)$$

Combining equations (4) and (6), the overall rate of mass transfer of A from gas phase to the external surface of the catalyst can be expressed as :

$$r_A = M_A (A^* - A_s) \quad (8)$$

where,

$$M_A = \left( \frac{1}{k_L a} + \frac{1}{k_s a_p} \right)^{-1} \quad (9)$$

The equation (9) is valid irrespective of the type of the kinetic model.

### 1.2.3.3 Rate of chemical reaction

Let us consider a case where the intraparticle diffusional resistance is negligible. In this case, the concentration of A is uniform throughout the catalyst particle and is equal to  $A_s$ . The rate of reaction per unit volume of the reactor is given by :

$$r_A = wk_m A_S^m \quad (10)$$

$A_S$  which is the unknown concentration in the above equation, can be eliminated using equation (8) and the equation for the overall rate in terms of the known parameters can be obtained. The results for various cases are as follows :

(a) First order reaction ( $m = 1$ )

From equation (10),

$$A_S = \frac{r_A}{wk_1} \quad (11)$$

Substituting for  $A_S$  in equation (8) and rearranging, we obtain,

$$r_A = A^* \left( \frac{1}{M_A} + \frac{1}{wk_1} \right)^{-1} \quad (12)$$

Substituting for  $M_A$  from equation (9), we get :

$$r_A = A^* \left( \frac{1}{k_L a} + \frac{1}{k_s a_p} + \frac{1}{wk_1} \right)^{-1} \quad (13)$$

(b) For  $m^{\text{th}}$  order reaction,

$A_S$  is obtained from equation (10), as

$$A_S = \left( \frac{r_A}{wk_m} \right)^{1/m} \quad (14)$$

Substituting for  $A_S$  in equation (8),

$$r_A = M_A \left( A^* - \frac{r_A}{wk_m} \right)^{1/m} \quad (15)$$

This equation can be solved by trial and error procedure to predict  $r_A$ .

#### 1.2.3.4 L - H Type kinetics

For the case of no intraparticle diffusion, the rate of chemical reaction, for a single - site mechanism can be obtained as,

$$r_A = \frac{wk_1 A_S}{1 + K_A A_S} \quad (16)$$

Here, it is assumed that the adsorption of other components is negligible. From the equation (8), which gives the rate of overall mass transfer,  $A_S$  is obtained as

$$A_S = A^* - r_A/M_A \quad (17)$$



Substituting this value of  $A_s$  into equation (16), a quadratic equation is obtained, which can be solved as,

$$r_A = \frac{M_A}{2K_A} \left[ 1 + K_A A^* + \frac{wk_1}{M_A} - \left[ \left( 1 + K_A A^* + \frac{wk_1}{M_A} \right)^2 - \frac{4 wk_1 K_A A^*}{M_A} \right]^{1/2} \right] \quad (18)$$

For a dual-site mechanism, the rate of reaction obtained, by assuming negligible adsorption of other components, is as follows :

$$r_A = \frac{wk_1 A_s}{(1 + K_A A_s)^2} \quad (19)$$

substituting for  $A_s$ , as given above, a cubic equation for  $r_A$  is obtained as,

$$r_A^3 - r_A^2 \left( \frac{2M_A}{K_A} + 2A^* M_A \right) + r_A \left[ -\frac{M_A^2}{K_A^2} + \frac{2M_A^2 A^*}{K_A} + M_A^2 A^{*2} + \frac{wk_1 M_A}{k_A^2} \right] - \frac{wk_1 A^* M_A^2}{K_A^2} = 0 \quad (20)$$

Equation (20) can be solved by standard methods as given by Perry and Chilton (1973).

Depending on the rate controlling steps, the overall rate will depend on various experimental parameters. Roberts (1976) has given a list of different variables, which affect the overall rate,  $r_A$ .

### 1.3 OBJECTIVE OF THE PRESENT WORK

The literature information on hydrogenation of m-nitrochloro benzene, is scarce and mostly patented. No attempts to investigate the reaction kinetics of this reaction have been made so far. The aim of this work was to study the kinetics of liquid phase catalytic hydrogenation of m-nitrochlorobenzene in batch autoclave. This reaction is an interesting three phase catalytic system and provides a good example to study the modelling of three phase slurry reactors. The aim of the present work was to study the applicability of the kinetics under integral conditions. Theoretical models for batch slurry reactors are proposed to be developed to compare the predictions with experimental data under both isothermal and non-isothermal conditions.

## 2.1 MATERIALS

The catalyst used for hydrogenation was sulfided 1% Pt-S/C, obtained from M/s Engelhard, U.K. (code no. 99804). The physical properties of the catalyst are given in Table 2.1. Hydrogen gas was supplied by M/s Indian Oxygen Ltd., Bombay, with a purity of > 99.8%, and was used directly from the cylinder. The reactant m-nitrochlorobenzene was procured from M/s Fluka AG, Switzerland and methanol was used as a solvent.

## 2.2 APPARATUS

All the hydrogenation experiments were carried out in a  $3 \times 10^{-4} \text{ m}^3$  capacity stirred autoclave of SS 316, supplied by M/s Parr Instrument Co. USA. The reactor was provided with a glass liner, automatic temperature control, heating mantle, variable stirrer speeds, sampling arrangement for gases and liquids, cooling coil, thermocouple and a pressure gauge. An intermediate vessel of  $1 \times 10^{-3} \text{ m}^3$  capacity, with a two stage pressure regulator was used as  $\text{H}_2$  reservoir in order to carry out the experiments at constant pressure. A schematic diagram of the experimental set up is shown in Figure (2.1), while the actual set up is shown in Figures (2.2) and (2.3).

### 2.3 EXPERIMENTAL PROCEDURE

In a typical hydrogenation experiment, known quantities of catalyst and m-nitrochlorobenzene alongwith the solvent were charged into the reactor and the contents flushed with nitrogen. Then the contents were flushed twice with hydrogen and heated to a desired temperature. During this period, a slow stirring was kept on. When the desired temperature was reached, stirring was put off and hydrogen gas was then introduced into the autoclave upto a required pressure and the reaction was started by switching the stirrer on, at full rpm. During an experiment, the pressure of hydrogen was maintained constant. In each experiment initial and final samples are analyzed, for reactant and product, in order to check the material balance, which was > 95% . The progress of the reaction was monitored by observing the drop in H<sub>2</sub> pressure vs. time. The liquid concentration Vs. time data was obtained by analyzing the liquid samples withdrawn from the autoclave at desired intervals of time. In all the experiments, the liquid volume was  $1.50 \times 10^{-4} \text{ m}^3$ .

### 2.4 ANALYSIS

The liquid analysis was carried out by a gas chromatographic method using HP 5840 gas chromatograph equipped with SS column. The details of the column and

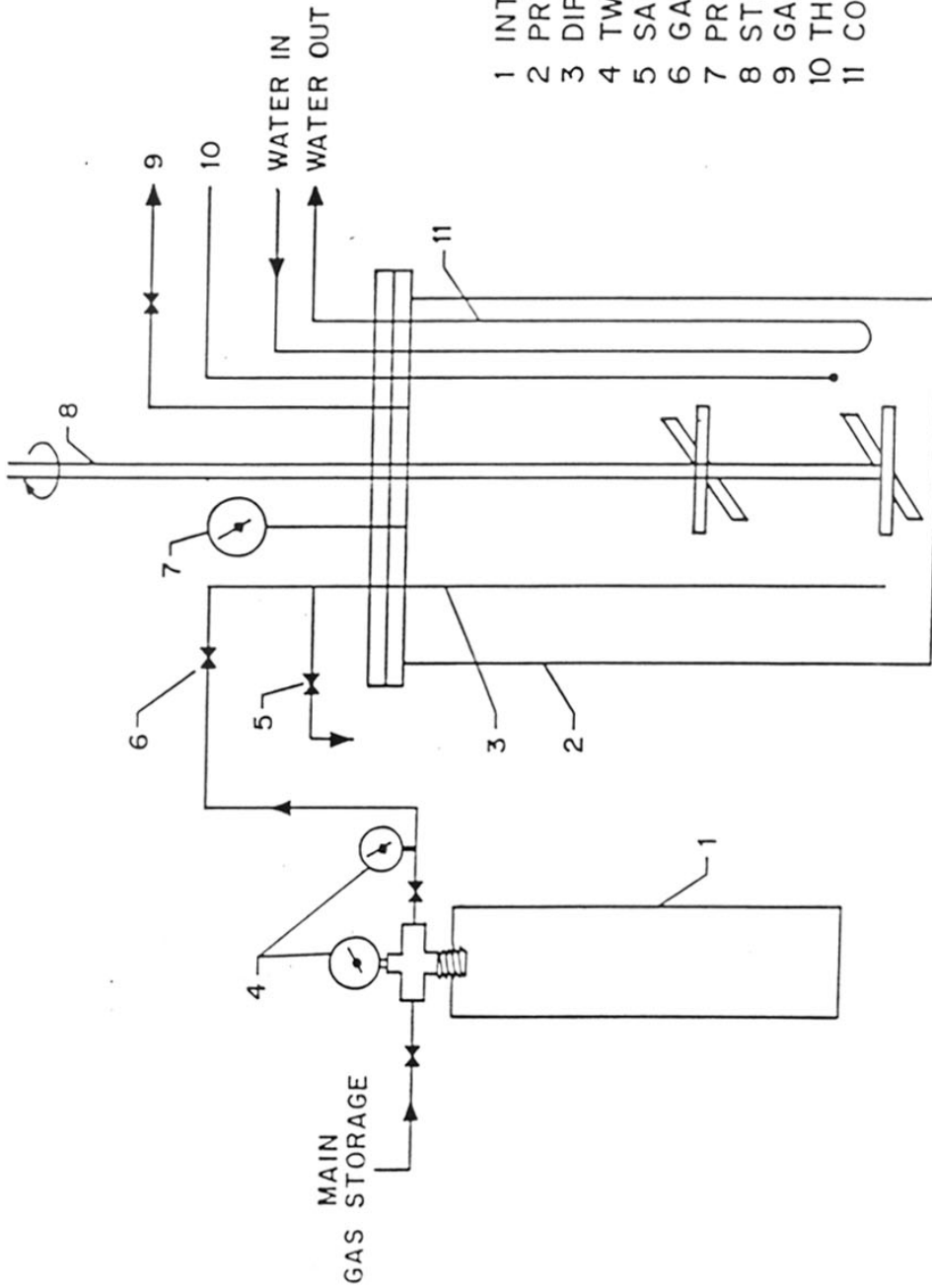
the other conditions of the GC analysis were as follows :

Column	:	5 % OV-17, on chromo- sorb, 3 m. long.
Column temperature	:	140°C
Detector (FID) temperature	:	350°C
Injection temperature	:	250°C
Carrier gas	:	N <sub>2</sub> , 1.2 x 10 <sup>-3</sup> m <sup>3</sup> /hr.

The peaks were identified by comparing the retention times with those of known standards. The quantitative analysis of reactant and product was carried out by using the external standard calibration method.

TABLE 2.1 : SPECIFICATIONS OF HYDROGENATION CATALYST

1.	Catalyst size ( $d_p$ )	1 - 4 microns
2.	Particle density ( $\rho_p$ )	$1.8 - 2.0 \times 10^3$ , kg/m <sup>3</sup>
3.	Pore volume	$4.5 \times 10^{-4}$ , m <sup>3</sup> / kg
4.	Porosity	0.90
5.	Surface area	$8 \times 10^5$ , m <sup>2</sup> / kg
6.	Pt content	1 %



- 1 INTERMEDIATE VESSEL FOR GAS
- 2 PRESSURE BOMB
- 3 DIP TUBE
- 4 TWO STAGE REGULATOR
- 5 SAMPLING VALVE
- 6 GAS INLET VALVE
- 7 PRESSURE INDICATOR
- 8 STIRRER
- 9 GAS VENT
- 10 THERMOCOUPLE
- 11 COOLING LOOP

FIGURE 2-1: SCHEMATIC OF EXPERIMENTAL REACTOR SET-UP

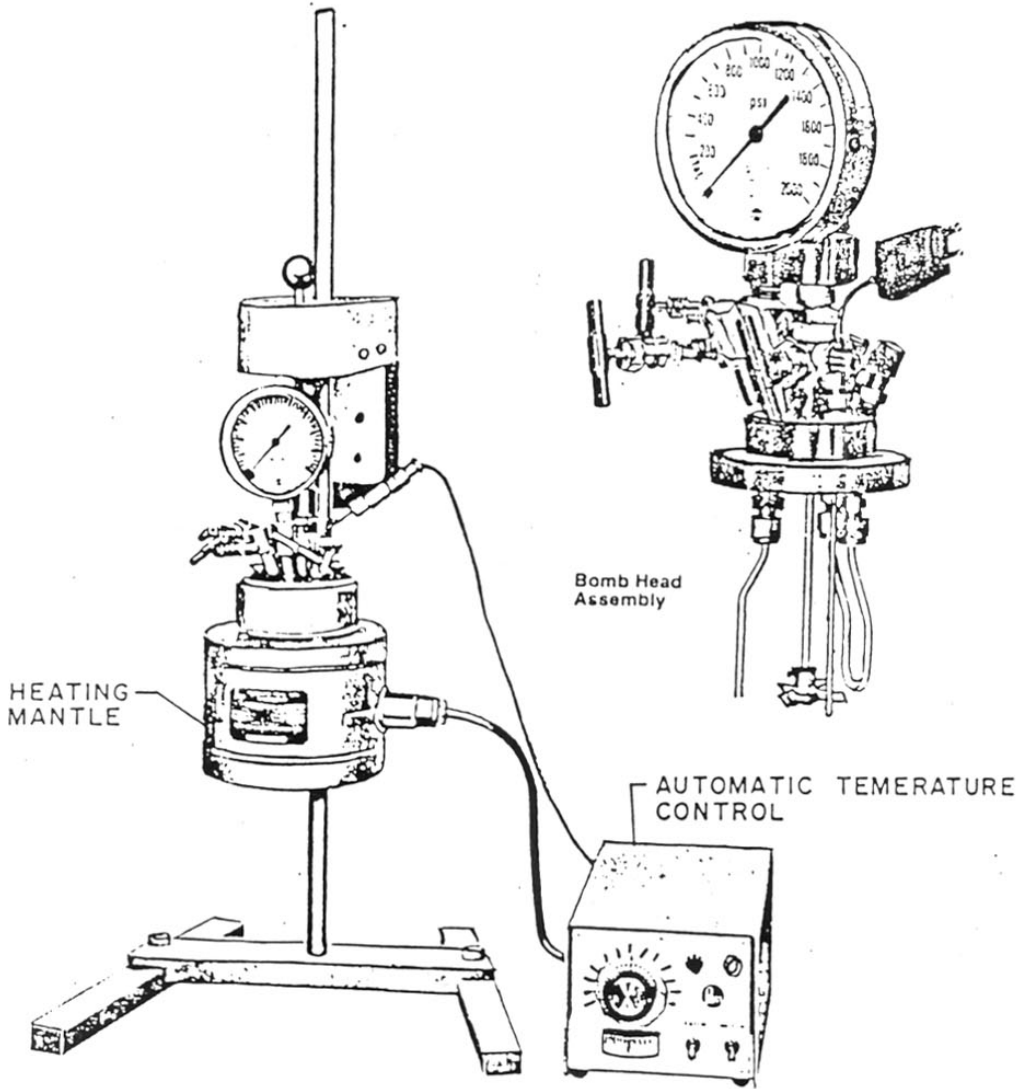


FIGURE 2-2 : EXPERIMENTAL REACTOR SET-UP



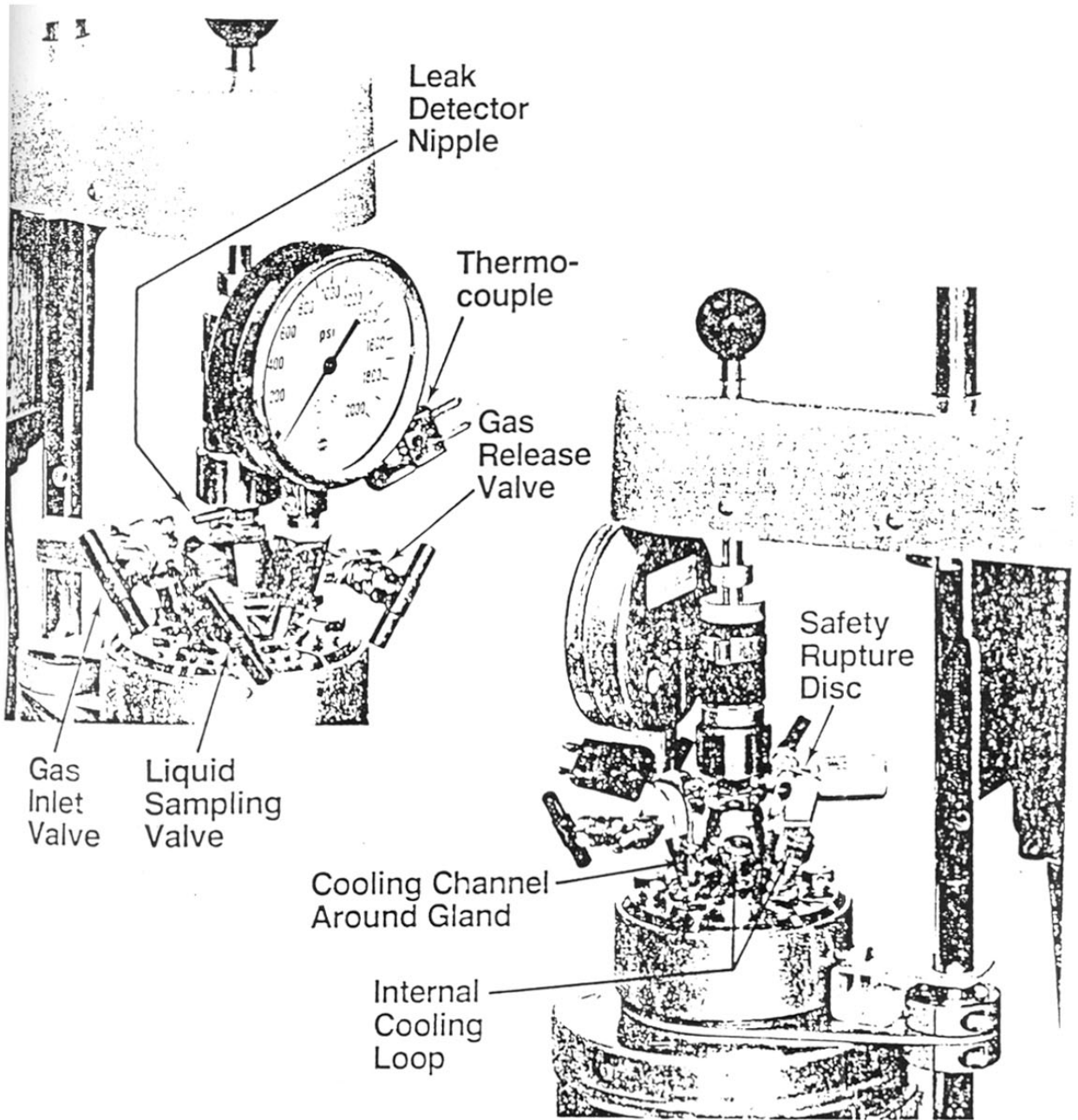
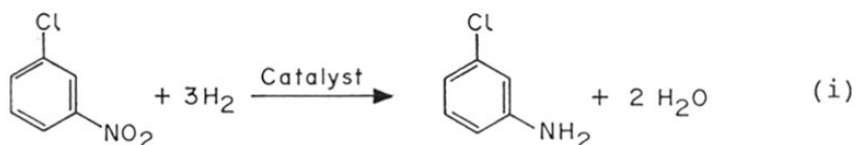


FIGURE 2.3 : EXPERIMENTAL SET-UP

## **CHAPTER 3**

### **RESULTS AND DISCUSSION**

Hydrogenation experiments were carried out in a stirred high pressure slurry reactor with the objective of investigating intrinsic kinetics and modelling of batch slurry reactor. The stoichiometry of hydrogenation of m-nitrochlorobenzene to m-chloroaniline is :



The reaction is highly exothermic with a heat of reaction of 540 kJ / mol. Before proceeding for the kinetic study, experiments were carried out to examine the following aspects :

- (a) Material balance and reproducibility
- (b) Possibility of homogeneous non catalytic reactions
- (c) Reusability of catalyst

The preliminary experiments showed that with Pt-S/C catalyst nearly complete conversion of MNCB with a selectivity > 98% for MCA was achieved. The material balance of the reactants consumed and the products formed was found to agree to the extent of 95 % and above (see Table 3.I), for all the conversion levels. The only side product formed was aniline, but in all cases, its concentration was negligible. A few experiments were

repeated under identical conditions to check the reproducibility which indicated the reproducibility within 3% error. In order to study the possibility of a non catalytic reaction, m-nitrochlorbenzene and methanol were charged into the reactor, pressurized with hydrogen and the reaction continued. The liquid sample, when analyzed showed no products and the contents were the same as initial values indicating absence of any non catalytic reaction.

Some experiments were carried out to ascertain the reusability of the catalyst which showed that the activity of the catalyst was constant even after repeated use. Figure (3.1) shows a plot of initial rate of hydrogenation Vs. number of recycles. This ensured that the catalytic activity was constant throughout any kinetic run.

In order to study the kinetics of reaction (i) the hydrogenation experiments were carried out in a temperature range of 313 - 363, K and at different concentrations of the catalyst, the substrate and the product. In each case, the amount of  $H_2$  consumed as a function of time was observed. The initial and final liquid samples were also analyzed for concentrations of MNCB and MCA. Only those runs, where  $H_2$  and MNCB consumption was corresponding to MCA formed were chosen

for kinetic analysis. The rate of hydrogenation was calculated from the plots of  $H_2$  consumed vs. time as

$$r_A = \frac{\text{Slope of } (H_2 \text{ consumed vs. time plot})}{\text{Volume of reaction mixture}}$$

A typical plot for  $H_2$  Vs. time for different temperatures is shown in Figure 3.2. Following this procedure rate of hydrogenation was calculated for differential conditions. The range of conditions varied is given in Table (3.II). The corresponding rate data are presented in Table (3.III). A detailed interpretation of these results is presented in the following sections.

The system under consideration being a three phase system, it was important to ensure that the mass transfer and hydrodynamic factors are either eliminated or accounted for in determining the kinetics. In order to eliminate the intraparticle and the liquid particle mass transfer resistances, finely divided particles ( $d_p = 1 - 4$  microns) of the catalyst were used.

### 3.1 ANALYSIS OF INITIAL RATE DATA

The analysis of initial rates is always useful in understanding the dependency of the reaction rate on individual parameters and also in the evaluation of the

TABLE 3. I : MATERIAL BALANCE OF MNCB CONSUMED AND MCA FORMED

Sr. No.	Temperature K	H <sub>2</sub> Pressure x 10 <sup>3</sup> , kP <sub>a</sub>	H <sub>2</sub> consumed x 10 <sup>4</sup> , kmol	MNCB consumed x 10 <sup>4</sup> , kmol	MCA formed x 10 <sup>4</sup> k mol	Material balance %
1.	313	0.656	3.78	1.26	1.245	98.4
2.	313	3.4	3.74	1.24	1.23	99.0
3.	313	0.656	1.776	0.06	0.590	98.33
4.	323	3.40	3.80	1.26	1.253	99.44
5.	333	6.83	3.71	1.237	1.212	97.97
6.	353	0.656	5.43	1.80	1.72	95.56
7.	363	0.656	1.771	0.588	0.571	96.93

Reaction conditions :

Catalyst loading = 0.36 kg/m<sup>3</sup>Volume of liquid = 1.50 x 10<sup>-4</sup> m<sup>3</sup>

rpm = 13.6 Hz.

TABLE 3.II : RANGE OF OPERATING CONDITIONS

---

1.	Catalyst loading	0.36 - 2.1 kg / m <sup>3</sup>
2.	Agitation speed	5 - 13.6 Hz
3.	H <sub>2</sub> pressure	0.656 x 10 <sup>3</sup> - 6.7 x 10 <sup>3</sup> k Pa
4.	Concentration of MNCB	0.20 - 1.2 kmol / m <sup>3</sup>
5.	Concentration of MCA	0.20 - 1.2 kmol / m <sup>3</sup>
6.	Temperature	313 - 363 K

---

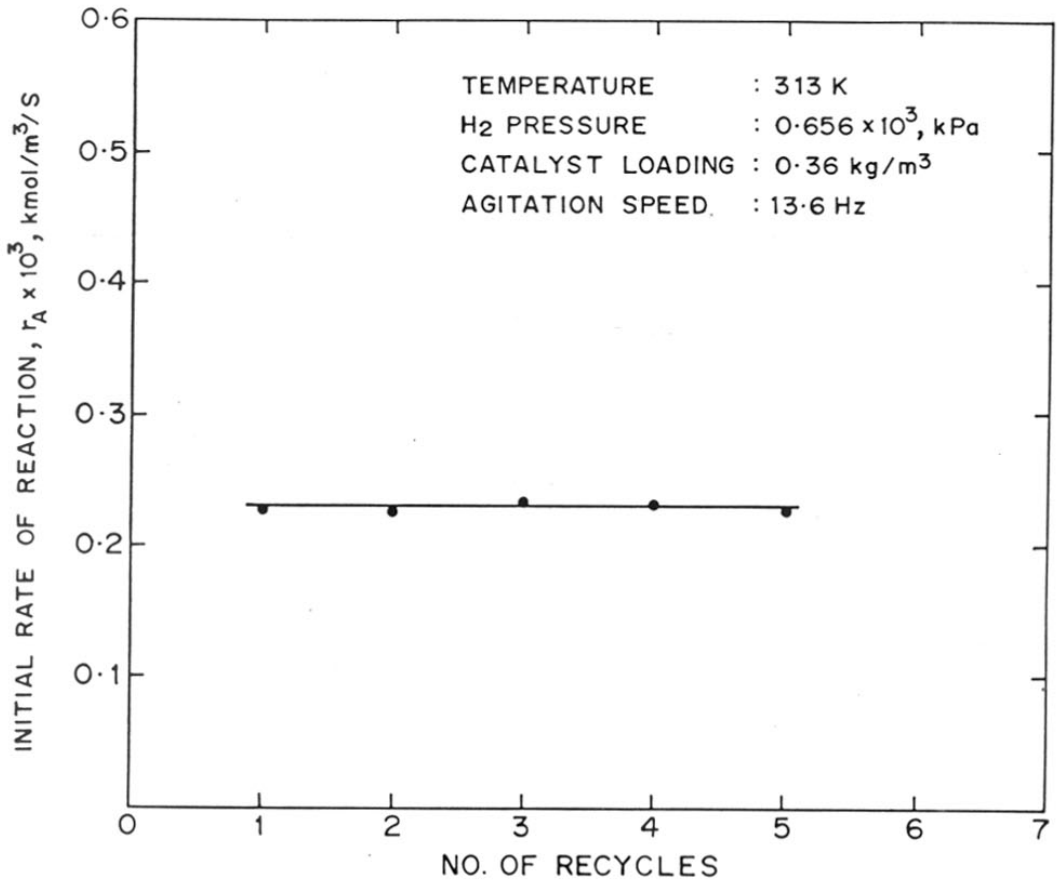


FIGURE 3-1: PLOT OF INITIAL RATE OF HYDROGENATION Vs. NUMBER OF RECYCLES



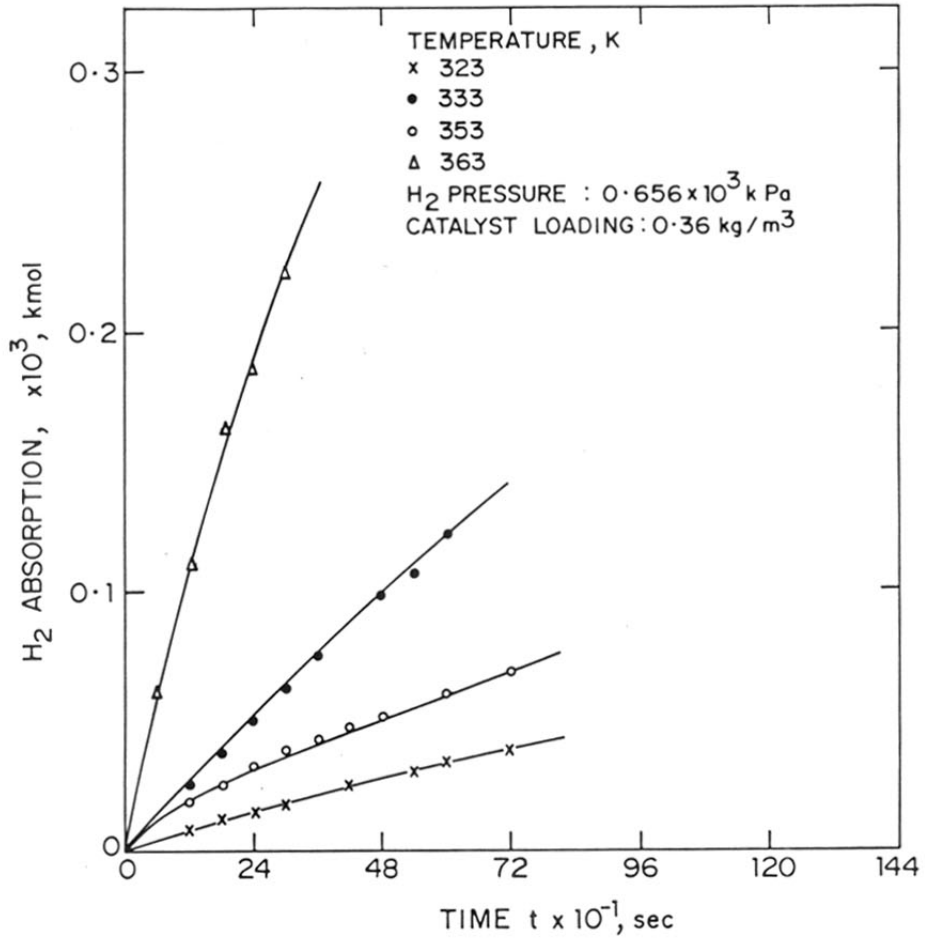


FIGURE 3.2: HYDROGEN ABSORPTION Vs TIME FOR DIFFERENT TEMPERATURES

significance of mass transfer effects. The effect of individual parameters or the rates is discussed below.

### 3.1.1 Effect of Catalyst Loading

Figure (3.3), show the influence of catalyst loading on the initial rate of hydrogenation of m-nitrochlorobenzene for the temperature range of 313 K - 363 K. It is clear from these results that the rate is linearly dependent on catalyst loading at 313-333 K, only, while it is independent of catalyst loading beyond a certain value for 353 K and 363 K indicating that gas-liquid mass transfer is being significant at 353 and 363K

### 3.1.2 Effect of Agitation Speed

In order to check the significance of gas-liquid mass transfer resistance, experiments were carried out at different agitation speeds, with lowest as well as the highest catalyst loadings. As can be seen from the Figures (3.4 and 3.5), for the temperature range of 313-333K, the rates were found to be independent of agitation speed, for both high and low catalyst loadings. However, at 353 K and 363 K, the rates were found to be strongly dependent on agitation speed even at the lowest catalyst loading (see Figure 3.5). These observations are consistent with the observations with respect to catalyst

loading and conclusion of gas-liquid mass transfer limitation at 353 and 363K.

### 3.1.3 Effect of Pressure

The effect of hydrogen pressure on the rate of reaction is shown in Figure (3.6) for different temperatures. The rate was found to vary with first order with  $H_2$  at all the temperatures.

### 3.1.4 Effect of Substrate and Product Concentration

As shown in Figure (3.7), the rates were found to be independent of concentrations of m-nitrochlorobenzene. In order to ascertain the effect of product concentrations, some experiments were carried out by adding a known quantity of m-chloroaniline, to the reaction mixture at the start of the experiment. The results observed at different initial m-chloroaniline concentrations are shown in Figure (3.8), which indicate that m-chloroaniline does not have any significant effect on the rate of reaction. Thus, a zero order kinetics was observed with respect to both the substrate as well as the product.

### 3.1.5 Analysis of Mass Transfer Effects

The initial rate data were also analyzed to check the significance of gas-liquid, liquid-solid and

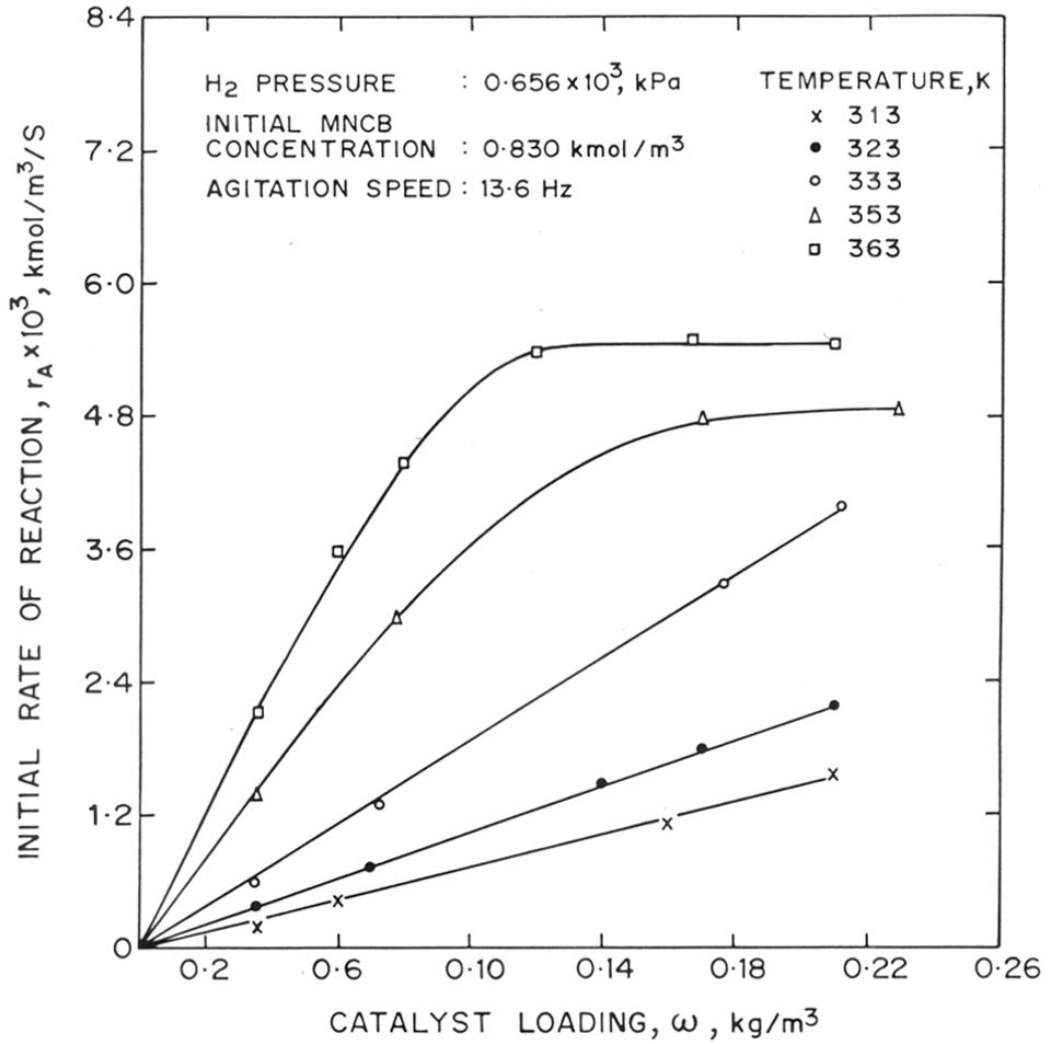


FIGURE 3.3: EFFECT OF CATALYST LOADING ON RATE OF HYDROGENATION

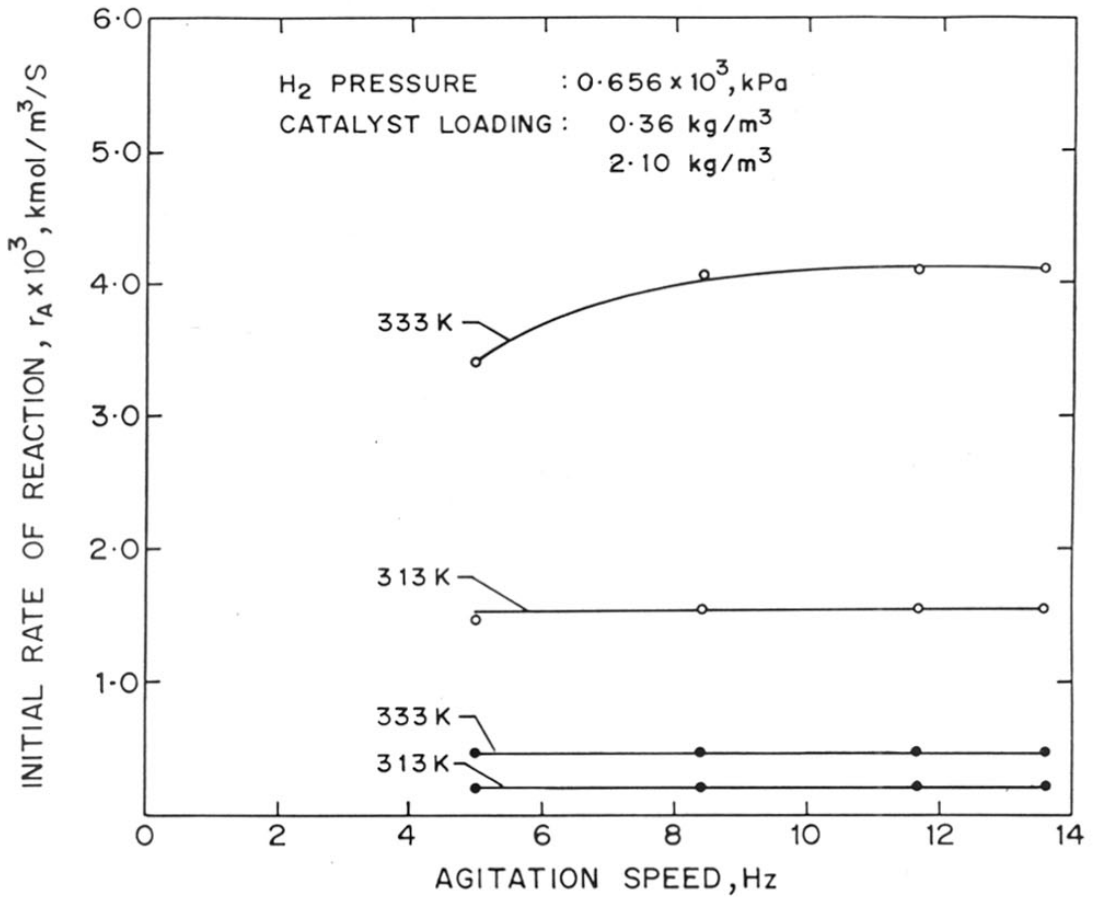


FIGURE 3.4: EFFECT OF AGITATION SPEED ON RATE OF HYDROGENATION AT 313 AND 333K, FOR DIFFERENT CATALYST LOADINGS

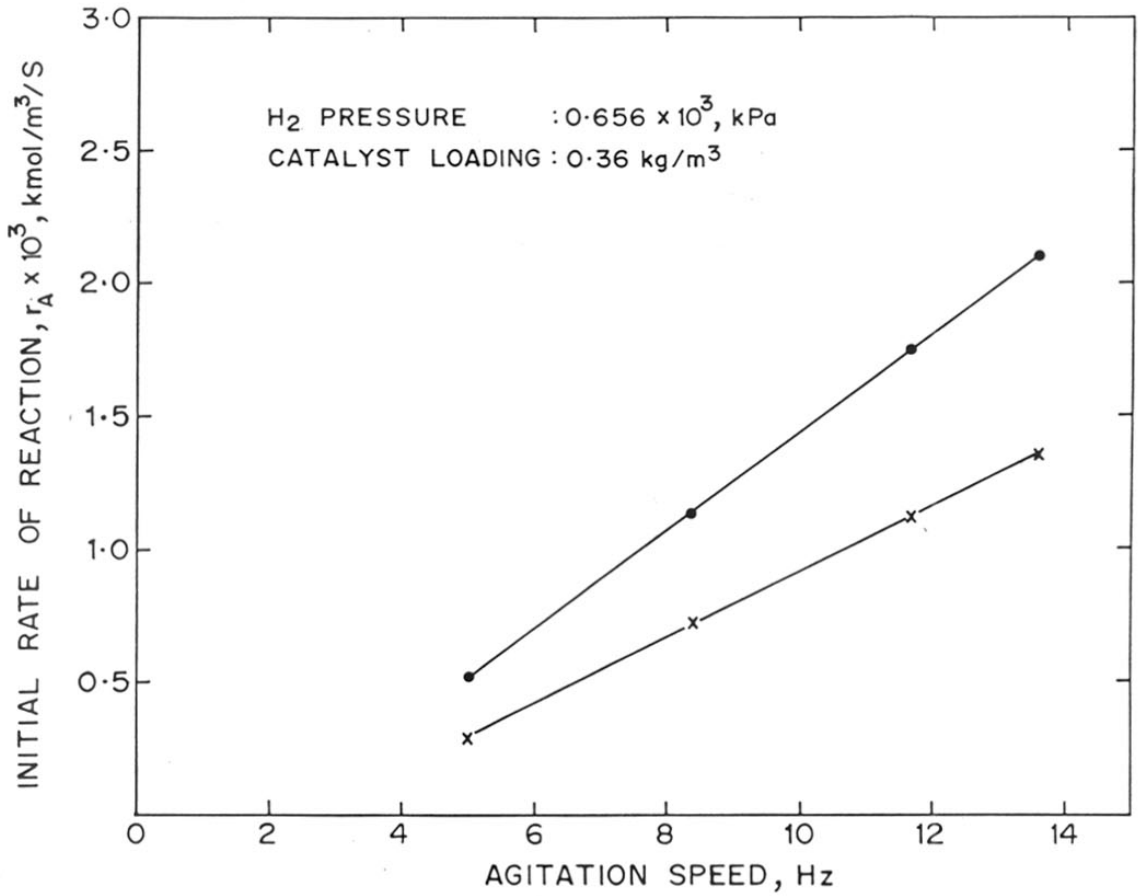


FIGURE 3-5 : EFFECT OF AGITATION SPEED ON REACTION RATE AT 353 K (x) AND 363 (•)

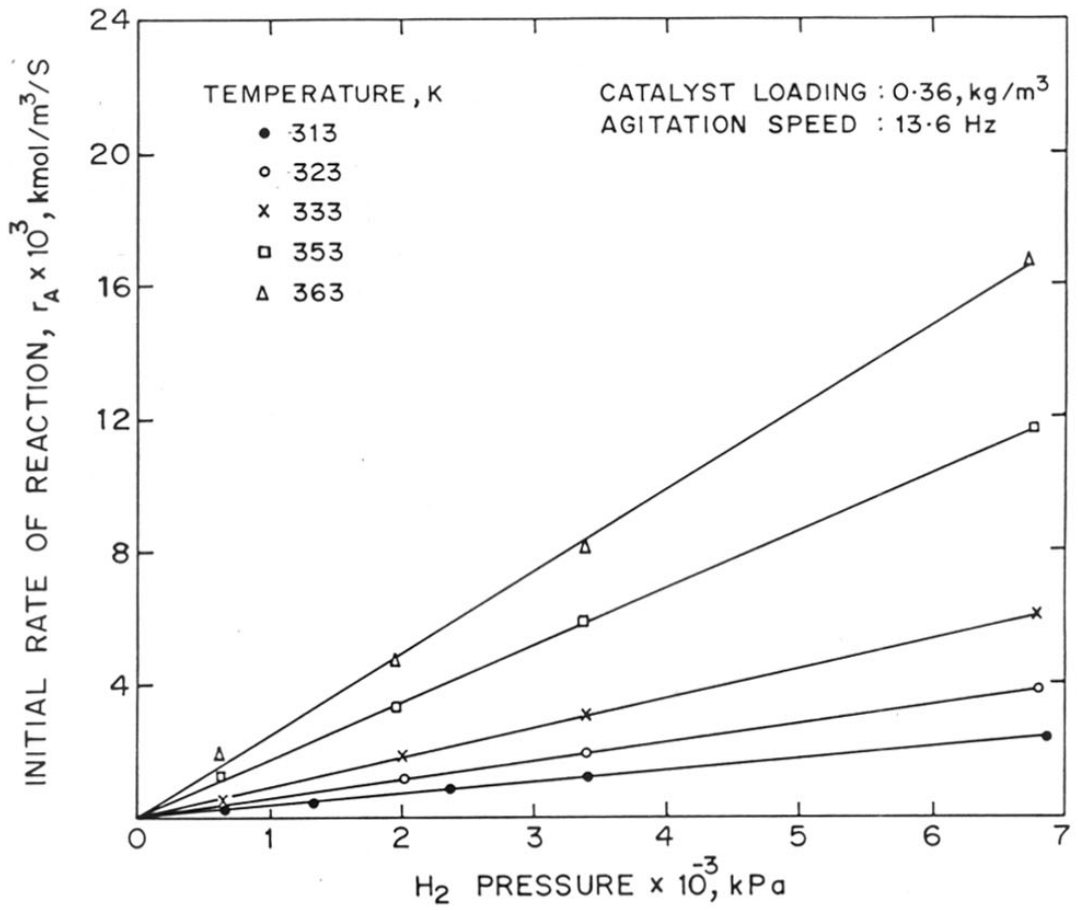


FIGURE 3.6: EFFECT OF H<sub>2</sub> PRESSURE ON THE RATE OF HYDROGENATION

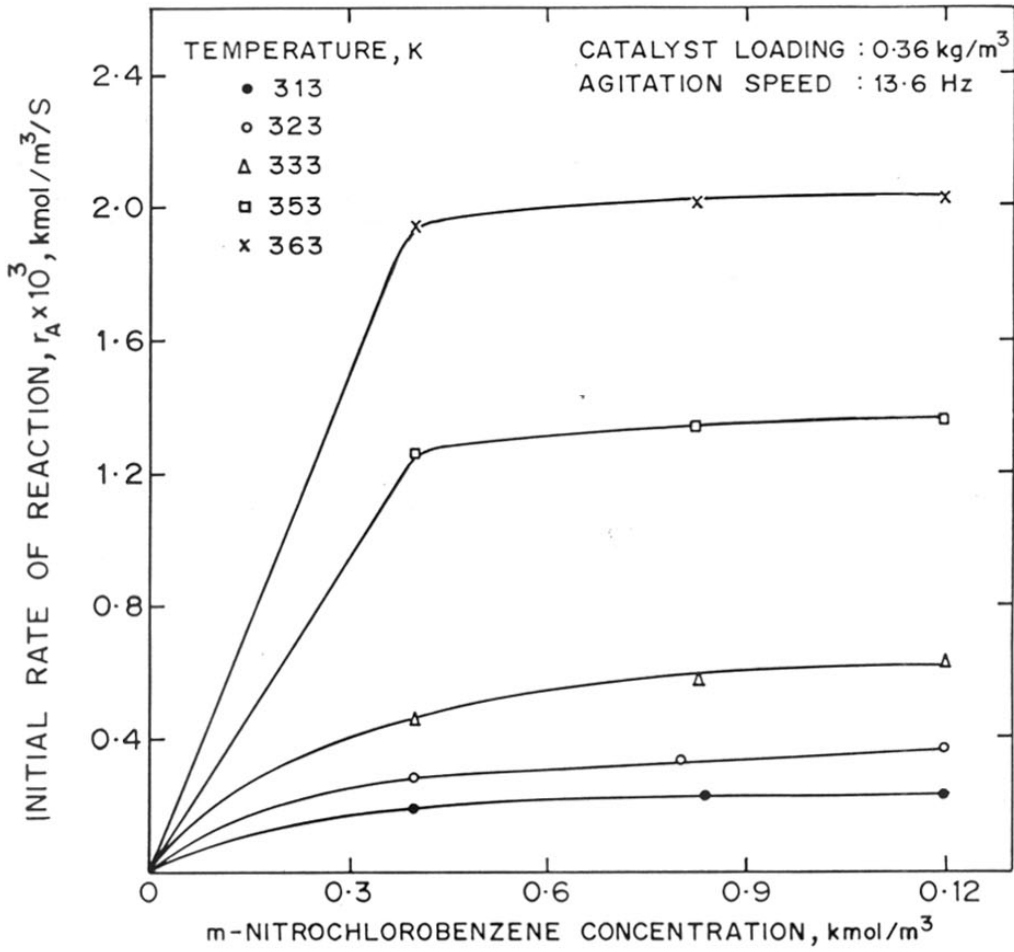


FIGURE 3.7: EFFECT OF m-NITROCHLOROBENZENE CONCENTRATION ON INITIAL RATES OF HYDROGENATION



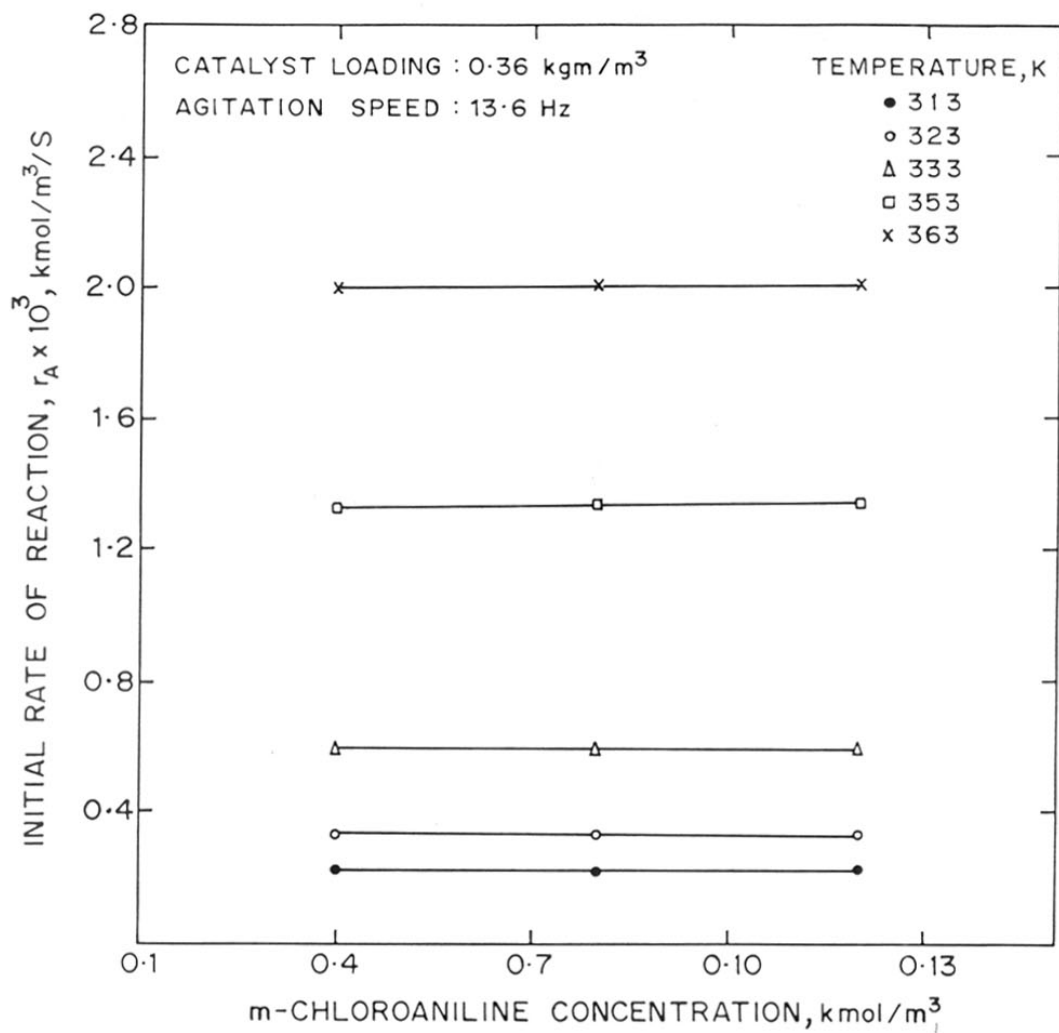


FIGURE 3-8 : EFFECT OF m-CHLOROANILINE CONCENTRATION ON INITIAL RATES OF HYDROGENATION

intraparticle mass transfer effects under the conditions used in this work. For this purpose, the criteria described by Ramachandran and Chaudhari (1983) were used. In these criteria, factors,  $\alpha_1$ ,  $\alpha_2$  and  $\phi_{exp}$ , are calculated which are defined as the ratios of the observed rates to the maximum rates of gas-liquid, liquid-solid and intraparticle mass transfer respectively. The calculation of these factors is given below.

### 3.1.5.1 Gas-liquid mass transfer

The gas to liquid mass transfer can be considered unimportant if,

$$\alpha_1 = \frac{r_A}{k_L a P_A H_A} < 0.1 \quad (1)$$

where,

- $r_A$  = Rate of hydrogenation,  $\text{kmol} / \text{m}^3 / \text{s}$
- $k_L$  = Gas liquid mass transfer coefficient,  $\text{m}/\text{sec}$
- $a$  = Effective gas-liquid interfacial area,  $\text{m}^2/\text{m}^3$
- $H_A$  = Henry's low constant of solubility for  $\text{H}_2$ ,  $\text{kmol} / \text{m}^3 \text{ kPa}$
- $P_A$  = Partial pressure of  $\text{H}_2$ ,  $\text{kPa}$ .

For calculation of  $\alpha_1$ , a knowledge of the solubility of  $H_2$  in the reaction medium is essential. The data for  $H_2$  methanol system, as reported by Seidell (1940), were used after correction for various temperatures. It was assumed that m-nitrochlorobenzene and m-chloroaniline have no influence on the solubility of  $H_2$  in methanol, in the range of concentrations used in this work. The solubility data are presented in Table (3.IV). The values of gas-liquid mass transfer coefficient ( $k_L a$ ), were calculated by using the correlation given by (Chaudhari et al. 1987) for the stirred reactor, and these are presented in Table (3.V).

### 3.1.5.2 Liquid-solid mass transfer

The liquid-solid mass transfer resistance can be considered to be negligible, if,

$$\alpha_2 = \frac{r_A}{k_S a_P P_A H_A} < 0.1 \quad (2)$$

where,

$k_S$  = Liquid-solid mass transfer coefficient,  
m/sec

$a_P$  = Effective liquid-solid interfacial area per  
unit volume of slurry,  $m^2/m^3 = 6w / \rho_P d_P$

$w$  = Catalyst loading,  $kg / m^3$

- $\rho_p$  = Particle density, kg / m<sup>3</sup>  
 $d_p$  = Particle diameter, m.

For calculation of  $k_s$ , the correlation, proposed by Sano et. al. (1974), was used.

$$\frac{k_s a_p}{DF_C} = 2 + 0.4 \left[ \frac{e d_p^4 \rho_L^3}{\mu_L^3} \right]^{1/4} \frac{\mu_L}{\rho_L^D} \quad (3)$$

Where,  $F_C$ , the shape factor can be assumed to be unity for spherical particles. The energy supplied to the liquid,  $e$ , was calculated as (Calderbank, 1958)

$$e = \frac{N_p N^3 d_I^5 \psi}{\rho_L V_L} \quad (4)$$

Where,

- $e$  = Energy supplied to liquid, kg / sec.  
 $N_p$  = Power number  
 $N$  = Agitation speed, Hz  
 $d_I$  = Diameter of agitator, m  
 $\rho_L$  = Density of liquid, kg / m<sup>3</sup>  
 $V_L$  = Volume of liquid, m<sup>3</sup>.

Here,  $\psi$  is a correction factor for the presence of gas bubbles and is given as (Calderbank, 1958)

$$\psi = 1.0 - 1.26 \left[ \frac{Q_g}{N d_I^3} \right]$$

$$\text{for } \frac{Q_g}{N d_I^3} > 3.5 \times 10^{-2}$$

$$= 0.62 - 1.85 \frac{Q_g}{N d_I^3} \quad (5)$$

$$\text{for } \frac{Q_g}{N d_I^3} > 3.5 \times 10^{-2}$$

Where,  $Q_g$  is the volumetric flow rate of gas,  $m^3/s$ . As in this work, a batch autoclave was used, gas was not continuously bubbled but was supplied as per the consumption to maintain a constant pressure. Therefore in the above calculations,  $Q_g$  was calculated as,

$$Q_g = r_{\max} \times V_L \times V_m \quad (6)$$

where,  $r_{\max}$  = maximum rate of hydrogenation,  $kmol/m^3/sec.$ ,  $V_m$  = molar gas volume,  $m^3/mol$ .

For actual calculation,  $Q_g$  was taken as 20% excess of that calculated by equation (6). The value of  $k_s$  calculated using the above equation was found to be 0.163.

3.1.5.3 Intraparticle diffusion

The significance of intraparticle diffusion can be evaluated using the criteria based on experimental Thiele parameter,  $\phi_{exp}$  (Satterfield, 1970, Chaudhari and Ramachandran, 1980) defined as :

$$\phi_{exp} = \frac{d_p}{6} \left[ \frac{\rho_p r_A}{w D_e P_A H_A} \right] \quad (7)$$

For  $\phi_{exp} < 0.2$ , the intraparticle diffusion can be assumed to be negligible. The effective diffusivity ( $D_e$ ) was calculated as :

$$D_e = \frac{D\epsilon}{\tau} \quad (8)$$

where,

- D = Diffusivity,  $m^2/sec$
- $\epsilon$  = Porosity of the catalyst
- $\tau$  = Tortuosity factor

The molecular diffusion coefficients were calculated from the equation by Wilke and Chang (1955) and the tortuosity factor was assumed as 3.0, the value observed for carbon particles (Komiyama and Smith, 1975). The diffusivity data are presented in Table (3.VI).

The values of these parameters  $\alpha_1$   $\alpha_2$  and

$\phi_{\text{exp}}$  were calculated for all the rate data and presented in Table 3.III. From this analysis it is clear that the liquid-solid mass transfer and the intraparticle diffusion effects are negligible. However, gas-liquid mass transfer is significant particularly at higher temperature and higher catalyst loadings. This conclusion is also consistent with the observations of the variation of rates with agitation speed and  $w$ , at 353K and 363K. Here, it is implied that at high temperatures and catalyst loadings the rate of reaction is very much higher compared to the rate of mass transfer and hence the latter becomes a controlling step.

### 3.2 KINETIC MODEL

The initial rate data in kinetic regime (313-333K), were fitted to several forms of rate equations, some purely empirical and some Langmuir-Hinshelwood type of models. In order to select the rate equation for fitting the rate data, several reaction schemes were considered. Each scheme involves several elementary steps such as adsorption, desorption and surface reaction and depending on the rate controlling step, various rate equations can be derived (Perry and Chilton, 1973). While deriving kinetic models, the following assumptions were made :

TABLE 3. III : INTIAL RATE DATA FOR HYDROGENATION OF  
m-NITROCHLOROBENZENE

Sr. No.	Catalyst loading, w, kg/m <sup>3</sup>	H <sub>2</sub> pressure x 10 <sup>-3</sup> , kPa	Initial MNCB concentration B <sub>10</sub> , kmol/m <sup>3</sup>	Initial rate of reaction, r <sub>A</sub> x 10 <sup>3</sup> , k mol/m <sup>3</sup> s	α <sub>1</sub>	α <sub>2</sub> x 10 <sup>2</sup>	φ <sub>exp</sub> x 10 <sup>2</sup>
1	2	3	4	5	6	7	8
Temperature 313 K,							
1.	0.36	0.656	0.20	0.136	0.0407	0.24	2.4
2.	0.36	0.656	0.40	0.190	0.057	0.34	9.1
3.	0.36	0.656	0.84	0.228	0.068	0.408	3.15
4.	0.36	0.656	1.20	0.225	0.067	0.403	3.13
5.	0.36	1.345	0.820	0.485	0.0709	0.424	3.21
6.	0.36	2.379	0.830	0.865	0.0716	0.429	3.23
7.	0.36	3.413	0.790	1.200	0.0690	0.414	3.17
8.	0.36	6.863	0.840	2.400	0.068	0.417	3.16
9.	0.60	0.656	0.840	0.422	0.096	0.454	3.32
10.	1.60	0.656	0.825	1.10	0.32	0.443	3.28
11.	2.10	0.656	0.825	1.56	0.4	0.48	3.41
Temperature 323 K							
12.	0.36	0.656	0.40	0.286	0.080	0.48	3.35
13.	0.36	0.656	0.80	0.338	0.09	0.57	1.15
14.	0.36	0.656	1.20	0.367	0.0887	0.62	3.80
15.	0.36	2.015	0.825	1.06	0.095	0.58	3.66



1	2	3	4	5	6	7	8
16.	0.36	3.394	0.825	1.92	0.10	0.625	3.80
17.	0.36	6.833	0.825	3.92	0.104	0.632	3.82
18.	0.70	0.656	0.825	0.73	0.20	0.64	3.84
19.	1.40	0.656	0.825	1.48	0.41	0.65	3.87
20.	1.70	0.656	0.825	1.80	0.50	0.65	3.875
21.	2.10	0.656	0.825	2.28	0.638	0.666	3.92
Temperature 333 K							
22.	0.346	0.656	0.40	0.476	0.092	0.781	4.18
23.	0.346	0.656	0.830	0.589	0.0962	0.967	4.65
24.	0.346	0.656	1.20	0.640	0.0973	1.05	4.85
25.	0.346	2.10	0.830	1.85	0.123	0.99	4.71
26.	0.346	3.39	0.830	3.06	0.151	0.974	4.67
27.	0.346	6.84	0.830	6.10	0.149	1.963	4.65
28.	0.733	0.656	0.830	1.34	0.34	1.038	4.83
29.	1.67	0.656	0.830	3.30	0.84	1.12	5.026
30.	2.13	0.656	0.830	4.12	1.05	1.09	5.00
Temperature 353 K							
31.	0.36	0.656	0.406	1.261	0.28	1.81	6.19
32.	0.36	0.656	0.825	1.340	0.30	1.92	6.39
33.	0.36	0.656	1.20	1.362	0.308	1.95	6.44
34.	0.36	2.00	0.825	3.3	0.246	1.56	5.75
35.	0.36	3.386	0.825	594	0.26	1.65	5.918
36.	0.36	6.83	0.825	11.70	0.254	1.61	5.85
37.	0.77	0.656	0.825	3.00	0.67	1.99	6.51

1	2	3	4	5	6	7	8
38.	1.70	0.656	0.825	4.784	1.08	1.45	5.55
39.	2.10	0.656	0.825	4.871	1.10	1.2	5.04
<b>Temperature 363 K</b>							
40	0.36	0.656	0.400	1.94	0.40	2.59	7.3
41.	0.36	0.656	0.825	2.10	0.43	2.81	7.6
42.	0.36	0.656	1.20	2.20	0.45	2.94	7.78
43.	0.36	2.00	0.825	4.80	0.325	2.11	6.6
44.	0.36	3.38	0.825	8.18	0.326	2.122	6.61
45.	0.36	6.83	0.825	16.82	0.332	2.16	6.66
46.	0.60	0.656	0.825	3.60	0.742	2.89	7.71
47.	0.80	0.656	0.825	4.46	0.919	2.68	7.43
48.	1.20	0.656	0.825	5.38	1.11	2.16	6.67
49.	1.66	0.656	0.825	5.48	1.13	1.59	5.72
50.	2.10	0.656	0.825	5.447	1.12	1.25	5.07

TABLE 3. IV : SOLUBILITY OF H<sub>2</sub> IN METHANOL \*

Temperature K	Solubility, x 10 <sup>4</sup> , kmol/m <sup>3</sup> . kPa
313	4.34
323	4.64
333	4.93
353	5.42
363	5.82

\* Siedell (1940)

TABLE 3. V : GAS-LIQUID MASS TRANSFER COEFFICIENTS\*

---

Temperature K	Gas-liquid mass transfer coefficient, $k_{L,a}$ , $s^{-1}$
313	0.117
323	0.119
333	0.121
353	0.1242
363	0.127

---

\* Chaudhari et.al. (1987).

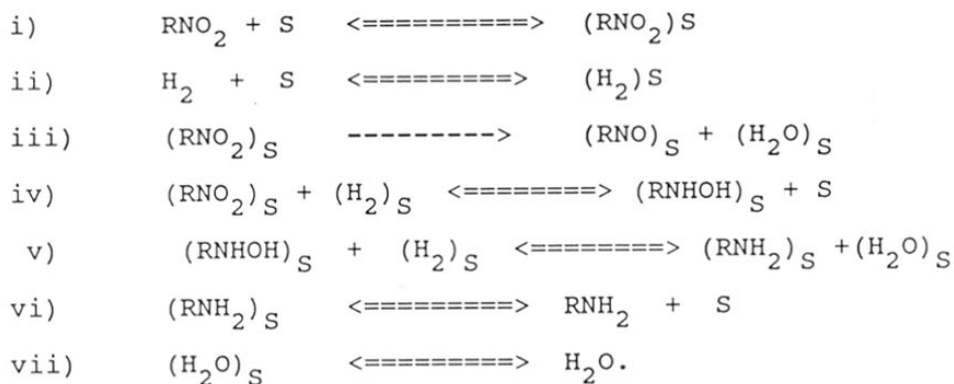
TABLE 3. VI : DIFFUSIVITY OF H<sub>2</sub> IN METHANOL

Temperature K	Molecular diffusivity D x 10 <sup>9</sup> , m <sup>2</sup> /s	Effective diffusivity De x 10 <sup>9</sup> , m <sup>2</sup> /s
313	6.70	1.116
323	6.91	1.175
333	7.13	1.212
353	7.55	1.284
363	7.77	1.320

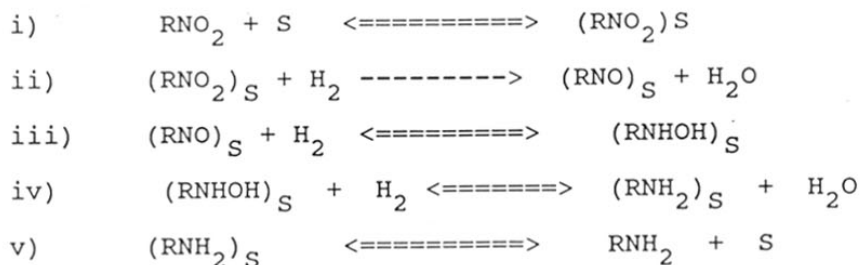
- o Catalyst is uniformly distributed with single type of sites (single type of sites implies that all the sites on the surface have uniform strength and nature).
- o Only one of the steps in reaction scheme is rate controlling.
- o The concentration of transient adsorbed species is negligible.
- o For a rate controlling step, the reverse reaction is negligible.

The following reaction schemes were considered :

**SCHEME 1 :** Molecular adsorption of  $H_2$ ; and MNCB, followed by surface reaction (Dual site).



SCHEME 2 : Molecular adsorption of  $H_2$ , and MNCB, followed by surface reaction (single site).



### 3.2.1 Model Discrimination and Parameter Estimation

In order to discriminate the several rate equations including those derived based on above schemes were considered as shown in Table 3.VII. Experimental rate data obtained in the kinetic regime (313-333 K) were considered for this purpose. A non-linear regression analysis was used for each rate equation in Table 3.VII to obtain the best values of rate parameters. For this purpose, an optimization program based on Marquardt's method was used, which involves a non-linear least square regression analysis. The values of rate parameters and  $\phi_{\min}$  are presented in Table 3.VII. It is well known that the model discrimination is not always easy on the basis of statistical analysis alone (Froment, 1975; Froment and Bischoff, 1979). Other criteria considered in selecting the best model are :

(a) The estimated kinetic parameters must have physico-chemical meaning. Some of the rules are given below (Boudart 1972; Vannice et al. 1979).

Rule 1 : reaction rate constant > 0  
 Rule 2 : activation energy > 0  
 Rule 3 : adsorption constants > 0

(b) The residuals ( $r_A' - r_A$ ) should be distributed with zero mean and these residuals should have no trend effects, as a function of the independent variables like  $pH_2$ , and MNCB concentration.

The values of the rate parameters evaluated for each model are presented in Table 3.VII. Considering the above criteria, it can be seen that all the models except (3) have model parameters less than zero, and hence can be rejected. The proposed rate equation is :

$$r_A = \frac{wk_1 A^* B_1}{1 + k_B B_1} \quad (9)$$

Also,  $\phi_{\min}$  was lowest for equation (9) at all temperatures. This rate equation (9) is also consistent with the reaction mechanism shown in scheme 2, (section 3.2).

Therefore, model (9) was considered as the best model to represent the kinetics of hydrogenation of m-

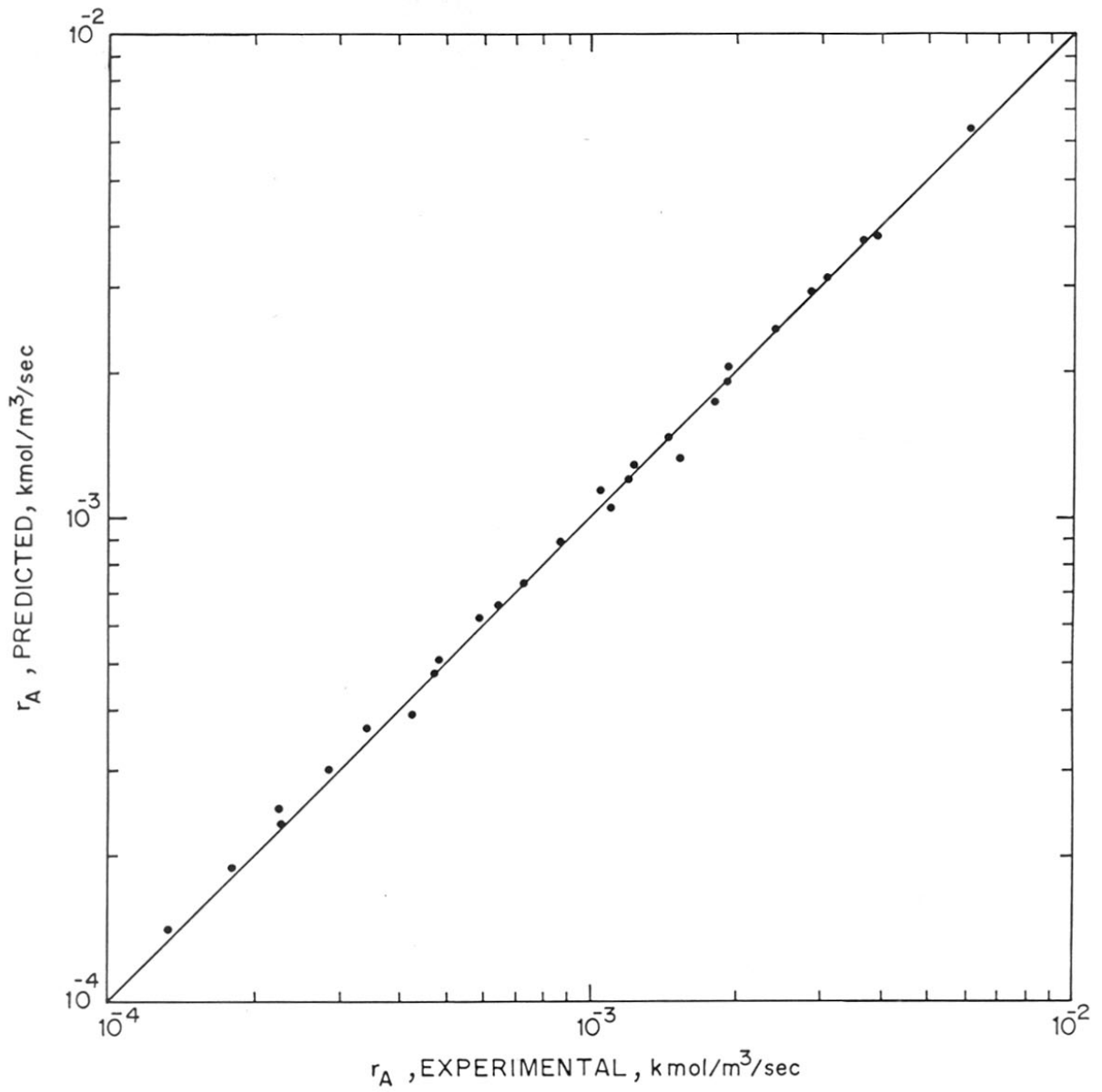


TABLE 3. VII : RATE EQUATIONS USED AND THE PARAMETERS OBTAINED

Serial No.	Rate Equation	Temperature K	$k_1$ ( $m^3/kg$ )( $m^3/kmol.s$ )	$k_A$ ( $m^3/kmol$ )	$k_B$ ( $m^3/kmol$ )	$\phi_{min}$
1	$w k_1 A^* B_l$ ----- ( $1 + K_A A + K_B B_l$ ) <sup>2</sup>	313 323 333	$8.3658 \times 10^{-3}$ $4.810 \times 10^6$ 0.2078	- 28.13 $1.6316 \times 10^3$ 0.3812	3.1231 $-1.344 \times 10^4$ 0.83326	$2.5 \times 10^{-12}$ $7.4 \times 10^{-12}$ $7.8 \times 10^{-13}$
2	$w k_1 A^* B_l$ ----- ( $1 + K_A A + K_B B_l$ )	313 323 333	0.133 0.18694 0.29927	1.862 -0.78266 1.93273	4.183 4.36132 3.7601	$2.3 \times 10^{-13}$ $3.7 \times 10^{-13}$ $8.2 \times 10^{-12}$
3	$w k_1 A^* B_l$ ----- ( $1 + K_B B_l$ )	313 323 333	0.1334 0.18869 0.27964	----- ----- -----	4.61888 4.21480 3.86400	$4.8 \times 10^{-14}$ $4.8 \times 10^{-14}$ $3.7 \times 10^{-13}$

4	$\frac{w k_1 \sqrt{A} B_l}{(1 + \sqrt{K_A} A + K_B B_l)}$	313	$-3.0801 \times 10^{-3}$	$3.052 \times 10^6$	$-3.820 \times 10^2$	$1.206 \times 10^{-9}$
		323	$-1.5640 \times 10^{-3}$	$8.537 \times 10^5$	$-4.585 \times 10^2$	$1.300 \times 10^{-11}$
		333	$-0.14$	$2.676 \times 10^5$	$-5.044 \times 10^2$	$7.900 \times 10^{-13}$

5	$\frac{w k_1 \sqrt{A} B_l}{(1 + \sqrt{K_A} A + K_B B_l)^2}$	313	$4.0220 \times 10^{-3}$	$3.840 \times 10^2$	$-14.80$	$1.40 \times 10^{-11}$
		323	$5.4000 \times 10^4$	$3.612 \times 10^8$	$-2.300 \times 10^4$	$1.04 \times 10^{-12}$
		333	$3.0130 \times 10^4$	$7.900 \times 10^7$	$-1.240 \times 10^4$	$3.110 \times 10^{-12}$

FIGURE 3-9: A LOG-LOG PLOT OF  $r_A$  EXPERIMENTAL Vs  $r_A$  PREDICTED

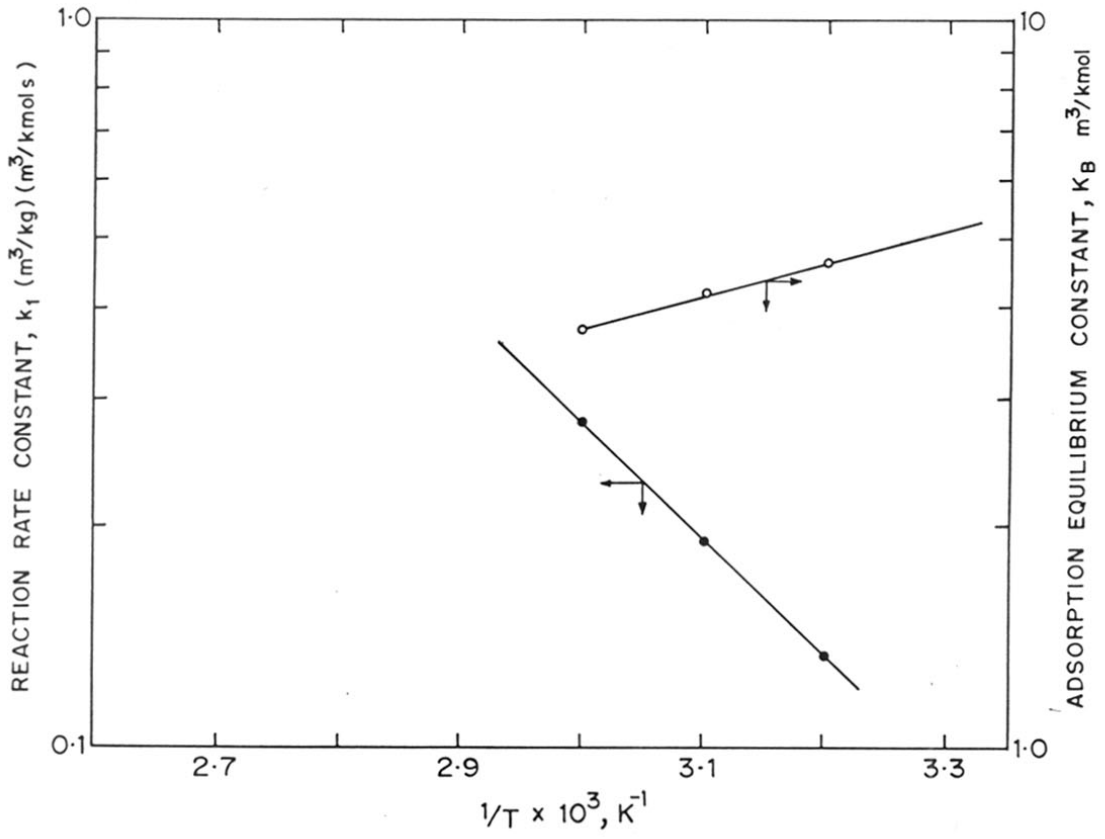


FIGURE 3.10: TEMPERATURE DEPENDENCE ON THE RATE PARAMETERS

nitrochlorobenzene to m-chloroaniline using 1% Pt-S/C, catalyst system. A comparison of the experimental and predicted rates is shown in Figure 3.9, which indicates an excellent agreement.

The temperature dependence of the rate and adsorption constants is shown in Figure 3.10, from which the activation energy was calculated, as 30.2 kJ/mole. The adsorption coefficients obtained for the above model, also show the usually expected trend of decrease in the values of adsorption coefficients with temperature (Table 3.VII, model 3). However, the temperature effect observed for the adsorption coefficient is very mild, and the heat of adsorption calculated from the Arrhenius plot is equal to 8.62 kJ/mol.

### 3.2.2 Interpretation of the rate data at 353 and 363 K

Since, the rate data at 353 and 363 K were found to be under conditions of gas-liquid mass transfer limitations, the overall rate of hydrogenation would be given as (Chaudhari and Ramachandran, 1980) :

$$r_A = k_L a (A^* - A_1) \quad (10)$$

$$= \frac{wk_1 A_1 B_1}{1 + K_B B_1} \quad (11)$$

Eliminating the unknown  $A_1$  in equation (10) and (11), the following equation for the overall rate of hydrogenation can be obtained :

$$r_A = A^* \left[ \frac{1}{k_L a} + \frac{1 + K_B B_1}{w k_1 B_1} \right]^{-1} \quad (12)$$

Here, liquid-solid and intraparticle diffusional resistances were not considered as they were found to be unimportant (section 3.1.5).

In order to use the equation (12) for calculating the rate of hydrogenation, a knowledge of  $k_1$ ,  $K_B$  and  $k_L a$ , is required in addition to the solubility data. The values of  $k_1$  and  $K_B$  were obtained by extrapolation of the Arrhenius plot in Figure 3.10, while  $k_L a$  values were evaluated from the following correlation proposed by (Chaudhari et al. 1987), for the type of equipment used in the present work.

$$k_L a = 1.48 \times 10^{-3} (N)^{2.18} (V_g / V_L)^{1.88} \times (d_I / d_T)^{2.16} \times (h_1 / h_2)^{1.16} \quad (13)$$

where,

- N = speed of agitation, Hz
- $V_g$  = volume of the gas in the reactor,  $m^3$
- $V_L$  = volume of the liquid in the reactor,  $m^3$
- $d_I$  = impeller diameter, m

- $d_T$  = tank diameter, m
- $h_1$  = height of the first impeller from the bottom, m
- $h_2$  = height of the second impeller from the bottom, m.

The values of  $k_1$  and  $K_B$  and  $k_L a$  thus obtained are presented in Table 3.VIII. The rates calculated using these parameters and equation (11) are compared in Table 3.IX with the experimental observations. Also, shown in Table 3.IX are the rates predicted using the equation (9) without incorporating the mass transfer effects. It was observed from this comparison that the experimental data agrees well with those predicted by the equation (12). The prediction of equation (9) are significantly higher than the observed data and this again confirms the importance of gas-liquid mass transfer resistances under these conditions. The agreement between the experimental results and the model predictions (equation 12) also confirms the applicability of the rate model given by equation (9) proposed here.

### 3.3 BATCH REACTOR MODEL

In order to verify the applicability of the kinetic model over a wider range of conditions, integral batch reactor data were also obtained at constant  $H_2$

TABLE 3. VIII : VALUES OF  $k_1$ ,  $K_B$  and  $k_{La}$  AT HIGHER TEMPERATURES

Temperature K	$k_1$ , ( $m^3/kg$ ) ( $m^3 / kmol^s$ )	$K_B$ ( $m^3 / kmol$ )	$k_{La}$ , $s^{-1}$
353	0.52	3.15	0.124
363	0.70	2.80	0.127



TABLE 3. IX : COMPARISON OF EXPERIMENTAL RATE DATA WITH MODEL PREDICTIONS WITH AND WITHOUT GAS-LIQUID MASS TRANSFER EFFECTS

Sr. No.	$r_A \times 10^3$ , kmol/m <sup>3</sup> .s. (Experimental)	$r_A \times 10^3$ , kmol/m <sup>3</sup> .s. (Predicted by Eq. 11)	$r_A \times 10^3$ , kmol/m <sup>3</sup> .s. (Predicted by Eq. 9)
Temperature 353 K			
1.	1.261	1.236	1.487
2.	1.340	1.334	1.530
3.	1.362	1.341	1.673
4.	3.30	3.276	4.634
5.	5.94	5.67	7.89
6.	11.70	11.793	15.92
7.	3.00	3.07	3.27
8.	4.784	4.581	7.214
9.	4.871	4.604	7.82
Temperature 363 K			
10.	1.94	1.86	2.33
11.	2.10	1.94	2.40
12.	2.20	2.08	2.65
13.	4.80	4.58	5.30
14.	8.18	7.89	10.34
15.	16.82	15.57	18.60
16.	3.60	3.76	4.00
17.	4.46	4.21	5.33
18.	5.38	5.12	6.78
19.	5.48	5.23	7.07
20.	5.447	5.72	6.86

pressures. In these experiments, the variation of the concentration of m-nitrochloro benzene and m-chloroaniline was observed as a function of time. The concentration-time behaviour can also be predicted from the batch reactor model since the kinetics is known from initial rate data compared with the experimental results.. The variation of the concentration of m-nitrochloro benzene and m-chloroaniline can be represented by the following mass balance equations :

$$-\frac{d[B_1]}{dt} = \frac{1}{3} A^* \left[ \frac{1}{k_L a} + \frac{1 + K_B B_1}{wk_1 B_1} \right]^{-1} \quad (14)$$

and for the product formation,

$$\frac{d[E_1]}{dt} = \frac{1}{3} A^* \left[ \frac{1}{k_L a} + \frac{1 + K_B B_1}{wk_1 B_1} \right]^{-1} \quad (15)$$

the initial conditions are

$$t = 0, \quad B_1 = B_{10}, \quad E_1 = 0$$

In case of data in the kinetic regime, the above equations are simplified as follows :

$$-\frac{d[B_1]}{dt} = \frac{wk_1 A^* B_1}{3 (1+K_B B_1)} \quad (16)$$

$$\frac{d[E_1]}{dt} = \frac{wk_1 A^* B_1}{3 (1+K_B B_1)} \quad (17)$$

Since the experiments were carried out at constant pressure of  $H_2$ , the value of  $A^*$  remains constant, at all times and also it was assumed that the presence of reactant and product do not affect the solubility of  $H_2$ , appreciably.

For data at constant pressure, the above equations can be solved numerically by using Runge-Kutta method to obtain concentrations of m-nitrochloro benzene and m-chloroaniline at different times. The concentration-time profile can then be predicted using the rate parameter and the solubility values from the previous section. The experimental and predicted concentration profiles of m-nitrochloro benzene and m-chloroaniline Vs. time are compared in Figures 3.11-3.14 for 313-333K. The agreement between the predicted and the observed results was found to be excellent.

The concentration time profiles for higher temperatures (353K and 363K) are shown in Figures 3.15 and 3.16. Here, it can be seen that the data is well represented by the above rate model (equation 9), after incorporating the mass transfer effects, while the predictions do not match if the data is assumed to be in

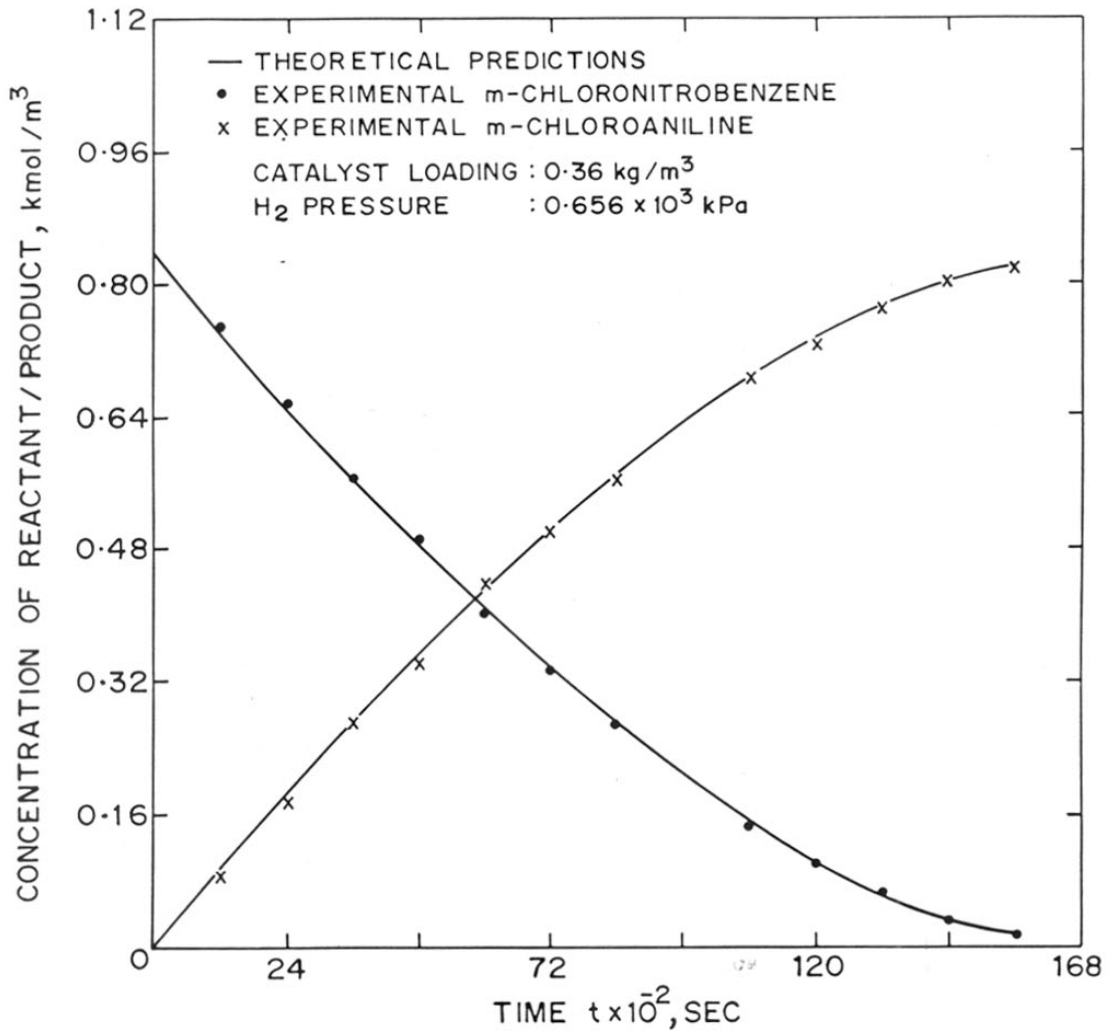


FIGURE 3.11 : LIQUID REACTANT/PRODUCT CONCENTRATION PROFILE FOR 313 K

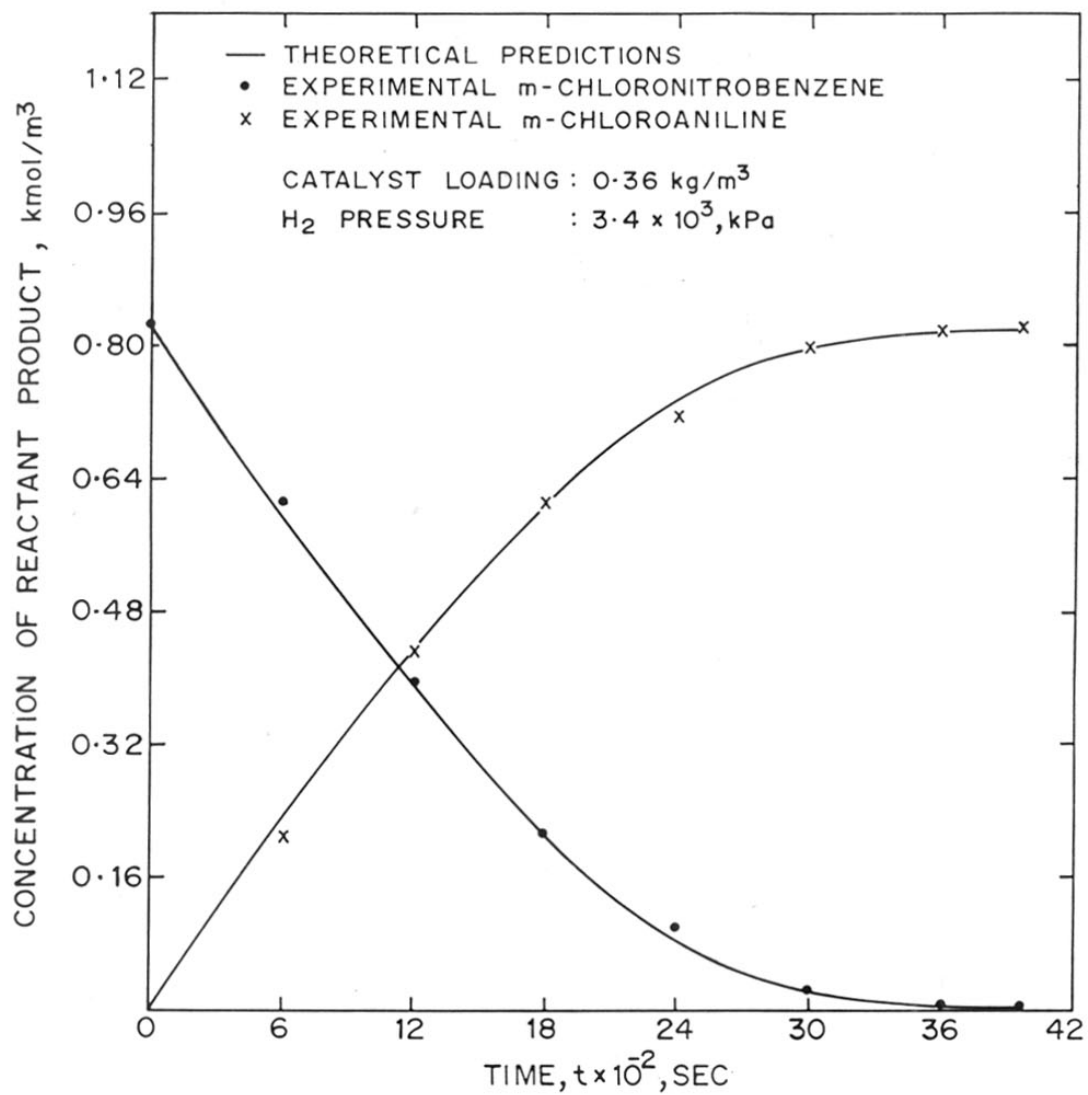


FIGURE. 3.12: LIQUID REACTANT /PRODUCT CONCENTRATION PROFILE FOR 313 K

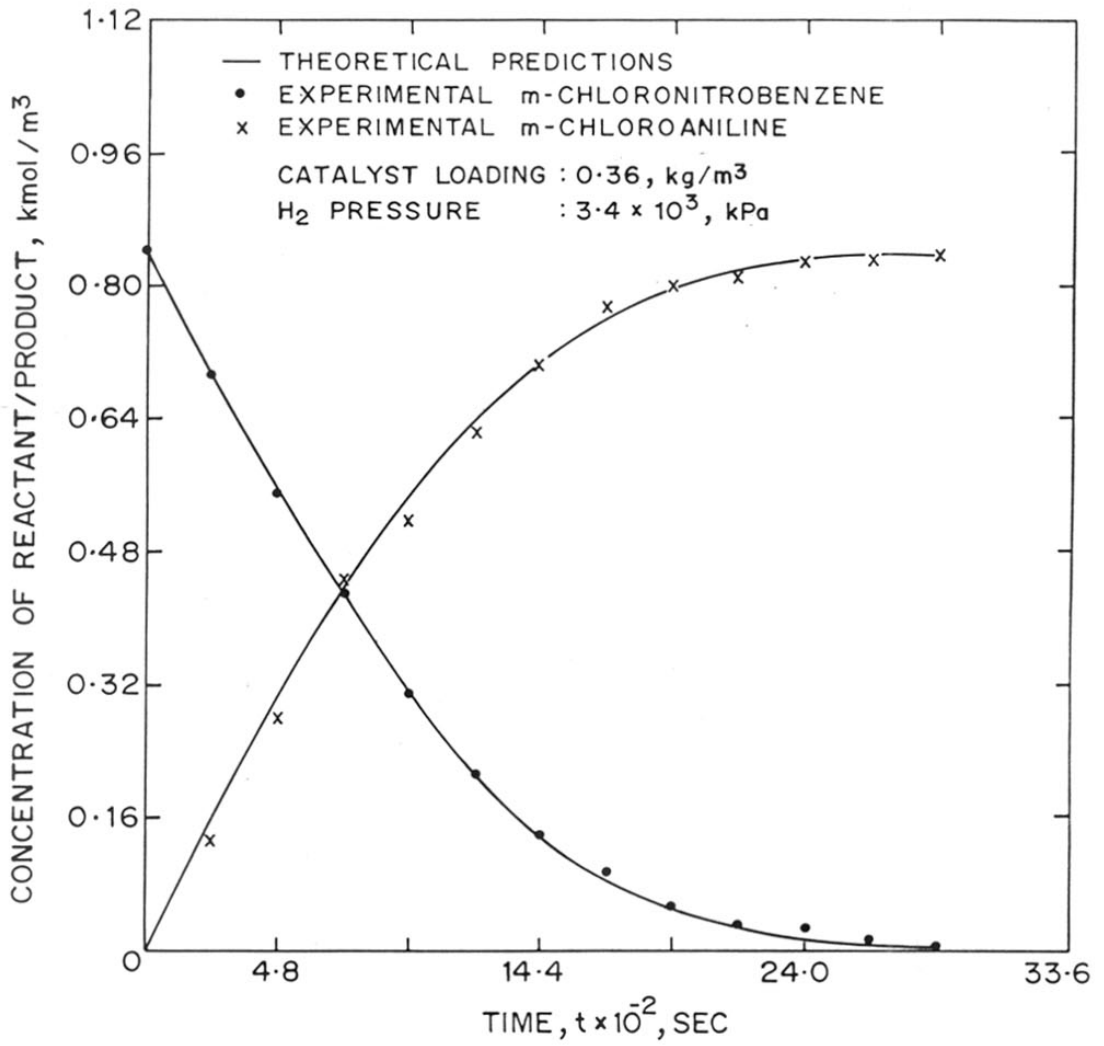


FIGURE 3-13 : LIQUID REACTANT/PRODUCT CONCENTRATION PROFILE, FOR 323 K

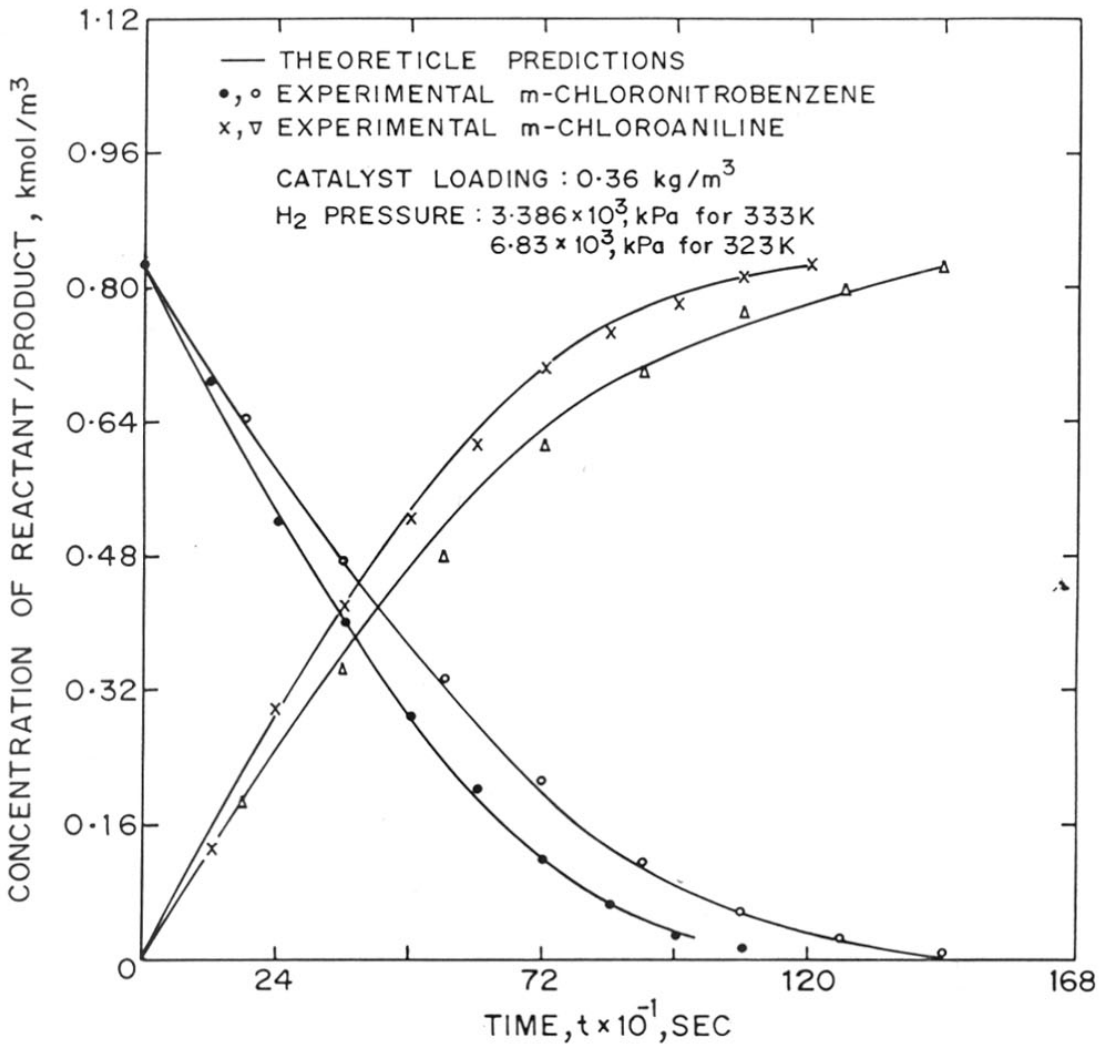


FIGURE 3-14 : LIQUID REACTANT/PRODUCT CONCENTRATION PROFILE , FOR 323K (•, x) AND 333 (◦, Δ)

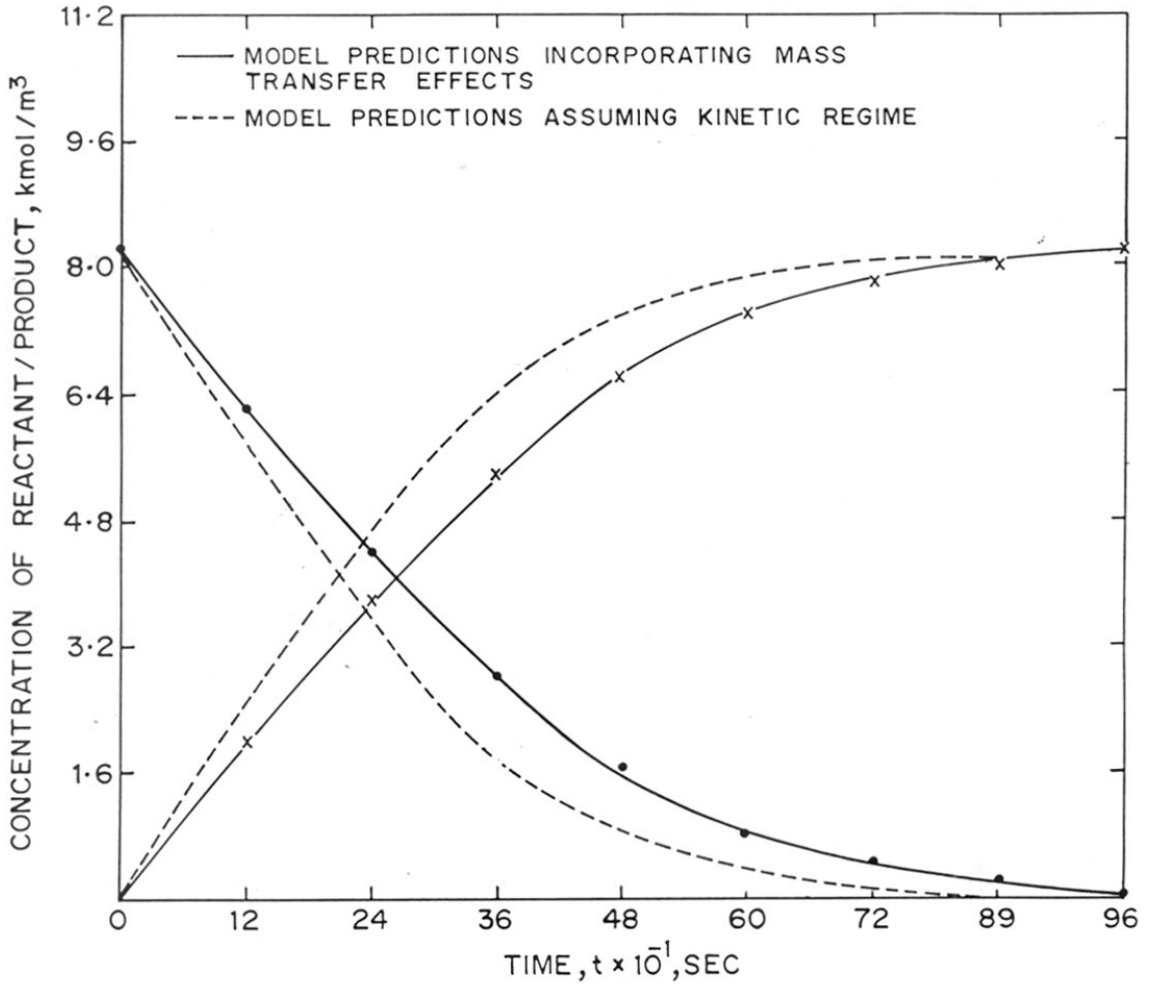


FIGURE 3-15: LIQUID REACTANT (•) AND PRODUCT (x), CONCENTRATION PROFILE FOR 353 K.



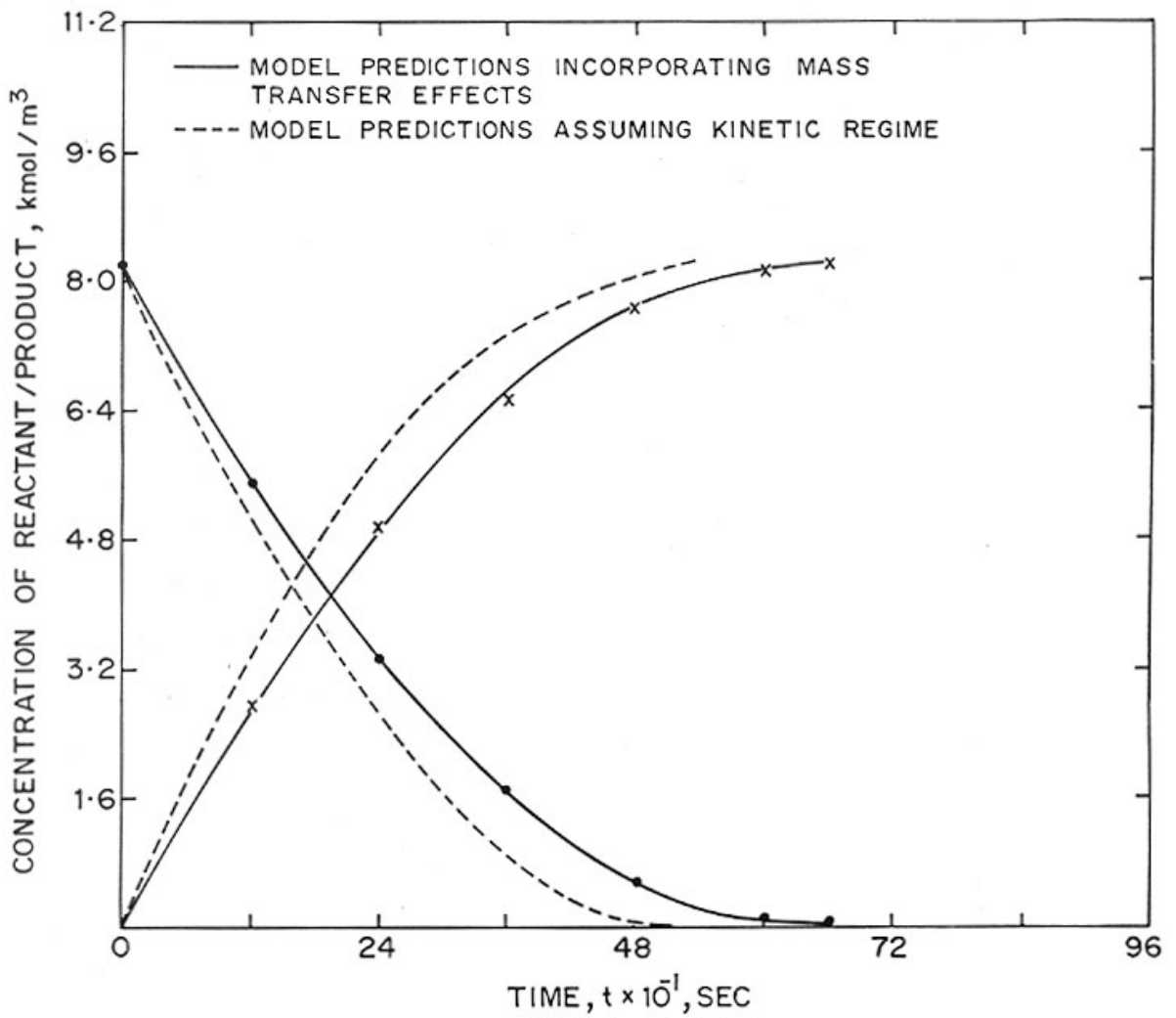


FIGURE 3-16: LIQUID REACTANT (•) AND PRODUCT (x), CONCENTRATION PROFILE FOR 363 K

the kinetic regime. Thus, the rate model proposed here, is applicable over a wide range of conditions and can be reliably used for design and scale-up purposes.

### 3.4 NON-ISOTHERMAL MODELLING

In the catalytic hydrogenation of the nitroaromatic compounds to the aromatic amines, the oxygen in the nitro group is progressively replaced by hydrogen. This reaction is highly exothermic and the heat of reaction is about 547 kJ/mol which would eventually lead to a rise in the temperature during the reaction. The objective of the present work was to carry out some hydrogenation experiments under non-isothermal conditions and to observe the temperature vs. time as well as H<sub>2</sub> consumption vs. time profiles. A theoretical non-isothermal model was also developed for this system based on the kinetics already reported in this work. Such a study would be useful in understanding the non-isothermal behaviour of the catalytic hydrogenation processes.

The non-isothermal experiments were carried out in the same setup as described earlier however, the procedure followed was as given below :

The contents of the autoclave were flushed first with N<sub>2</sub> and then with H<sub>2</sub>, then the reactants were heated

to a desired initial temperature by circulating the hot water through the outer jacket of reactor. After the initial reaction temperature was observed to be constant,  $H_2$  was introduced into the reactor to a desired pressure and the reaction was started. The rise in temperature and the pressure drop in the intermediate hydrogen reservoir were recorded as a function of time. This was continued until there was no further absorption of hydrogen. In these experiments no cooling fluid was circulated through the internal coil.

The material balance equations for the reactant, product, and hydrogen consumption, under non-isothermal conditions are given as :

$$\frac{-d[B_1]}{dt} = \frac{1}{3} A^* e^{-E_s/RT} \left[ \frac{1}{(k_L a)_{T_0} (T_1/T_2)^{1/2}} + \frac{(1 + K_{Bo} e^{-E_{ad}/RT} B_1)}{w B_1 k_{1(0)} e^{-E_r/RT}} \right]^{-1} \quad (18)$$

$$\frac{d[B_1]}{dt} = \frac{1}{3} A^* e^{-E_s/RT} \left[ \frac{1}{(k_L a)_{T_0} (T_1/T_2)^{1/2}} + \frac{(1 + K_{Bo} e^{-E_{ad}/RT} B_1)}{w B_1 k_{1(0)} e^{-E_r/RT}} \right]^{-1} \quad (19)$$

$$\frac{dH_2}{dt} = V_R A^* e^{-E_s/RT} \left[ \frac{1}{(k_L a)_{T_0} (T_1/T_0)^{1/2}} + \frac{(1 + K_{Bo} e^{-E_{ad}/RT} B_1)}{w B_1 k_{1(0)} e^{-E_r/RT}} \right]^{-1} \quad (20)$$

The heat balance for the present system can be written as :

Heat released due to reaction

- Heat lost to the surroundings
- Heat required to raise the inlet gas temperature.
- = Heat accumulated in the reactor

The corresponding heat balance equation is :

$$\begin{aligned} V_R \Delta H_{rA} dt - U_A A_R (T - T_w) - Q_g C_{pg} (T - T_w) dt \\ = \epsilon_g V_R \rho_g - (1 - \epsilon_g - w/\rho_s) C_{pl} \rho_l V_L + w V_R C_{ps} dt \end{aligned} \quad (21)$$

Equation (21) can be rewritten as :

$$\frac{dT}{dt} = \frac{V_R \Delta H_r A - (U_A A_R + Q_S C_{pg})(T - T_w)}{\epsilon_g V_R s + (1 - \epsilon_g - w/\rho_g) C_{pl} \rho_l V_R + w V_R C_{ps}} \quad (22)$$

The initial conditions are :

$$t = 0, B_1 = b_{10}, H_2 = 0, T = T_0 \quad (23)$$

The solution of equations (17), (18), and (21) with initial conditions given in equation (23) allows the prediction of  $H_2$  consumed and temperature rise as a function of time. These equations are non-linear and solved simultaneously to obtain the temperature-time and the hydrogen consumption-time profiles. While solving these equations the following points were considered :

- (1) Variation of  $k_1$  and  $K_B$  with temperature.
- (2) Variation of  $H_2$  solubility ( $A^*$ ) with temperature.
- (3) Variation of vapour pressure of solvent with temperature.
- (4) Mass transfer (gas - liquid) effects and variation of  $k_L a$  with temperature.

It was also assumed that the heat of reaction and the heat transfer coefficient remained constant in the temperature range covered here.

It is well known that the heat transfer coefficient  $U_A$  is highly equipment sensitive, therefore, its value in the present case was estimated by simulating a part of our own experimental data. For this purpose, at a given temperature, the value of  $U_A$  was estimated so that the predicted temperature rise and the experimentally observed one matched closely. This estimated value was found to be  $1.045 \times 10^4 \text{ J/m}^2/\text{s/K}$  which was then used to predict the temperature-time profiles for other temperatures. The results are presented in Figures 3.17 - 3.19 for different initial temperatures. It was found that the agreement between the predicted and the experimental results was excellent. It is important to note that the non-isothermal data at different initial temperatures were represented well by the non-isothermal model developed here, after accounting for the gas-liquid mass transfer resistance.

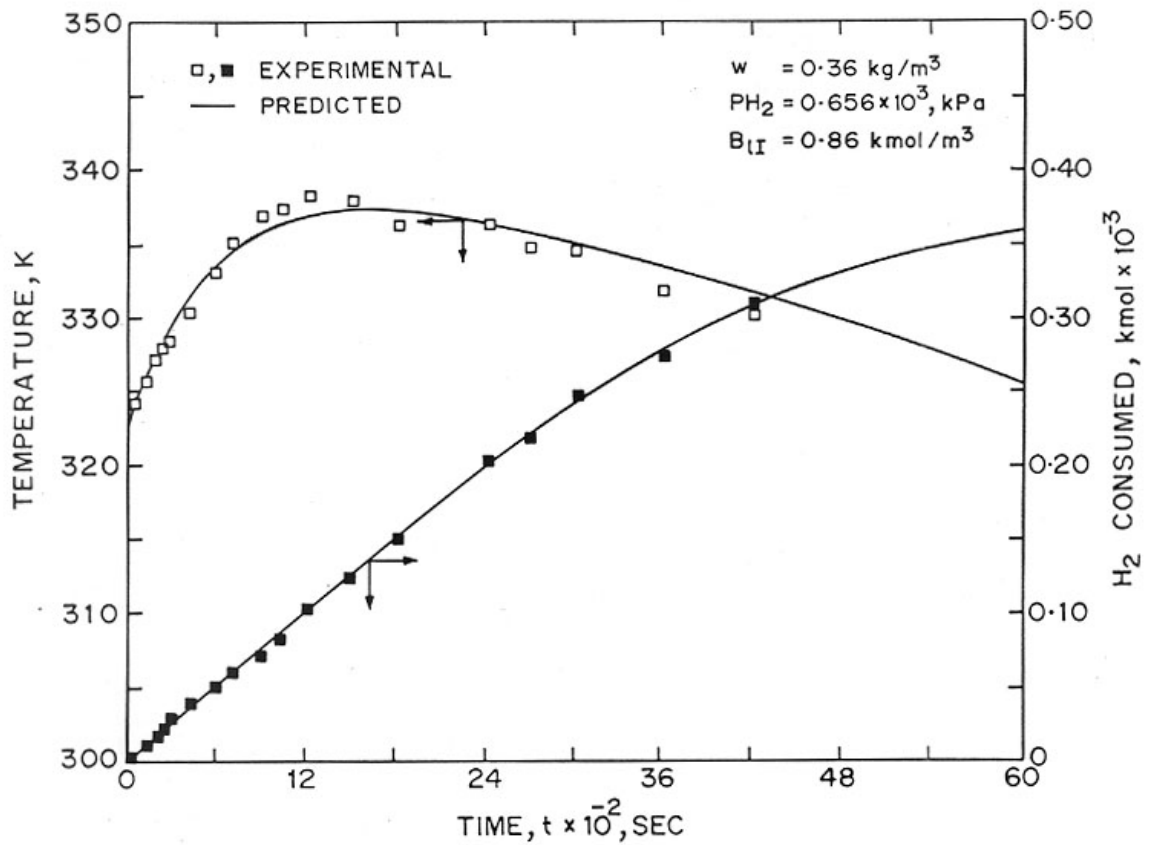


FIGURE 3-17: TEMPERATURE AND H<sub>2</sub> CONSUMPTION PROFILES, UNDER NONISOTHERMAL CONDITIONS, AT INITIAL TEMPERATURE 323 K

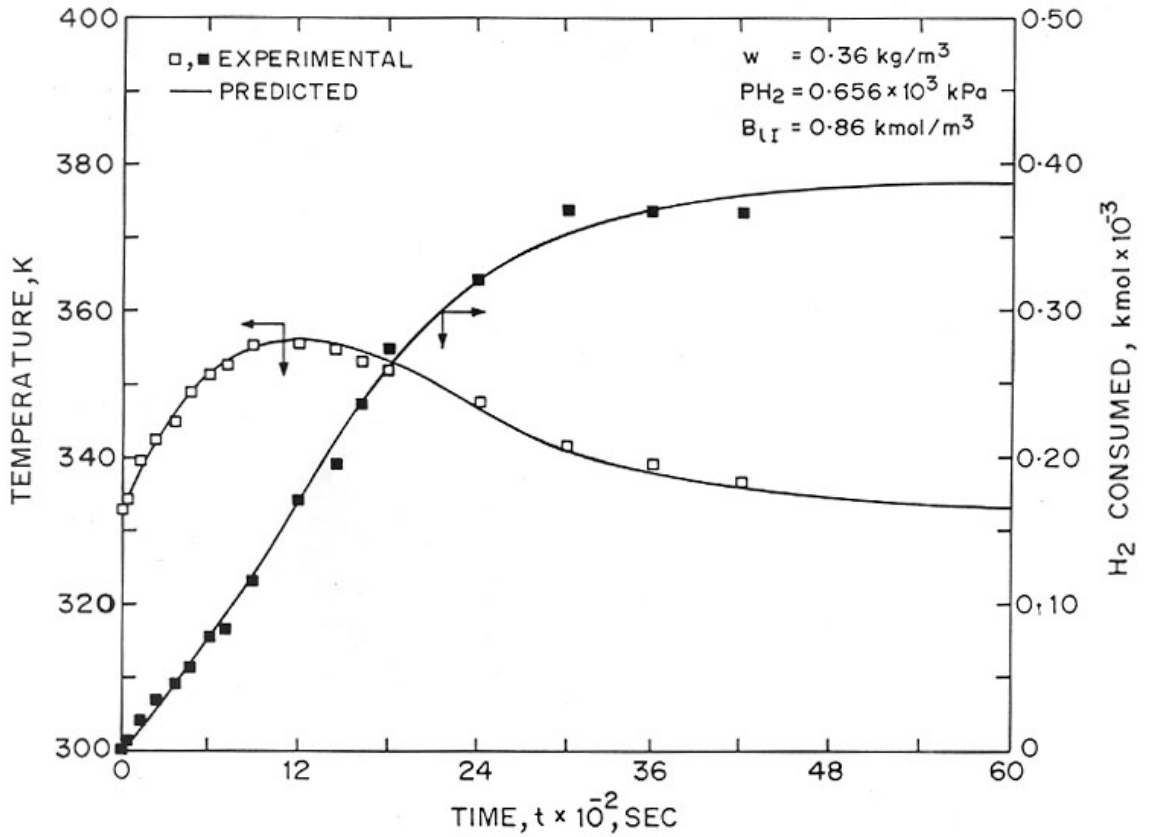


FIGURE 3-18: TEMPERATURE AND H<sub>2</sub> CONSUMPTION PROFILES UNDER NONISOTHERMAL CONDITIONS WITH INITIAL TEMPERATURE = 333 K



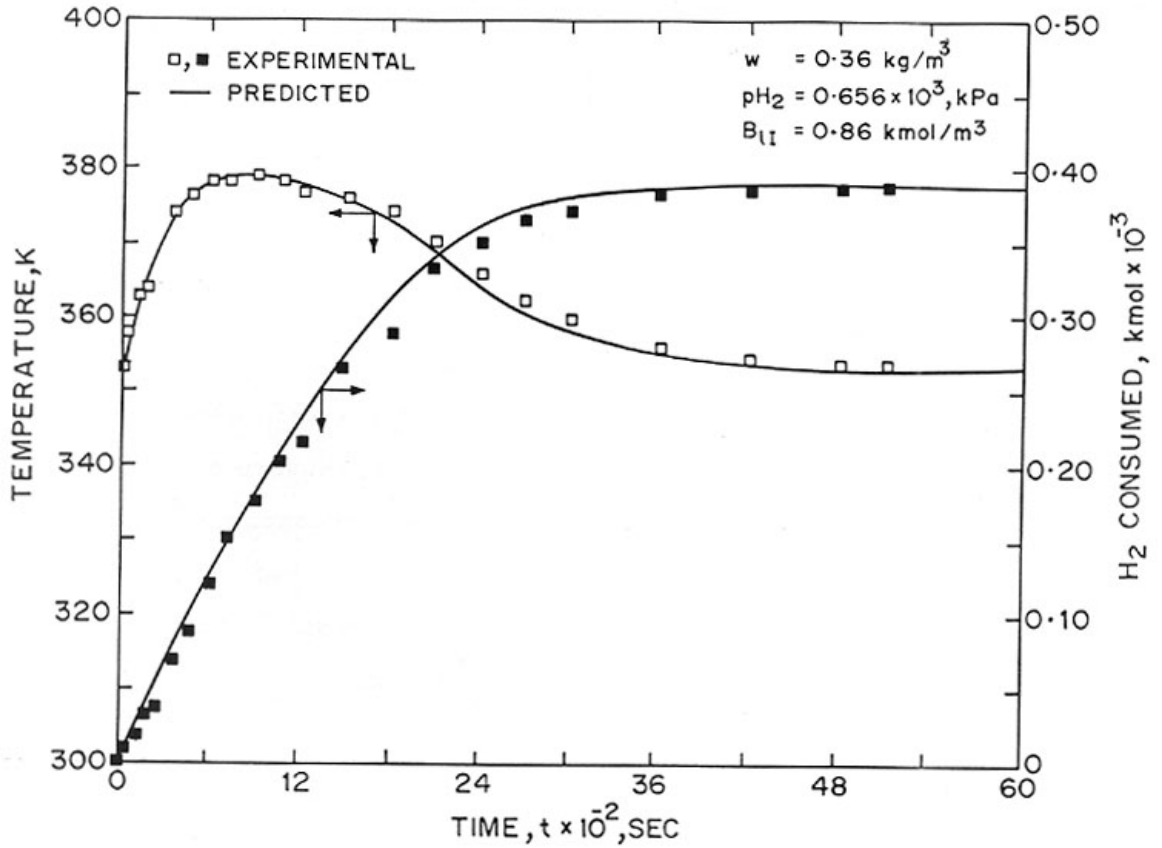


FIGURE 3-19: TEMPERATURE AND H<sub>2</sub> CONSUMPTION PROFILES UNDER NON-ISOTHERMAL CONDITIONS WITH INITIAL TEMPERATURE = 353 K

### 3.5 CONCLUSIONS

The hydrogenation of m-nitrochlorobenzene was studied using 1% Pt-S/C catalyst in a high pressure slurry reactor over a wide range of temperatures. From the initial rate data, a Langmuir - Hinshelwood type rate model was found to represent the data satisfactorily. The rate was found to be linearly dependent on  $H_2$  pressure while it was zero order with respect to both the substrate as well as the product concentration. The initial rate data were analyzed for the significance of mass transfer effects. It was found that in the temperature range of 313-333K, mass transfer effects were unimportant, while at 353 and 363, gas-liquid mass transfer resistance was significant. The data at higher temperatures could be represented by the rate equation, after accounting for the gas-liquid mass transfer effects.

In order to verify the applicability of the rate equation under integral reactor conditions, experimental data in a batch reactor were obtained. A theoretical model was developed, to predict the concentration-time profile in a batch reactor. The predicted and observed results were found to agree within 5 - 7% error.

Finally, the values of activation energy and the heat of adsorption evaluated were found to be 30.2

kJ/mole and 8.62 kJ/mole, respectively.

A few experiments were carried out under non-isothermal conditions, with different initial temperatures. The experimental data were interpreted by developing a non-isothermal model using the kinetics studied in this work. The agreement between the model predictions and the experimental results was excellent indicating the applicability of the kinetics and reactor model over a wide range of conditions.

## NOMENCLATURE

$A^*$	:	concentration of dissolved hydrogen in the bulk liquid, kmol/m <sup>3</sup>
$a$	:	effective gas-liquid interfacial area per unit volume of the reactor, m <sup>2</sup> /m <sup>3</sup>
$a_p$	:	effective liquid-solid interfacial area per unit volume of slurry, m <sup>2</sup> /m <sup>3</sup>
$B_{lo}$	:	Initial concentration of m-nitrochlorobenzene, kmol/m <sup>3</sup>
$D$	:	Diffusivity of hydrogen, m <sup>2</sup> /sec
$d_t$	:	diameter of agitator, m
$d_p$	:	average diameter of the catalyst particles, m
$e$	:	energy supplied to liquid, kg/sec
$F_c$	:	shape factor of the catalyst
$H_A$	:	Henry's law constant for solubility of A, m <sup>3</sup> /kmol/kPa
$K_B$	:	adsorption equilibrium constant, m <sup>3</sup> /kmol
$k_1$	:	reaction rate constant, (m <sup>3</sup> /kg) (m <sup>3</sup> kmol <sup>-1</sup> s) (defined by Eq. 9)
$k_L$	:	gas - liquid mass transfer coefficient, m/sec.
$k_s$	:	liquid-solid mass transfer coefficient, m/sec.
$N$	:	speed of agitation employed, s <sup>-1</sup> . Hz.
$N_p$	:	Power number
$p$	:	Power consumption for agitation, kg/m <sup>2</sup> /sec <sup>3</sup>
$P_A$	:	partial pressure of H <sub>2</sub> , k Pa
$Q_g$	:	volumetric gas flow rate of gas, m <sup>3</sup> /s
$r_A$	:	overall rate of reaction, kmol/m <sup>3</sup> /s

- $r_{\max}$  : maximum rate of hydrogenation,  $\text{kmol} / \text{m}^3/\text{s}$
- $U_A$  : heat transfer coefficient,  $\text{J}/\text{m}^2/\text{s}/\text{K}$
- $w$  : catalyst concentration,  $\text{kg}/\text{m}^3$

### Greek symbols

- $\alpha_1, \alpha_2$  : parameters defined by Equations (1) and (2)
- $\gamma_B$  : stoichiometric coefficient for species, B
- $\rho_p$  : particle density,  $\text{kg}/\text{m}^3$
- $\rho_L$  : density of liquid,  $\text{kg}/\text{m}^3$
- $\mu_L$  : viscosity of the liquid,  $\text{kg}/\text{m}/\text{sec}$ .

## REFERENCES

1. Acres, G.J.K., and Cooper, B.J., *J. Appl. Chem. Biotechnol.*, **22** (1972), 769.
2. Baltzly, R., *J. Org. Chem.*, **41** (1976), 920.
3. Bavin, P.M.G., *Can. J. Chem.*, **36** (1958), 238.
4. Bechamp, A., *Annales de Chemie (Paris)*, **42**, (3), (1854a), 186.
5. Bechamp, A., *Ann. Chem.*, **92**, (1854b), 401.
6. Blicke, F.F., *Organic Reactions*, **1**, (1942), 303.
7. *Belg. Pat.*, 654597, (1965), to I C Ind.,  
C A, 63 : 11425D (1965).
8. *Brit. Pat.*, 982 902, (1968), C A, 64 : 641F(1966).
9. *Brit. Pat.*, 1, 125,811, (1968), to I C Ind.,  
C A, 69 : 110354a (1968).
10. *Brit. Pat.*, 1, 433 517, (1975), to Shell oil co.  
C A, 84 : 43583u (1976).
11. Boudart, M., *AICh E J.*, **18** (1972), 465.
12. Burge, H.D., and Collins, D.J., *Ind. Eng. Chem. Prod. Res. Develop.*, **19**, (1980), 389
13. Calderbank, P.H., *Trans. Inst. Chem. Engrs.*, **36** (1958), 443.
14. Chaudhari, R.V., Gholap, R.V., Emig, G., and Hofmann, H., *Can. Chem. Eng.*, **65** (1987), 744.
15. Chaudhari, R.V. and Ramachandran, P.A., *AIChE J.*, **26**, (1980), 177.

16. Chaudhari, R.V., Shah, Y.T. and Foster, N.R.,  
Catal. Rev. Sci. Eng., **28** (4), (1986), 431.
17. Degussa AG, unpublished results (1980).
18. Dovell, F.S., Fergusson, W.E. and Greenfield,  
H.J., Ind. Eng. Chem. Prod. Res. Develop., **9**,  
(1970), 224.
19. Dovell, F.S. and Greenfield, H., J. J. Org. Chem.  
**32** (1967), 3670.
20. Du Pont, U.S. Pat., 2,619,503 (1952), C A, 47 : 9356  
(1953)
21. Du Pont, U.S. Pat., 2, 823, 235 (1958), C A, 53 :  
6155 (1959).
22. Every, R.L. and Riggs Jr., O.L., Mater. Protect., **3**,  
(1964), 46.
23. Fr. Pat., 1, 440 419 (1966), to Englehard Ind.,  
C A, 66 : 28497D (1966)
24. Fr. Pat., 1, 503 153 (1967), to Universal oil  
products, C A, 69 : 106200E (1968)
25. Fr. Pat., 2, 211 448 (1974), C A, 82 : 139631t (1975)
26. Froment, G.F., AICh E J., **21** (1975), 1041.
27. Froment, G.F., and Bischoff, K.B., 'Chemical reactor  
analysis and design', J. iley, New York, (1979).
28. General Aniline and Film Corp., U.S. Pat., 3,093,  
685 (1963).
29. Ger. Offen., 939, 289 (1956), C A, 52 : 13315h  
(1958).

30. Ger. offen., 2, 156 051, (1971), to Hoechst AG.,  
C A, 79 : 43680v  
(1973).
31. Ger. offen., 2, 343 959, (1973), to Hoechst AG,  
C A, 83 : 58402n (1975).
32. Ger. Pat., 2, 426 879, (1974). to BASF
33. Haber, F., Z. Electrochem., 4, (1898), 506.
34. Hopkins, T.R., neighbors, R.P., Strickler, P.D. and  
Philips, L.V., J. Org. Chem., 24, (1959), 2040.
35. Komiyama, H., and Smith, J.M., AICh E J., 21 (1975),  
670.
36. Kosak, J. R., 'Catalysis in organic synthesis', Ed.,  
W.H. Jones, Academic Press, New York (1980).
37. McNab, J.I., Inst. Chem. Eng. Symp. Ser., 68,  
3/s : 15 (1981).
38. Meldola, R., J. Chem. Soc., 93, (1908), 2214.
39. Meschke, R.W. and Hostung, W.H., J. Org. Chem., 25,  
(1960), 137.
40. Metcalfe, A., and Rowden, M.W., J. Cat., 22 (1971),  
30.
41. Pascoe, W., 'Catalysis of organic reactions',  
Eds., P.N. Rylander, H. Greenfield, and R.L. Augustine,  
Marcel Dekker, Inc., New York (1988).
42. Perry, R.H. and Chilton, C.H. Chemical Engineers  
Hand -Book, 5th Edition, Mc Graw-Hill, New York  
(1973).



43. Rajadhakshya, R.A., and Karwa, S.L., Chem. Eng. Sci., **41** (1986), 1765.
44. Ramachandran, P.A. and Chaudhari, R.V., 'Three Phase Catalytic Reactors', Gordon and Breach Science Publishers (1983).
45. Roberts, G.W., 'Catalysis In Organic Synthesis', Academic Press New York (1976).
46. Sano, Y., Yamaguchi, N., and Adachi, T., J. Chem. Eng. Japan, **1** (1974), 255.
47. Satterfield, C.N., 'Mass Transfer in Heterogeneous Catalysis', MIT Press Cambridge Mass (1970).
48. Shah, Y.T., 'Gas-Liquid-Solid Reactor Design', New York, McGraw-Hill International (1979).
49. Sherwood, T.K. and Farkes, E.J., Chem. Eng. Sci., **21**, (1966), 573.
50. Seidell, A.D., 'Solubility of Inorganic and Organic Compounds', Van Nostrand Co. Inc. New York (1940)
51. Stratz, A.M., 'Catalysis of Organic Reactions', Ed. Kosak, J.R., Murcel Dekker, Inc., New York (1984).
52. Surrey, R.A. and Hammer, H.F., J. Am. Chem. Soc., **68**, (1948), 115.
53. Talati, J.D. and Pandya, J.M., Corros, Sci., **16**, (1976), 603.
54. Tolochemie, Belg. Pat., 846, 341 (1977), C A, 87 : 2010574u (1977).
55. U.S. Pat., 2,458,214 (1949), to Shell Devlop. Co.
56. U.S. Pat., 2,464,044 (1949) to Boyle-Midway Inc.

57. U.S. Pat., 2,670,327 (1954), to Universal Oil Products, C A, 48 :4738b (1954)
58. U.S. Pat. 2,716,135 (1955), to Allied Chem. Corp.
59. U.S. Pat. 2,772,313 (1956), to Columbia Southern Chem. Corp., C A, 51 :10570f (1957)
60. U.S. Pat. 2,791,613 (1957), to Columbia Southern Chem. Corp., C A, 52 :1226h (1958).
61. U.S. Pat. 3,051,753 (1962), to Dow Chem. Co., C A, 58 :473F (1963).
62. U.S. Pat. 3,683,025 (1972), to Pons, H.W., C A, 77 :139594e (1972).
63. Vannice, M.A., Hyum, S.H., Kalpakci, B., and Liauch, W.C., J. Cat. **56** (1979), 358.
64. Venkatraman, K., 'Chemistry of Synthetic Dyes', Vol. I, Academic Press, New York (1952).
65. Wilke, C.R., and Chang, P., AICh E J., **1** (1955), 264.
66. Wisniak, J., and Klein, M., Ind. Eng. Chem. Prod. Res. Dev., **23** (1984), 44.
67. Yao, H.C., and Emmett, P.H., J. Am. Chem. Soc., **81**, (1959), 4125.
68. Yao, H.C. and Emmett, P.H., J. Am. Chem. Soc., **83**, (1961a), 796.
69. Yao, H.C. and Emmett, P.H., J. Am. Chem. Soc., **83**, (1961b), 799.
70. Yao, H.C. and Emmett, P.H., J. Am. Chem. Soc., **84**, (1962), 1086.